

IBEHS 5P06 (2024-2025)

# Capstone Project: RhythmGuard

A Real-Time Arrhythmia Detection System Powered by TinyML

Team 16

**Supervisor:** Dr. Mohamed Hassan

**Instructor:** Vincent Leung

**Co-instructor:** Dr. Allan Wassyng

## **Members:**

Noor Al-Rajab | alrajabn | 400291137 | Mechatronics & BME

Kavya Sundaresan | sundarek | 400307169 | Mechatronics & BME

Maryem Abdullatif | abdulm41 | 400297192 | Mechatronics & BME

Sarah Alabdulrazzak | alabdus | 400326083 | Mechatronics

## Summary

Heart arrhythmias are characterized by irregular heart rhythms and can lead to severe health complications if left untreated. Early diagnosis can play a crucial role in preventative care and early intervention. However, detecting arrhythmias often requires access to specialized and costly equipment and is commonly restricted to medical settings. Although wearable devices for arrhythmia detection exist, they face challenges such as insufficient accuracy, poor usability, and limited accessibility.

Rhythm Guard addresses these challenges with an affordable, compact, and user-friendly solution for real-time arrhythmia detection. The system collects ECG and PPG data through a wearable device and processes it internally on an ESP32 controller. By integrating a one-lead ECG sensor, PPG technology, and a TinyML-based algorithm, the ESP32 efficiently analyzes signals directly on the device. Leveraging advanced signal processing and machine learning, Rhythm Guard ensures high sensitivity and specificity while maintaining a fast response rate for real-time actionable feedback. Designed for user comfort and practicality, it provides a seamless solution for daily monitoring.

Rhythm Guard's expected impact includes improving access to arrhythmia detection by offering a cost-effective and portable solution that empowers individuals to monitor their heart health. By bridging the gap between accessibility and reliability, Rhythm Guard aims to improve early detection rates, reduce healthcare costs, and improve health outcomes.

Rhythm Guard is an innovative system that collects data through a wearable device and processes it locally using ECG and PPG technologies with AI-driven algorithms to provide real-time arrhythmia detection. Designed for accuracy, affordability, and comfort, Rhythm Guard empowers users to monitor their heart health while offering personalized insights and timely alerts, enhancing proactive healthcare management.

## **Declaration of Academic Achievement and Consent**

As a future member of the engineering profession, the student is responsible for honestly performing the required work without plagiarism and cheating. Submitting this work with my name and student number is a statement of understanding that this work is my own and adheres to the Academic Integrity Policy of McMaster University and the Code of Conduct of the Professional Engineers of Ontario.

Submitted by [**Noor Al-Rajab, alrajabn, 400291137**]

As a future member of the engineering profession, the student is responsible for honestly performing the required work without plagiarism and cheating. Submitting this work with my name and student number is a statement of understanding that this work is my own and adheres to the Academic Integrity Policy of McMaster University and the Code of Conduct of the Professional Engineers of Ontario.

Submitted by [**Sarah Alabdulrazzak, alabdus, 400326083**]

As a future member of the engineering profession, the student is responsible for honestly performing the required work without plagiarism and cheating. Submitting this work with my name and student number is a statement of understanding that this work is my own and adheres to the Academic Integrity Policy of McMaster University and the Code of Conduct of the Professional Engineers of Ontario.

Submitted by [**Maryem Abdullatif, Abdulm41, 400297192**]

As a future member of the engineering profession, the student is responsible for honestly performing the required work without plagiarism and cheating. Submitting this work with my name and student number is a statement of understanding that this work is my own and adheres to the Academic Integrity Policy of McMaster University and the Code of Conduct of the Professional Engineers of Ontario.

Submitted by [**Kavya Sundaresan, sundarek, 400307169**]

## Table of Contents

<b>List of Abbreviations and Symbols.....</b>	<b>8</b>
<b>List of Figures.....</b>	<b>9</b>
<b>List of Tables.....</b>	<b>11</b>
<b>1.1 User Needs: Understanding User Requirements for Device Usability and Effectiveness...</b>	
<b>12</b>	
1.1.1 Background and Rationale for Continuous Arrhythmia Monitoring.....	12
<b>1.1.2 Impact and Benefits of Continuous Arrhythmia Monitoring System.....</b>	<b>13</b>
<b>1.2 Design Inputs.....</b>	<b>17</b>
1.2.1 Functional Requirements for Continuous Monitoring and Real-Time Prediction.....	17
1.2.2 Performance Criteria for Accurate Detection.....	18
1.2.3 System Feedback Requirements for Communication and Alerts.....	18
1.2.4 Physical and Durability Specifications for Wearability.....	18
1.2.5 Environmental and Sustainability Considerations.....	19
1.2.6 Considerations from Literature for Performance Optimization.....	19
<b>1.3 Design Process: Approach to Building a Wearable Arrhythmia Monitoring Device.....</b>	<b>20</b>
1.3.1 Signal Selection and Device Design: Choosing the Right Biosignals for Detection.....	20
1.3.2 Feedback Mechanism and Integration Considerations: Providing Clear User Alerts.....	21
1.3.3 Data Processing and Algorithm Development: Advanced Methods for Arrhythmia Detection.....	21
1.3.4 Validating Feature Detection Methods.....	24
<b>1.4 Preliminary Risk Assessment: Evaluating Health, Safety, and Ethical Implications for Wearable Technology.....</b>	<b>27</b>
1.4.1 Health and Safety Risks: Evaluating Electrical, Battery, and Allergic Concerns...	27
1.4.2 Ethical Implications: Addressing Data Privacy, Security, and Inclusivity.....	27
1.4.3 Standards and Regulatory Compliance: Ensuring Device Safety and Performance.....	28
<b>2.1 Design Outputs and Verification Tools for Performance Assessment.....</b>	<b>29</b>
<b>2.2 Final Decision Concept: Balancing Affordability, Accuracy, and Usability.....</b>	<b>32</b>
2.2.1 Final Design Overview: System Architecture and Features.....	32
Accuracy of Arrhythmia Detection: Achieving High Sensitivity and Specificity.....	32
Real-Time Processing: Optimizing Speed and Efficiency.....	33
Compliance with Medical Device Regulations: Adhering to Safety Standards.....	34
2.2.2 Final Design Concept Justification: Ensuring Performance and Compliance.....	35
Algorithmic Accuracy: Evaluating Sensitivity, Specificity, and Generalizability.....	35
Signal Sampling and Filtering: Optimizing ECG Signal Accuracy.....	36

Wearable Design: Size, Comfort, and Material Selection for Continuous Monitoring.....	36
Battery Life Considerations: Ensuring 24-Hour Continuous Monitoring.....	37
Power Consumption Optimization: Enhancing Energy Efficiency for Extended Device Operation.....	37
Real-Time Feedback Mechanism and Data Privacy: Ensuring User Interaction and Security.....	37
2.2.4 Assumptions, Limitations, and Constraints of Design Implementation.....	37
Assumptions: Defining Usage and Operational Guidelines.....	37
Limitations: Identifying Constraints on Detection and Data.....	38
Constraints: Addressing Hardware and Battery Limitations.....	38
<b>2.3 Final Decision: Risk and Compliance Management Plan.....</b>	<b>38</b>
2.3.1 Scope of Risk Management Activities in the Project Lifecycle.....	38
2.3.2 Responsibility, Authorities, and Stakeholder Roles in Risk Management.....	38
2.3.3 Criteria for Accepting and Managing Risks in Medical Device Development.....	39
2.3.4 Risk Identification, Analysis, and Evaluation Process.....	39
2.3.5 Mitigation Strategies and Control Measures for Identified Risks.....	41
2.3.6 Verification and Testing of Risk Control MeasuresReviewing training materials to ensure users are well-informed about device operation and limitations [67].....	41
2.3.7 Comprehensive Evaluation of Residual Risks and Their Impact.....	41
2.3.8 Ethical, Safety, and Environmental Considerations in Risk Management.....	42
Informed Consent and Transparency in Device Use.....	42
Ensuring Safety and Compliance with Medical Standards.....	42
Managing Algorithmic Fairness and Minimizing Bias.....	43
Environmental Responsibility and Sustainability in Production.....	44
<b>2.4 Final Decision: Proof-of-Concept and Verification.....</b>	<b>45</b>
2.4.1 Transferability of Wearable Device Data.....	45
Objective.....	45
Verification Methodology.....	45
Modeling and Analysis.....	47
2.4.2 Technical Feasibility of Data Acquisition and Processing.....	48
Objective.....	48
Verification Methodology.....	48
Modeling and Analysis.....	49
<b>3.1 Design Prototype Plan.....</b>	<b>50</b>
3.1.1 Overview of Hardware Architecture and Integration.....	50
3.1.2 Overview of Software Architecture and Integration.....	51
Data Preparation and Processing.....	52
Feature Extraction and Clustering.....	53
Real-Time Identification and Classification of Arrhythmia Types.....	56

Real-Time Scheduling for Signal Processing.....	57
3.1.3 Overview of Casing for Hardware Hiding Design.....	58
3.1.4 Assumptions, Limitations, and Constraints.....	61
3.1.5 Implementation of Mitigation Strategies.....	62
<b>3.2 Design Verification Plans.....</b>	<b>63</b>
3.2.1 Verification Setup.....	63
Test environment and components.....	63
Verification strategy.....	63
3.2.2 Test Cases.....	66
3.2.3 Verification Plans for Design Outputs.....	68
Test 1: Battery Life Validation and Compliance with IEC 61960 Standards.....	69
Test 2: Sensitivity and Specificity Assessment of Heart Arrhythmia Detection.....	69
Test 3: Sampling Frequency Verification Based on ECG Signal Requirements.....	70
Test 4: Verification of Non-Invasiveness and Class I Medical Device Compliance.....	70
Test 5: Wearable Adjustability Assessment for Diverse Wrist Sizes.....	70
Test 6: Allergenicity Assessment via Human Repeated Insult Patch Test (HRIPT).....	70
Test 7: Scratch Resistance Testing of Wearable Casing Materials.....	71
Test 8: Drop Resistance Testing Based on Average Adult Height.....	71
Test 9: Water Resistance Evaluation Using 1-Metre Submersion Test.....	71
Test 10: Hardware Response Time Measurement for Real-Time User Feedback.....	71
3.2.4 Verification Plans for Mitigation Strategies.....	72
Risk: inaccurate arrhythmia detection.....	72
Verification plan.....	72
Risk: delayed or inaccurate arrhythmia detection.....	73
Verification plan.....	73
Risk: device firmware crashes.....	74
Verification plan.....	74
<b>4.1 Implementation.....</b>	<b>74</b>
Embedded Software Architecture and Pipeline Overview.....	74
Core Software Implementation Pipeline Components.....	74
Hardware Prototype Design and Implementation for Real-Time ECG and PPG Data Processing.....	78
Mechanical.....	78
<b>4.2 Results and Discussion.....</b>	<b>79</b>
Software.....	79
Signal Sampling and Threading Performance on the ESP32.....	79
Feature Extraction and Class Variability.....	80
Machine Learning Model Accuracy and Verification Results.....	84
Dataset Limitations and Software Implications.....	86

Hardware.....	86
Memory Overflow.....	86
LCD Screen.....	87
<b>4.3 Future Work.....</b>	<b>87</b>
Software.....	87
Hardware.....	88
Mechanical.....	89
<b>4.4 Reflections and Recommendations.....</b>	<b>89</b>
Kavya.....	90
Noor.....	91
Sarah.....	91
Maryem.....	91
<b>Conclusion.....</b>	<b>91</b>
<b>References.....</b>	<b>93</b>

# List of Abbreviations and Symbols

ECG: Electrocardiogram

PPG: Photoplethysmography

Hz: Hertz

IoT: Internet of Things

ML: Machine Learning

WHO: World Health Organization

SDG: Sustainable Development Goals

FDA: Food and Drug Administration

LCD: Liquid-Crystal Display

CNN: Convolutional Neural Network

RNN: Recurrent Neural Network

HRV: Heart Rate Variability

ISO: International Organization for Standardization

IEC: International Electrotechnical Commission

EMC: Electromagnetic Compatibility

PIPEDA: Personal Information Protection and Electronic Documents Act

HRIPT: Human Repeat Insult Patch Test

ASTM: American Society for Testing and Materials

MIL-STD: Military Standard

FFT: Fast Fourier Transform

FMEA: Failure Mode and Effects Analysis

RPN: Risk Priority Number

E-waste: Electronic waste

RoHS: Restriction of Hazardous Substances

GUI: Graphical User Interface

CSV: Comma-separated values

FPU: Floating-point unit

DSP: Digital Signal Processing

SRAM: Static random-access memory

UMAP: Uniform Manifold Approximation and Projection

TD: Time Domain

I2C: Inter-Integrated Circuit

## List of Figures

**Figure 1:** Design decisions (rectangles) and potential choices (ellipses) to find a continuous arrhythmia monitoring solution according to the need statement.

**Figure 2:** RR interval, as detected with the Python package SciPy [22]. A smooth line or curve would mean the measurements are consistent, otherwise either some ECG peaks are not getting detected (spike down) or false peaks are detected (spike up).

**Figure 3:** Top plots are healthy ECG, bottom plots are ECG signals of atrial fibrillation episodes. Left plots are the time-domain representation, right plots are frequency-domain (Fourier Transform) representation. Shaded region is the normal range for heart rate in Hz. Even though time-domain signals look fairly similar, the two signals can be distinguished easily through frequency-domain plots.

**Figure 4:** FFT of a healthy sinus rhythm (left) compared to an atrial fibrillation ECG (right) in waveforms from the Charlton et al. dataset.

**Figure 5:** Time constraints of data processing on the wearable. Schedule A shows a schedule that meets the time constraints, where processing ends before the next sampling point is acquired. If processing, including FFT calculation, takes longer than the time between sampling actions (Schedule B), some samples will either be skipped or delayed, the former case compromising accuracy and the latter case causing a continuously increasing lag.

**Figure 6:** Data acquisition using the wearable through bluetooth.

**Figure 7:** Circuit used for the 3-lead signal acquisition, consisting of amplifiers and a combination of high-pass and low-pass filters.

**Figure 8:** Raw ECG signals (top) and processed ECG signals (bottom) from the wearable (left), 3-lead lab circuit (middle), and MIMIC (right). Since MIMIC waveforms had minimal noise, no filtering or smoothing was required.

**Figure 9:** The FFT of the wearable, 3-lead lab circuit, and MIMIC samples, respectively. All three samples displayed the healthy peaks at the heart rate frequency and its multiples. The red arrows show the main peak which represents the heart rate frequency.

**Figure 10:** FFT of healthy ECG signal as calculated on the ESP32, graphed in real-time on the laptop.

**Figure 11:** FFT of atrial fibrillation ECG signal as calculated on the ESP32, graphed in real-time on the laptop.

**Figure 12:** The hardware system consists of two separate components, the wearable and the ESP32 portion.

**Figure 13:** A flow chart outlining the process from signal acquisition and processing to feature extraction, optimization, classification, and output.

**Figure 14:** The counts of 8-second samples collected from the Clifford et al. and Charlton et al. datasets combined.

**Figure 15:** Time-domain signal (left) and frequency domain signal (right) of a sample signal. Annotations on the right graph represent some features found to be useful in distinguishing some arrhythmias from healthy rhythms and from each other.

**Figure 16:** Visual representation of the specific features extracted from the PPG waveform, highlighting the morphological characteristics critical for analysis. Adapted from [80].

**Figure 17:** Detection of peaks and valleys within the PPG waveform, illustrating their significance in segmenting the signal for feature extraction.

**Figure 18:** Stacked ML model to form a decision based on both ECG and PPG data. ECG and PPG data are extracted from both datasets and separated so that each is fed to its corresponding model. The final result is determined by a meta model that forms the decision based on the outputs of the two models.

**Figure 19:** The management of sampling and processing real-time tasks. Although the usage of interrupts increases the duration of processing, it leads to all tasks meeting their deadlines since processing (every second) is less frequent than sampling (250 times per second).

**Figure 20:** Initial iteration sketch for the hardware casing

**Figure 21:** Engineering Drawings of the Final Mechanical Component

**Figure 22:** Data transmission and processing verification test flow chart.

**Figure 23:** Power and signal verification test flow chart (Left) and alert and system durability verification test flow chart (right)

**Figure 24:** Power and signal verification test flow chart (Left) and alert and system durability verification test flow chart (right)

**Figure 25:** Diagram showing the multithreading architecture with separate circular FIFO buffers for ECG and PPG data. One thread handles sampling every 8 ms, while the other performs FFT, feature extraction, and arrhythmia prediction without data interference.

**Figure 26:** Final 3D printed mechanical design

**Figure 27:** resultant sampling period after threading

**Figure 28:** Confusion matrices before and after feature elimination. The left matrix shows the model's performance with all features, while the right reflects improved classification accuracy after removing less informative features.

**Figure 29:** Scatter plot showing the variance in num\_peaks and num\_valleys across selected arrhythmia types, highlighting their potential for distinguishing between classes.

**Figure 30:** UMAP projection illustrating the variance between healthy, tachycardia, and bradycardia samples.

**Figure 31:** UMAP visualization highlighting the variance between healthy and atrial fibrillation samples.

**Figure 32:** UMAP showing variance between ventricular tachycardia and ventricular flutter/fibrillation

**Figure 33:** Confusion matrices comparing classification accuracy across four setups. Top left: PPG model; top right: ECG model; bottom left: combined PPG and ECG model; bottom right: final optimized model.

**Figure 34:** Updated Gantt chart to reflect changes

## List of Tables

**Table 1:** Summary of Design Inputs for the Wearable Arrhythmia Detection Device

**Table 2:** Key Design Requirements and Their Associated Verification Outputs

**Table 3:** FMEA Table [31, 32]

**Table 4:** A comparison between the ESP32-PICO-D4 and the MAX32666 wearable device [2, 3]

**Table 5:** Summary of key frequency-domain and time-domain features extracted from preprocessed ECG signals

**Table 6:** Summary of key morphological and time-domain features extracted from preprocessed PPG signals

**Table 7:** The verification tests that can be conducted to check each design output corresponding to each design input.

**Table 8:** Summary of overall classification results, including true positives (TP), true negatives (TN), false positives (FP), false negatives (FN), precision, and sensitivity for each arrhythmia type.

## 1.1 User Needs: Understanding User Requirements for Device Usability and Effectiveness

### 1.1.1 Background and Rationale for Continuous Arrhythmia Monitoring

Cardiac arrhythmia is a serious condition characterized by irregular heartbeats, which can lead to severe complications such as stroke, heart failure, and sudden cardiac arrest if left undetected. Globally, cardiovascular diseases account for approximately 17.9 million deaths annually, representing 32% of all deaths, with arrhythmias playing a significant role in many of these cases [1]. Early detection and continuous monitoring are crucial for timely medical intervention, particularly for high-risk patients.

Traditional electrocardiogram (ECG)-based monitoring remains the gold standard for arrhythmia detection. However, it is primarily limited to clinical settings, requiring specialized equipment and trained personnel for interpretation, which restricts continuous long-term monitoring [1]. Wearable ECG devices, such as Holter monitors and smartwatches with ECG functionality, have attempted to bridge this gap, but they often suffer from issues related to signal noise, limited battery life, and the need for frequent manual assessments by healthcare professionals [1]. Furthermore, the increasing burden on healthcare systems to collect and interpret large volumes of ECG data contributes to delays in diagnosis and treatment.

Despite the rise of Internet of Things (IoT)-based healthcare solutions, current methods still face challenges such as data security concerns, high power consumption, and inaccurate classification of arrhythmic events due to artifacts and signal distortions [2]. Many existing techniques rely on manual detection, which is time-consuming and prone to errors, potentially leading to misdiagnosis. Machine learning (ML) and deep learning approaches have demonstrated significant promise in automating arrhythmia classification, improving both accuracy and efficiency in real-time detection [2]. Thus, there is a strong need for robust, automatic methods that enhance the classification and prediction of arrhythmias, ensuring more reliable and continuous patient monitoring.

Existing literature has identified several key user needs, particularly from the perspectives of patients and cardiologists, who are the primary users of arrhythmia monitoring systems. Patients require a non-invasive, user-friendly wearable device that enables continuous heart monitoring without compromising their quality of life [2]. Wear comfort, ease of use, and uninterrupted daily activity are critical factors influencing patient adherence to long-term monitoring solutions. Additionally, real-time alerts are essential, allowing patients to take immediate action when an abnormal event is detected. Furthermore, patients benefit from clear,

interpretable, and actionable data, empowering them to understand their condition and seek timely medical intervention when necessary [2].

On the other hand, healthcare professionals emphasize the need for an accurate and reliable system that minimizes both false positives and false negatives, ensuring precision in arrhythmia detection [3]. High false-positive rates can lead to unnecessary interventions and increased workload, while false negatives pose a risk of missing life-threatening conditions. Cardiologists also require a system that delivers clinically relevant insights without overwhelming them with excessive or redundant data, thereby streamlining diagnosis and decision-making. Additionally, minimizing the delay in arrhythmia detection and diagnosis is crucial for effective patient management.

These user needs underscore the importance of integrating wearable technology with machine learning to enable real-time, continuous heart rhythm monitoring while maintaining diagnostic accuracy. An efficient, real-time arrhythmia detection system that is user-friendly, minimizes false diagnoses, and reduces the burden on healthcare professionals is urgently needed. Such a system would not only improve patient outcomes but also enhance the overall efficiency of cardiovascular care by facilitating early detection and timely intervention outside the clinical setting.

Patients suffering from, or at risk of arrhythmia need an accurate, real-time, and user-friendly arrhythmia detection system that can be used for continuous monitoring outside clinical settings, minimizing false diagnoses while reducing the workload on healthcare professionals.

#### 1.1.2 Impact and Benefits of Continuous Arrhythmia Monitoring System

The proposed continuous arrhythmia monitoring and detection system aims to address the critical gaps identified in cardiac health monitoring literature. Research highlights significant limitations in existing detection systems, including high false-positive and false-negative rates, as well as the inability to ensure real-time monitoring—especially outside clinical environments [4]. These shortcomings contribute to delayed diagnoses and increased strain on healthcare professionals, underscoring the urgent need for an improved solution.

The final system will incorporate real-time continuous monitoring and automatic arrhythmia detection, directly addressing the immediate needs of both patients and healthcare providers. By enabling timely intervention, reducing diagnostic errors, and extending monitoring beyond clinical settings, this system will not only enhance individual patient care but also drive positive societal change.

### *Benefits for Arrhythmia Patients*

The proposed system is expected to significantly enhance the quality of life for arrhythmia patients by providing real-time, continuous monitoring while reducing the need for frequent clinical visits. This aligns with the growing patient preference for non-invasive, user-friendly devices that seamlessly integrate into daily life without causing discomfort or disruption. Studies have shown that patients increasingly value wearable technologies that offer continuous monitoring capabilities, as they allow for real-time tracking without interfering with normal daily activities [5]. These devices are also perceived as empowering patients, giving them a greater sense of control over their health and well-being.

By enabling continuous monitoring, the system helps alleviate anxiety and empowers patients with greater autonomy over their health. Research has demonstrated that the peace of mind provided by such systems is invaluable to patients, as it ensures that any potential arrhythmia is instantly diagnosed, allowing for timely medical intervention [5]. In fact, studies have highlighted that patients with access to continuous monitoring report reduced stress and improved quality of life due to the reassurance provided by real-time health tracking [5].

Furthermore, this system has the potential to prevent severe health events, such as stroke and sudden cardiac arrest, by minimizing the risk of undetected arrhythmias and facilitating early identification and response. According to recent studies, early detection of arrhythmias is directly linked to improved patient outcomes, as it enables interventions that can prevent life-threatening complications [6]. With its timely alerts and continuous data tracking, the system can substantially reduce the chances of missing critical arrhythmias, thereby enhancing overall patient safety and long-term health outcomes.

### *Benefits for Healthcare Providers*

Clinically, the proposed system would address critical challenges related to diagnostic accuracy in arrhythmia detection. One of the most significant issues in current systems is the high rate of false positives, which can overwhelm healthcare providers with irrelevant information, delaying diagnosis and treatment [4]. By automating the detection process and filtering out noise from the data, the system would present the results in the most relevant and interpretably formatted manner, helping to reduce the burden of unnecessary information and enabling quicker, more informed decision-making.

Recent studies indicate that false positives are a major concern in arrhythmia monitoring, as they not only increase the workload for healthcare providers but also lead to unnecessary

interventions, which can cause patient distress and resource strain [5]. By incorporating machine learning-based algorithms that refine the data, the system would minimize false positives and negatives, thereby improving overall diagnostic accuracy.

Furthermore, the system's ability to automate the detection process would free up valuable time for healthcare professionals, allowing them to focus on direct patient care rather than spending excessive time on intensive data interpretation. This would enhance clinical workflows by streamlining the decision-making process, reducing diagnostic delays, and improving the efficiency of healthcare delivery. As a result, healthcare professionals would be better equipped to provide timely and accurate care, leading to better patient outcomes.

### *Health, Safety, and Resource Utilization*

Continuous monitoring for the early detection of arrhythmias has been shown to significantly enhance patient outcomes. Early medical intervention is critical, as studies have demonstrated that it can decrease hospitalization rates, reduce the incidence of medical emergencies, and even lower mortality rates from untreated or undiagnosed heart conditions [6]. Research consistently highlights the importance of early detection in preventing the progression of arrhythmias, which can lead to more severe cardiovascular events like stroke, heart failure, and sudden cardiac arrest [1].

The proposed system would also contribute to better utilization of healthcare resources, particularly by reducing the burden on emergency services and hospitals. By providing real-time, continuous monitoring, the system enables early identification of potential arrhythmias before they escalate into emergencies. This would help mitigate the load on rescue services and hospital emergency departments, particularly during peak seasons, such as flu outbreaks or high-pressure periods (e.g., holiday seasons). Studies have shown that preventive care systems that enable early detection and intervention significantly reduce emergency room visits, thereby allowing healthcare facilities to allocate resources more effectively and efficiently [2].

Additionally, the reduction in emergency hospitalizations directly translates to cost savings for the healthcare system, improving overall resource management and enhancing the sustainability of healthcare delivery, especially in resource-constrained environments.

### *Economic and Environmental Impact*

The economic benefits of early arrhythmia detection are well-documented in the literature. Early diagnosis significantly reduces the financial burden on the healthcare system by preventing the need for lengthy hospital stays, emergency interventions, and the ongoing management of chronic heart conditions. A study by Smith et al. (2020) found that early

detection and intervention for arrhythmias can lower hospitalization costs by as much as 30%, as it reduces the likelihood of severe complications that would otherwise require extended care [6].

Furthermore, by enabling a shift toward a more preventive care model, early detection helps minimize the need for urgent care, leading to lower healthcare expenditure in the long term. As arrhythmias are identified and managed early, patients can avoid emergency situations, reducing the strain on hospitals and emergency services, which are often burdened by preventable cases. This model not only alleviates pressure on healthcare infrastructure but also saves resources, ultimately contributing to more efficient allocation of healthcare funds [6].

The economic burden extends beyond the healthcare system, impacting patients and their families. Chronic diseases such as arrhythmias are expensive to manage, and by detecting them early, patients can avoid the high costs associated with prolonged hospital stays, emergency procedures, and long-term treatment regimens. Research indicates that preventive care can lower out-of-pocket costs for patients by reducing the frequency of hospital visits and the need for intensive treatments, fostering a more sustainable healthcare approach [6].

The integration of machine learning technology into wearable devices for continuous arrhythmia monitoring not only enhances healthcare efficiency but also offers significant environmental and sustainability benefits. By reducing the need for frequent hospital visits, the system can help lower transportation-related emissions, which contribute to carbon footprints. Research has shown that a significant portion of healthcare's environmental impact comes from patient transportation to and from medical facilities, which can be alleviated through the use of remote monitoring solutions [7].

Furthermore, the system minimizes the reliance on high-energy-consuming hospital-based monitoring equipment. Traditional medical devices used in clinical settings require considerable power and infrastructure, adding to the overall ecological footprint of healthcare operations. Wearable devices, on the other hand, are designed to be energy-efficient and more portable, reducing the need for such large-scale, energy-intensive equipment. This reduction in energy use aligns with the global push for more sustainable healthcare practices, which are a key aspect of environmental goals set by international organizations like the World Health Organization (WHO) and UN Sustainable Development Goals (SDGs) [7].

Additionally, the development of greener medical devices that require fewer resources and generate less waste is a priority for advancing sustainability in healthcare. Eco-friendly wearable devices, coupled with machine learning algorithms, can help reduce not only energy consumption but also the use of materials in the manufacturing process, contributing to a more sustainable healthcare model. Research highlights that such innovations are critical to ensuring

that healthcare systems can meet the growing demand for services without disproportionately contributing to environmental degradation [7].

### *Legal, Social, and Regulatory Considerations*

The design and deployment of wearable medical devices must adhere to established regulatory standards to ensure patient safety and privacy. The proposed system will be developed in full compliance with FDA medical device guidelines, which set forth stringent criteria for the safety, effectiveness, and quality of medical technologies. As the system operates locally, without relying on cloud services or internet connectivity, the device will prioritize local data storage and ensure secure processing of sensitive health information on the device itself. This approach reduces the risk of data breaches that are often associated with cloud-based storage and transmission, further protecting patient privacy.

Moreover, accessibility will be a core design principle, ensuring that the system is usable by a diverse range of patients, including those with varying levels of education, physical ability, or technological literacy. This consideration is crucial in addressing the equitable distribution of healthcare technologies, as outlined in the literature. Studies emphasize that technological solutions must be inclusive, providing equal access to all patients, regardless of socioeconomic background, education level, or physical capability [8]. By ensuring that the wearable device is user-friendly and adaptable to different needs, the system can help bridge the gap in healthcare accessibility, particularly for underserved populations.

Furthermore, the legal and social implications of healthcare technology extend beyond privacy and accessibility concerns. The system will be designed to foster trust between patients and healthcare providers, ensuring that patients feel confident in the accuracy and security of the technology. As wearable medical devices become more integrated into daily life, building trust is essential for widespread adoption and for addressing public concerns about the ethical use of health data in a rapidly evolving technological landscape [8].

## 1.2 Design Inputs

### 1.2.1 Functional Requirements for Continuous Monitoring and Real-Time Prediction

The main goal of the final wearable device is to accurately predict arrhythmia in patients in real-time. The device will be worn continuously to monitor heart rate, so it must have a battery life of at least 24 hours. This allows the user to wear the device for the majority of the day, providing adequate time for recharging (during nighttime, for example).

Additionally, the system must be capable of delivering predictions or alerts within a time period longer than the prediction time. The signal sampling rate must be sufficiently long to allow for data storage while keeping the system real-time and meeting deadlines. Based on similar devices in the literature, a sampling rate of 250-500 Hz is often found adequate, ensuring data acquisition accuracy without unnecessary power consumption. Research suggests that time delays and data storage must be managed to ensure that data is not lost between predictions, thus supporting real-time monitoring [9].

#### 1.2.2 Performance Criteria for Accurate Detection

For arrhythmia detection, current one-lead ECG solutions have demonstrated a sensitivity of 98% and a specificity of 99% with 12-lead ECG as gold standard[10]. The system will simulate ECG data at a sampling frequency of around 250 Hz to provide a balance between data accuracy and power efficiency, suitable for real-time arrhythmia detection. However, for the first iteration, the wearable device will aim to achieve sensitivity and specificity values greater than or equal to 90% in preliminary trials using ECG data, ensuring a reliable starting point for further refinement of the detection algorithm.

#### 1.2.3 System Feedback Requirements for Communication and Alerts

The wearable device should include a power on/off feature to optimize battery life. When not in use, this will allow the patient to store energy efficiently and use the device for extended periods. The USB Type-C charging port is recommended for compatibility with a wide range of current devices, enhancing the device's usability and accessibility [12].

The wearable must be able to convey arrhythmia prediction results to a user-friendly interface. This could be achieved through a visual or auditory alert system, ensuring the patient receives immediate feedback on their condition. The wearable will also need a visual display or mobile app interface for conveying predictive alerts and any necessary actionable steps.

#### 1.2.4 Physical and Durability Specifications for Wearability

The physical dimensions of the wearable should be small, ideally measuring no more than 5 cm in diameter for ease of wearability and comfort. Literature suggests that smaller, lighter devices improve patient compliance [13]. The device must be non-invasive and compact, with the outer casing made from durable, hypoallergenic materials such as medical-grade silicone to ensure comfort during prolonged use and reduce potential skin reactions. The device must have a water resistance rating of at least IPX7 to allow use in wet conditions such as rain or the shower, ensuring robustness for daily activities [14].

## 1.2.5 Environmental and Sustainability Considerations

In terms of environmental sustainability, the wearable should be produced with environmentally friendly materials, minimizing harmful toxins upon disposal and promoting recyclability. The total cost of the materials used in production should not exceed \$1000, based on cost-benefit analyses of similar devices, ensuring the system remains affordable for both consumers and healthcare providers [14].

## 1.2.6 Considerations from Literature for Performance Optimization

Upon reviewing the literature on wearable arrhythmia detection, studies highlight several key factors influencing device effectiveness. Many research papers emphasize the importance of data quality in arrhythmia detection (e.g., sensitivity and specificity), with some suggesting that 500 Hz sampling frequency strikes a balance between data accuracy and power consumption [9]. However, studies also note challenges related to false positives and false negatives, especially when dealing with noisy or incomplete datasets [5]. Therefore, it is crucial that the system's design includes algorithms to mitigate these issues, optimizing performance while maintaining user-friendly operation.

Table 1: Summary of Design Inputs for the Wearable Arrhythmia Detection Device

<b>Functional Requirements</b>	<ul style="list-style-type: none"> <li>- Real-time arrhythmia prediction</li> <li>- Battery life: 24 hours</li> <li>- Sampling rate: 250-500 Hz</li> <li>- Manage time delays and data storage.</li> </ul>
<b>Performance Requirements</b>	<ul style="list-style-type: none"> <li>- Sensitivity: <math>\geq 90\%</math>, Specificity: <math>\geq 90\%</math> in trials</li> <li>- Simulate ECG data at <math>\sim 250</math> Hz.</li> </ul>
<b>Interface Requirements</b>	<ul style="list-style-type: none"> <li>- Power on/off for battery optimization</li> <li>- USB Type-C charging</li> <li>- User-friendly prediction alerts.</li> </ul>
<b>Physical Requirements</b>	<ul style="list-style-type: none"> <li>- Size <math>\leq 5</math> cm diameter</li> <li>- Hypoallergenic silicone casing</li> <li>- IPX7 water resistance</li> <li>- Cost <math>\leq \\$1000</math>.</li> </ul>
<b>Environmental Considerations</b>	<ul style="list-style-type: none"> <li>- Use eco-friendly, recyclable materials.</li> </ul>
<b>Literature Review Considerations</b>	<ul style="list-style-type: none"> <li>- Focus on data quality and noise management.</li> <li>- Mitigate false positives and negatives.</li> </ul>

## 1.3 Design Process: Approach to Building a Wearable Arrhythmia Monitoring Device

### 1.3.1 Signal Selection and Device Design: Choosing the Right Biosignals for Detection

Continuous monitoring of arrhythmias can be implemented either via an under-skin chip or a wearable device (Figure 1). The wearable option is generally considered more feasible due to its non-invasive nature and minimal concerns related to biocompatibility. While under-skin chips offer an advantage in terms of discreteness, they might raise issues regarding biocompatibility, device removal, and long-term safety, making wearables a more practical solution for this kind of application.

The most commonly used biosignal for arrhythmia detection is ECG (electrocardiogram), which is the gold standard for diagnosing arrhythmias in clinical settings [15,16]. ECG works by measuring the electrical activity of the heart, providing detailed insights into the heart's rhythm and electrical state. However, PPG (photoplethysmography) has recently gained traction as a complementary method for arrhythmia detection [17]. PPG measures blood volume changes in the microvascular bed of tissue, typically through the use of light sensors. When used in conjunction with ECG, PPG can offer additional information regarding vascular health and heart rate dynamics, thus providing a more complete picture of the heart's function, particularly for detecting conditions such as atrial fibrillation [18].

The location of the wearable device is influenced by the choice of biosignal. ECG requires a minimum of two sensors on different spots in the body, commonly near the ribcage for optimal signal capture. This placement is more suitable for detecting heart activity related to electrical conduction but requires careful consideration of device placement for comfort and convenience. On the other hand, PPG is more flexible in terms of sensor placement, with common sites including the earlobe, fingertip, and wrist[19]. These areas are easily accessible and minimally invasive, making them ideal for a wearable device.

A critical factor for device design is the convenience of signal detection, particularly if continuous monitoring is required. For example, if ECG signals are to be detected from the chest, the device may need to be placed in a way that makes it visible to the patient, especially for feedback purposes. This could result in the need for a wireless communication system running from the sensor placement to the feedback system, such as an LCD screen or vibration motor, which would be more complex to design. Alternatively, PPG-based devices could offer more freedom in terms of sensor placement (e.g., wristband-style), which could eliminate the need for complex communication systems across the body.

### 1.3.2 Feedback Mechanism and Integration Considerations: Providing Clear User Alerts

**Feedback Mechanism** For feedback when an arrhythmia is detected, an LCD screen is chosen to provide immediate, clear, and detailed information. While LCD screens can be bulkier than other feedback options, they allow the delivery of essential information, such as heart rate, the specific arrhythmia detected, and the time of occurrence. This approach ensures that the patient is promptly made aware of the issue and can access comprehensive details if needed. Given that older individuals may have difficulty feeling vibrations, vibrations will not be used in this design, and the device will rely solely on the LCD for feedback [121].

### 1.3.3 Data Processing and Algorithm Development: Advanced Methods for Arrhythmia Detection

**Data Processing and Algorithm Development** Assuming the tool has access to relevant signals, it should be equipped with the ability to utilize these signals as predictors for arrhythmia detection. The two most relevant types of models for this purpose are mathematical models and machine learning models. Both approaches offer high flexibility and customizability, but the key distinction lies in how they treat the data and the underlying signal relationships.

#### *Mathematical Models*

Mathematical models, such as statistical models, rely on domain knowledge of the signals and their relationship to the desired outcome (in this case, arrhythmia). These models are based on predetermined mathematical equations or heuristics that are designed to capture specific characteristics of the signals. For example, mathematical models might rely on the RR interval, QT interval, or other well-established metrics that correlate directly with arrhythmia events. While these models can be efficient, they often require in-depth knowledge of the biological processes and can struggle to generalize to new or unseen data. However, they are computationally efficient and easy to interpret, making them suitable for real-time, low-resource applications.

#### *Machine Learning Models*

In contrast, machine learning models do not require explicit knowledge of the signal's relationship to arrhythmia but instead learn patterns directly from the data. The choice of machine learning model depends on the complexity of the data and the specific task at hand. There are several types of machine learning models, each with distinct strengths and challenges: Some of which are:

- Network-based methods: These include neural networks, convolutional neural networks (CNNs), and recurrent neural networks (RNNs), which have demonstrated considerable

success in medical signal processing. Neural networks and CNNs can capture spatial hierarchies in data, while RNNs are well-suited for handling temporal sequences, such as ECG or PPG data. These models can be powerful, especially when the relationships between features are complex, but they are also computationally expensive, are prone to overfitting, and require large amounts of data for effective training [20].

- 
- Tree-based methods: such as decision trees and random forests. These are simpler than network-based models and less computationally expensive. Two additional advantages are interpretability, which makes them easier to validate, and resilience to overfitting due to their automatic feature-selection operation.
- Linear methods: such as logistic regression, lasso, and ridge regression. These models are the simplest and they happen to be the least powerful, but they're the most computationally efficient. Introducing an L1 or L2 penalty (a penalty imposed on increased number of features to encourage feature selection) greatly reduces overfitting.

Despite the variety of models available, their success is largely dependent on the data.

High-quality, well-labeled data is critical for training any model. In addition, for some models with temporal support, raw sequential data may be acceptable, but feature extraction from raw data often improves the model's performance. Features such as the RR interval, QT interval, and heart rate variability (HRV) are proven to be relevant for arrhythmia detection [21]. These features can be extracted either directly in the time domain or through frequency-domain methods.

### *Time Vs Change in State*

In designing an arrhythmia detection system, the model's focus could either be on the current state or the change in state over a given time period. For instance, the current RR interval may provide useful information for detecting arrhythmias, but the change in RR interval over the last 5 seconds may be even more predictive in certain cases, especially when detecting transient arrhythmias. Therefore, models that capture dynamic changes in the signal over time, such as RNNs, might be more effective than those relying on static values.

### *Frequency Domain Approaches*

In addition to time-domain analysis, frequency-domain methods, such as the Fourier Transform or wavelet transform, can offer significant insights into the cardiac state. Frequency-domain methods analyze how the frequency components of a signal change over time, which can reveal underlying rhythms or abnormalities that are not immediately obvious in the time domain. Differences between normal and arrhythmic states often become more apparent when looking at the frequency content of the signal. For example, a normal ECG signal might

exhibit strong, consistent peaks in the frequency domain corresponding to the heart rate, while an ECG of a patient with atrial fibrillation might show more erratic and less regular frequency components [20].

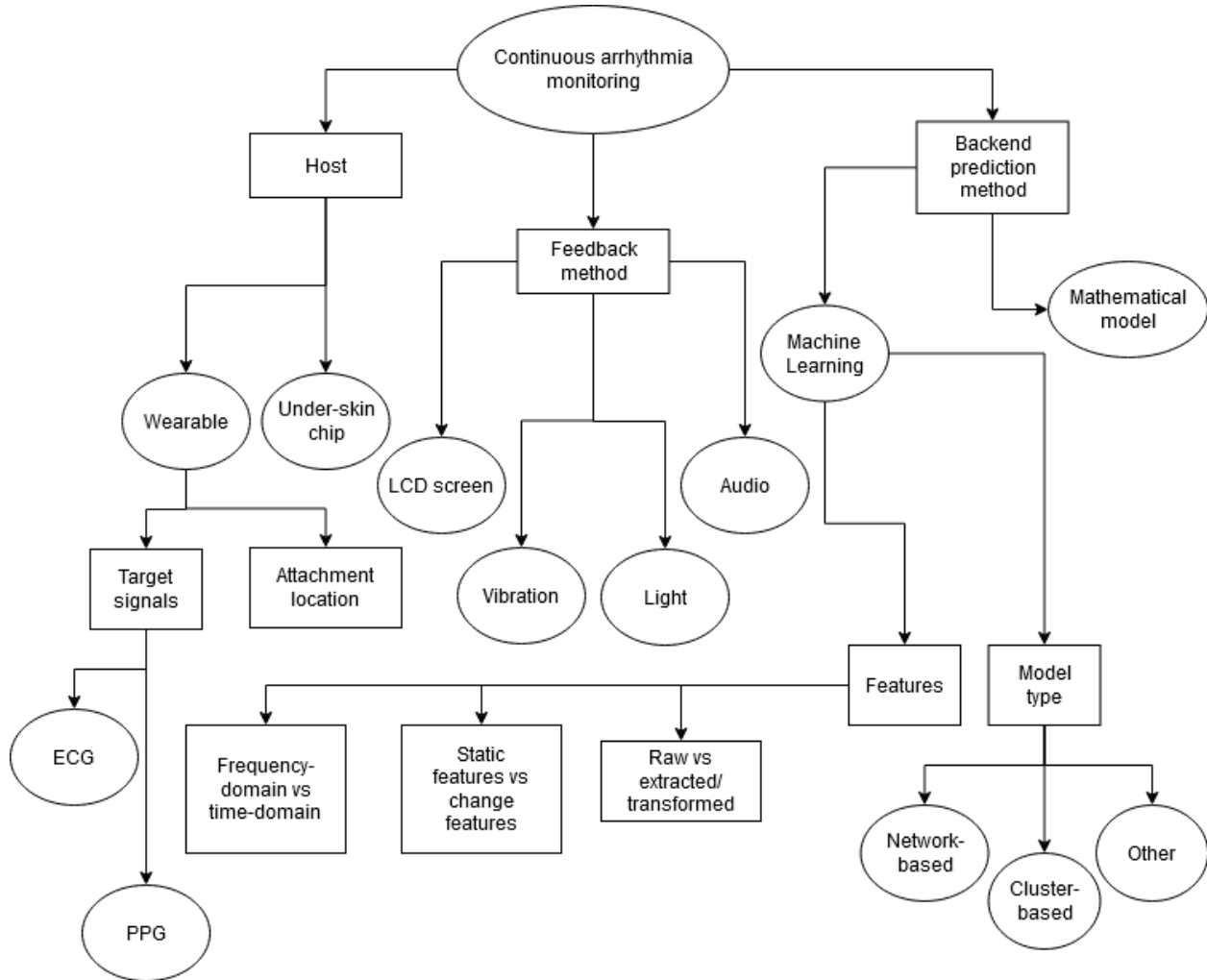


Figure 1: design decisions (rectangles) and potential choices (ellipses) to find a continuous arrhythmia monitoring solution according to the need statement.

### 1.3.4 Validating Feature Detection Methods

As seen in Figure 1, the design of a continuous arrhythmia monitoring solution involves multiple key decisions, each influencing the final implementation. One of the foundational assumptions of the design is that the backend software must be able to distinguish an arrhythmia from a normal signal, whether using ECG, PPG, or a combination of both. A well-thought-out approach is needed to translate raw biosignals into meaningful features that can be used for arrhythmia detection.

### Feature Extraction

To start the design process, we explored two methods for extracting relevant features from ECG signals. The first method involved using the SciPy package to detect peaks in the ECG signal, specifically identifying RR intervals. However, a challenge emerged with the time-domain peak detection method, as seen in Figure 2. Ideally, the RR interval should be consistent and smooth, but in practice, the method displayed spikes, indicating erratic measurements across different patients. This behavior could result from various factors such as noise, variability in patient data, or limitations of the detection algorithm.

To address this, further parameter tweaking and data scaling could help refine the results. However, this approach also highlighted the limitations of time-domain methods, particularly when applied to real-world, noisy ECG signals.

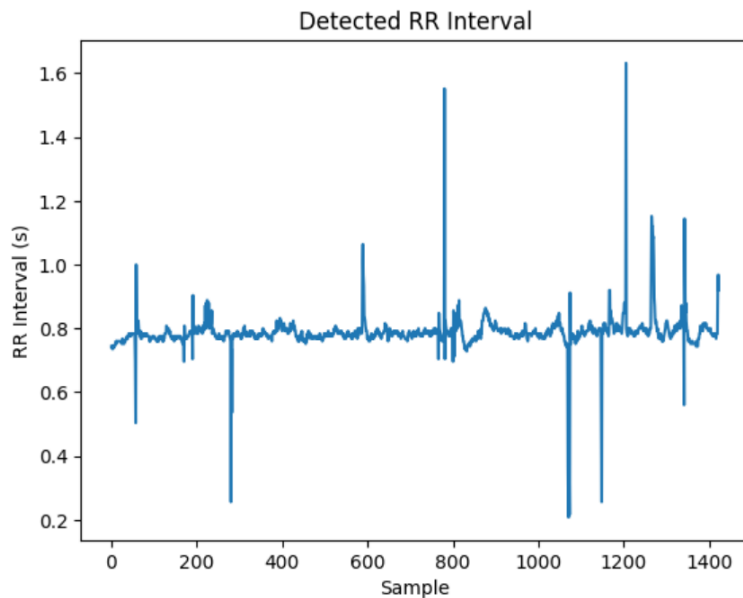


Figure 2: RR interval, as detected with the Python package SciPy [22]. A smooth line or curve would mean the measurements are consistent, otherwise either some ECG peaks are not getting detected (spike down) or false peaks are detected (spike up).

### Exploration of Frequency-Domain Methods

In response to the inconsistencies observed in time-domain analysis, we shifted focus to frequency-domain methods, which involve using techniques like the Fourier Transform to extract features from the signal. This approach can be particularly useful for detecting specific patterns and characteristics in the heart's rhythm, such as regularity and frequency components.

From the frequency-domain analysis, interesting insights were gained. Figure 3 illustrates the contrast between a healthy ECG signal and one exhibiting atrial fibrillation. The key observation here is that healthy ECG signals show distinct, regular peaks in the frequency domain, which correspond to the heart rate. In contrast, atrial fibrillation signals exhibit a less regular frequency pattern, with reduced prominence in the heart rate frequency range. This suggests that frequency-domain analysis may offer an effective way to distinguish between normal rhythms and arrhythmic events, particularly in conditions like atrial fibrillation.

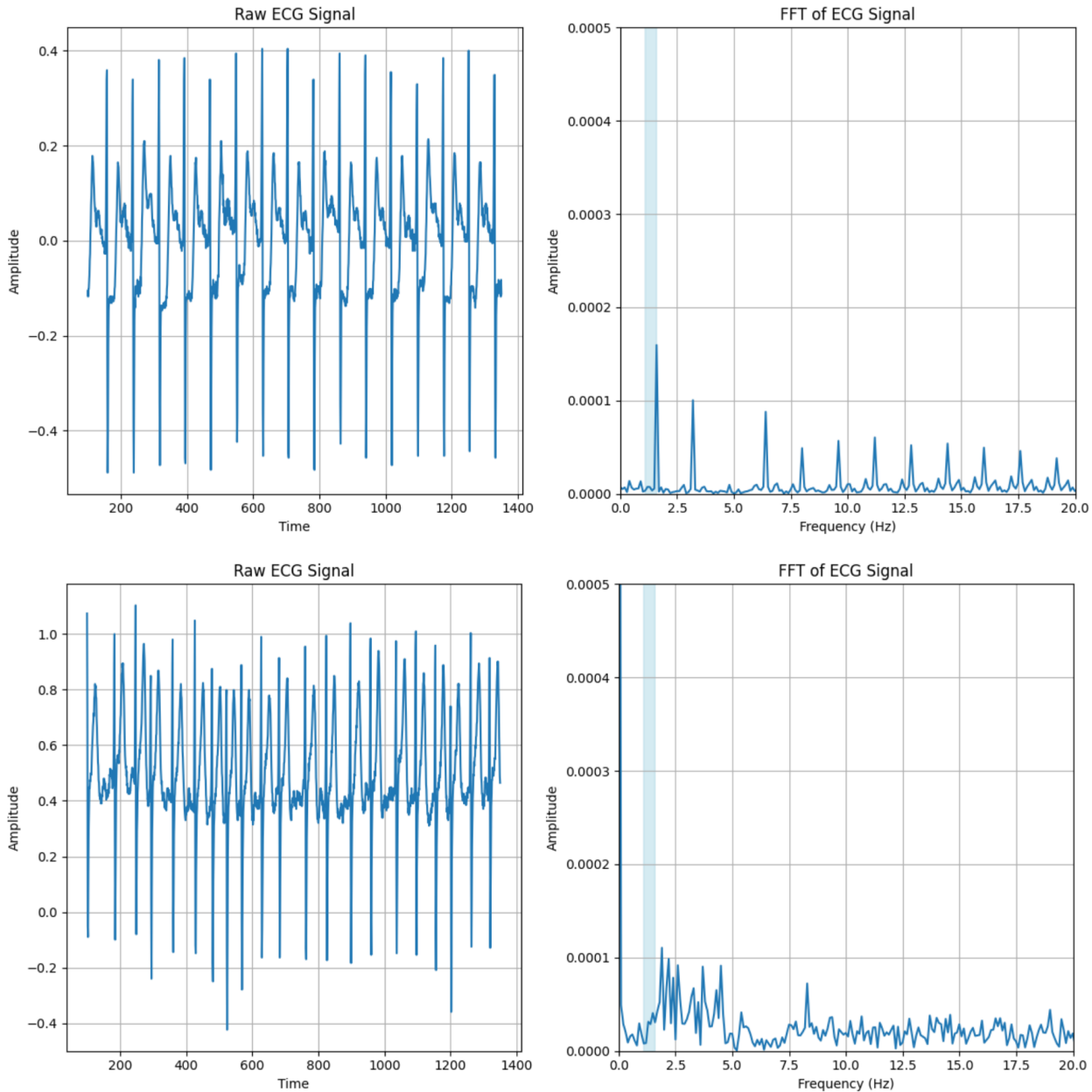


Figure 3: Top plots are healthy ECG, bottom plots are ECG signals of atrial fibrillation episodes. Left plots are the time-domain representation, right plots are frequency-domain (Fourier Transform) representation. Shaded region is the normal range for heart rate in Hz. Even though time-domain signals look fairly similar, the two signals can be distinguished easily through frequency-domain plots.

#### *Design Implications for Arrhythmia Detection*

These exploratory analyses have significant implications for the overall system design. First, they confirm that distinguishing between atrial fibrillation and normal heart rhythms is indeed feasible using ECG data alone, as long as appropriate feature extraction methods are employed. This discovery supports the decision to prioritize ECG as a primary signal for arrhythmia detection.

The next step in the design process will involve refining feature extraction techniques and evaluating the predictive power of additional biosignals, such as PPG. Although ECG has proven effective, the integration of PPG data could potentially enhance the system's robustness and accuracy by providing complementary information about heart function.

#### *Iterative Design and System Refinement*

As the design process evolves, ongoing adjustments will be made to improve signal processing algorithms, model selection, and overall system performance. The goal is to ensure that the arrhythmia detection system operates effectively in real-time, offering reliable predictions while minimizing false positives and negatives.

In conclusion, while the design decisions in Figure 1 remain under review, these initial simulations and analyses provide strong evidence that a continuous arrhythmia monitoring solution, based on ECG signals, is both practical and promising. Further refinement of the signal processing pipeline and model selection will be necessary to optimize the system for real-world use.

### 1.4 Preliminary Risk Assessment: Evaluating Health, Safety, and Ethical Implications for Wearable Technology

This preliminary risk assessment identifies and evaluates key health, safety, and ethical risks associated with the wearable device to ensure both user safety and regulatory compliance throughout its lifecycle.

#### 1.4.1 Health and Safety Risks: Evaluating Electrical, Battery, and Allergic Concerns

There are several health and safety risks for end-users associated with this device, including electrical hazards, potential battery malfunctions, and risks of skin irritation or allergic

reactions. Since the wearable device relies on sensors and electronics, users may be exposed to electrical risks, particularly if the components are vulnerable to water exposure. Moisture can lead to short circuits, resulting in electric shocks, device malfunctions, or even injuries [23]. Battery safety is crucial as well; wearables, especially flexible ones, are subjected to frequent physical stresses, which can heighten the chance of battery failure or even explosions [24]. These incidents can occur due to thermal runaway, a condition triggered by mechanical, electrochemical, or thermal abuse of the battery [24].

Silicone is commonly used in wearable device straps for its durability, flexibility, and biological inertness [25,26]. However, although rare, silicone allergies can still occur, leading to allergic contact dermatitis in some users [25, 26, 27]. Another critical safety concern involves the potential for incorrect diagnoses or false positives or negatives if the device fails to accurately interpret cardiac signals [28,29]. Issues such as poor electrocardiographic signal quality or false atrial fibrillation and tachycardia alerts may cause misinterpretation, leading to unnecessary medical referrals and tests [28]. Conversely, false negatives can falsely reassure the user, causing diagnostic delays and potentially serious health risks [29].

#### 1.4.2 Ethical Implications: Addressing Data Privacy, Security, and Inclusivity

With the collection of sensitive health data, this device raises ethical considerations about data privacy and security. Many wearable devices share user data with third-party apps and services, often without clear information on how this data will be used [30]. This ambiguity can lead to privacy concerns, as personal health information may be sold to advertisers or used for other purposes without the user's knowledge or consent [30]. Such practices compromise individual privacy, making it crucial to address these ethical concerns with transparency and proper user consent processes [30].

Data bias is another issue in wearable health devices, especially regarding accessibility and inclusivity for underrepresented groups or those with unique physiological characteristics [30]. Many wearables, like heart rate monitors and fitness trackers, may not perform equally across various skin tones or body types [30]. Devices that use light-based technologies, such as photoplethysmography (PPG), may have decreased accuracy on individuals with darker skin due to reduced light penetration [31]. This inconsistency in data accuracy can reinforce existing healthcare disparities if left unaddressed, emphasizing the need for inclusive and representative device design to ensure equal benefit across diverse populations [31].

#### 1.4.3 Standards and Regulatory Compliance: Ensuring Device Safety and Performance

Medical device standards, such as ISO 13485, IEC 60601, and ISO 14971, are essential for ensuring that health technology devices meet rigorous quality, safety, and

performance criteria. ISO 13485 is an international standard that specifies requirements for quality management systems in medical devices, addressing regulatory compliance throughout the device lifecycle, from design and development to production and post-market activities. It also includes provisions for evaluating and monitoring suppliers to ensure that all materials and components meet necessary safety and quality standards, making it a cornerstone for organizations that produce medical technology [32]. IEC 60601 outlines essential requirements for the safety and efficacy of medical electrical equipment. It is widely applied in the design and construction of devices used in clinical settings to ensure their safe operation. This standard covers device performance factors such as accuracy, reliability, and effectiveness and includes provisions for electromagnetic compatibility (EMC) to prevent devices from interfering with each other in environments with multiple electronic devices, like hospitals [33]. ISO 14971 establishes principles and a framework for the risk management of medical devices, including those with software components. It guides manufacturers in identifying and assessing device-related hazards, evaluating risks, implementing risk controls, and monitoring their effectiveness [34].

For data protection, PIPEDA (Personal Information Protection and Electronic Documents Act) is critical in Canada for devices collecting health information. Compliance with PIPEDA ensures that users' personal health data is collected, used, and shared responsibly, with transparency and consent. Additionally, users have rights to access, correct, and request deletion of their data, maintaining control over their personal information, thus safeguarding user privacy [35].

Non-compliance with these standards can have severe implications, including regulatory penalties, barriers to market entry, and increased liability in cases of device failure or malfunction, underscoring the importance of adherence for patient safety and organizational accountability [34].

## 2.1 Design Outputs and Verification Tools for Performance Assessment

It's crucial to have appropriate verification tools to guide the design process and ensure that the final prototype meets the appropriate standards and user requirements. The design inputs listed below address the key goals that the device must meet. The design outputs are verification tools that will be used later to assess whether the device met the respective design input's requirements.

Table 2: Key Design Requirements and Their Associated Verification Outputs

<b>Design Inputs</b>	<b>Design Outputs</b>
The device must have a long lasting battery life of 24 hours.	The device must comply with IEC 61960 standards for Secondary Lithium Cells and Batteries for Portable Applications to prove the battery's ability to continuously provide power under various circumstances [36]. The device must have a long battery life so the user can wear the device for long time periods which allows more data to be collected and analysed for diagnosis.
The device must achieve a minimum sensitivity and specificity of 90% for detection of heart arrhythmia.	<p>Sensitivity and specificity can be calculated using the equations below and the patient dataset which marks the presence/absence of arrhythmia for each individual.</p> $\text{Sensitivity} = \frac{\text{True Positives}}{\text{True Positives} + \text{False Negatives}}$ $\text{Specificity} = \frac{\text{True Negatives}}{\text{True Negatives} + \text{False Positives}}$ <p>True positive would be when the device correctly identifies heart arrhythmia. True negative would be when the device correctly identifies the absence of heart arrhythmia. False positive would be when the device concludes the individual has heart arrhythmia but they don't in reality. False negative would be when the device concludes that the individual doesn't have heart arrhythmia but they actually do [37].</p>
The sensors must have a sampling frequency greater than or equal to 300 Hz.	The Fast Fourier Transform (FFT) can be applied to the waveform to find the maximum frequency. Applying the Shannon Nyquist Theorem, the sampling frequency must be greater than or equal to twice the highest frequency that the device can measure [38]. The highest frequency in an ECG signal is 150 Hz [11]. After applying the FFT to the ECG signal, if a spike is found at 150 Hz then it can be concluded that the sampling frequency requirement is met. It's crucial to have an appropriate sampling frequency to avoid aliasing in the signal.
The device must be compatible with USB Type-C charging.	The wearable must have a USB Type C connector receptacle component that can be accessed externally. USB Type C connectors are used

	commonly across devices for charging and data transfer between devices. Having a USB Type C connector on the wearable will make it more compatible with other devices and allow for efficient charging.
The wearable must be small, noninvasive and compact.	The device must comply with the Medical Devices Regulations (SOR/98-282) definition of a Class I Medical Device from sections 10 to 20 to validate that the device is noninvasive [39]. The device is intended to be used independently by the user without any supervision so it must be noninvasive and easy to use as specified in the definition of Class I Medical Devices.
	The wearable must accommodate for circumferences from 10 cm to 25 cm which is the range of wrist sizes in adults [40]. The size of the wearable can be measured manually using a ruler. The wearable will be used by a variety of individuals of different sizes so it must be adjustable for all users' wrist sizes and comfortable.
The wearable enclosure must be made of a durable and hypoallergenic material.	Verify Human Repeated Insult Patch Test (HRIPT) results on all materials used in the casing which will assess if the materials can pose allergies [41]. The wearable will be used for long time periods regularly by the user so it shouldn't trigger any allergic reactions that would cause the user to discontinue its usage.
The device should be able to withstand scratches. The device must survive falls and should remain functional.	Successful scratch test results based on the ASTM D7027/ISO 19252 standards on materials used in the wearable casing [42]. Since the user will be wearing the device for long time periods regularly, the device may be handled roughly by accident. The device should be able to withstand the slight rough handling and still be functional.
	Successful test results from Drop and Shock testing according to MIL-STD-810G [43]. The device will be dropped 10 times from a height of 168.27 cm after which the device must still be functional. The average height of adults in Canada from ages 60 to 79 is 165.32 cm so this height will account for patient falls with the

	wearable as well as accidental dropping of the wearable.
The device must have a water resistance rating of at least IPX7.	Successful results from a 1 metre water submersion test of the final device for 30 minutes [44]. While the device is not intended to be used while engaging with water, it's possible that light splashes can occur while washing hands for example or rain can come in contact with the device. The device must be able to survive these mild contact scenarios with water and still remain functional.
The total cost of materials must not exceed \$1000.	A bill of materials must be produced breaking down the cost of the materials used to make the wearable. The total cost of materials must not exceed \$1000.
The device response rate must not exceed 5 seconds.	Successful results from performance testing of the device under different scenarios (e.g. presence/absence of arrhythmia) where the device responds in less than 5 seconds and the software doesn't freeze in an infinite wait state [45]. Users tend to lose attention or become disinterested once a software takes more than 5 seconds to respond. Thus to make the device easy to use and satisfactory for users its response rate must be reasonable. It's also important to have a quick response rate to have the effect of real time data collection and feedback response effect on the user.
The device must provide feedback to the user regarding the absence/presence of arrhythmia.	The device must provide auditory, visual and haptic feedback to the user to inform if they have arrhythmia or not. The target population of elderly happen to have poor vision and hearing. Thus, by providing notifications with a combination of sensory alerts the user is more likely to be made aware of their diagnosis.

## 2.2 Final Decision Concept: Balancing Affordability, Accuracy, and Usability

The final decision for the RhythmGuard design concept balances affordability, accuracy, and usability, addressing the identified problem and aligning with project objectives. This section outlines the chosen design, its practical implementation, and the rationale behind the decision.

### 2.2.1 Final Design Overview: System Architecture and Features

The system integrates real-time health monitoring capabilities to detect and classify arrhythmias using a combination of ECG (single-lead) and PPG signal processing. The device features the following:

- TinyML-based algorithms trained on medical datasets like MIMIC, enabling on-device processing.
- Real-time alerts delivered to users via an integrated LCD screen.
- Power-efficient design to ensure continuous monitoring.
- Compact, user-friendly form factor meeting regulatory standards for medical devices.

By combining wearable technology with machine learning, the design provides a portable and non-invasive solution for arrhythmia detection.

### 2.2.2 Final Design Concept Justification: Ensuring Performance and Compliance

Accuracy of Arrhythmia Detection: Achieving High Sensitivity and Specificity

**Output Requirement:** Accuracy  $\geq 90\%$

The accuracy of arrhythmia detection is crucial for the effectiveness of the device. A high sensitivity ensures that arrhythmias are detected when they are present (reducing false negatives), while high specificity ensures that healthy rhythms are not mistakenly identified as arrhythmias (reducing false positives) [46].

The wearable will employ a TinyML-based algorithm that processes ECG and PPG signals directly on the device. The algorithm will be trained on the Clifford et al. Computing in Cardiology Challenge 2015 dataset, and the Charlton et al. MIMIC PERform AF dataset [78, 79] to ensure robust detection capabilities across various arrhythmia types. Advanced signal processing techniques, including noise filtering and feature extraction from the QRS complex, P wave, and T wave, will be implemented to further enhance detection accuracy. Additionally, integrating real-time data processing and employing hybrid sensing approaches (PPG and ECG) will ensure the device meets high-performance requirements while maintaining reliability in diverse real-world conditions. A methodology similar to the one employed by Sun et al. [48] in their research on using ECG and PPG signals for blood pressure estimation in wearable devices will be employed. This approach leverages the synergy between these biosignals to extract relevant features and apply them within a predictive framework, ensuring the device's effectiveness and reliability within the project's scope [48].

A study that was aimed to evaluate the sensitivity and specificity of wearable devices for atrial fibrillation detection in older adults has demonstrated that a combination of PPG and single-lead ECG achieves high accuracy, with sensitivity and specificity often exceeding 95%, particularly when advanced machine learning techniques, such as Deep Neural Networks (DNNs), are utilized. For example, algorithms trained on R-R intervals and PPG waveforms have achieved sensitivity of 97.6% and specificity of 96.5% [49].

Within the scope of the project, the device will aim to achieve a minimum specificity and sensitivity of 90%. This baseline ensures reliable arrhythmia detection, with a reduced likelihood of false positives (high specificity) and false negatives (high sensitivity). While the ultimate goal for medical-grade devices might be even higher accuracy, this level is practical and achievable given the constraints of the project.

### Real-Time Processing: Optimizing Speed and Efficiency

**Output Requirement:** Device response  $\leq$  5 seconds

Real-time feedback is crucial for arrhythmia detection, as early intervention can significantly improve health outcomes. The device will process signals on the wearable in real time, using optimized TinyML models that perform FFT to extract key features. The device's microcontroller capability and power efficiency will be considered to ensure that the system meets the response time requirement without exceeding the device's memory and computational constraints. The optimization of both hardware and software ensures that the device can offer timely alerts to the user for immediate action.

The study by Haque et al. demonstrates the effectiveness of using FFT for extracting features from ECG signals, particularly in identifying abnormalities that are challenging to detect through conventional graphical methods [50]. This was also observed during exploration of waveforms from the Charlton et al. dataset, where we examined FFT representations of normal sinus rhythm and atrial fibrillation (Figure 4). Additionally, Sun et al. propose innovative hardware/software collaborative techniques to accelerate TinyML inference on microcontrollers, achieving up to a 71% reduction in inference latency without compromising model accuracy or size. Inspired by the techniques outlined by their work, this project incorporates architecture- and application-aware optimizations to enhance the efficiency of machine learning inference for health monitoring applications, particularly focusing on wearable devices leveraging PPG and ECG signals [51].

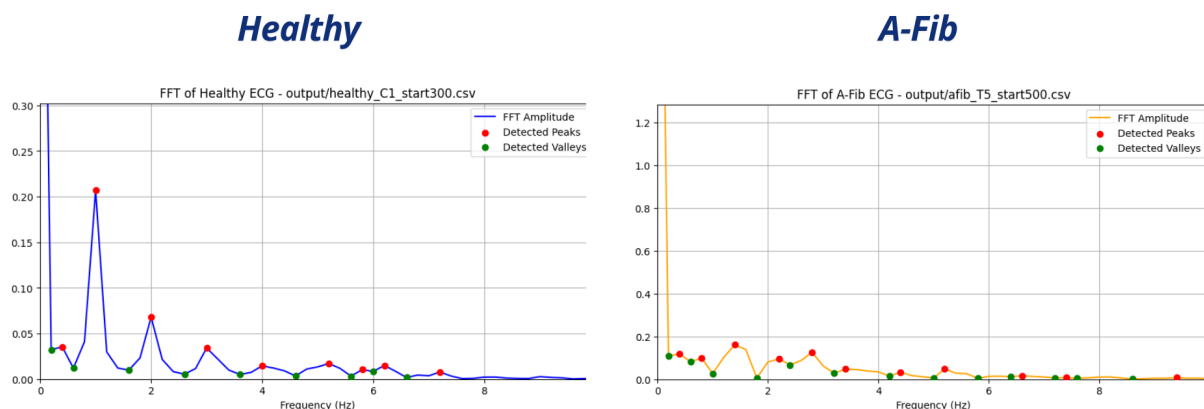


Figure 4: FFT of a healthy sinus rhythm (left) compared to an atrial fibrillation ECG (right) in waveforms from the Charlton et al. dataset.

The fact that the wearable device's processor has a single core imposes a time constraint, which is that the data processing (including FFT and prediction) must have a shorter execution time than the available time between sample collections. In other words:

$$e_p \leq P_s - e_s$$

Where  $e_p$  is the processing execution time,  $e_s$  is the sampling execution time, and  $P_s$  is the sampling period. Figure 2 shows a schedule that meets the time constraint (Schedule A) and a schedule that doesn't (Schedule B). Since the FFT is expected to have a substantial execution time, this time constraint will be tested within the prototype.

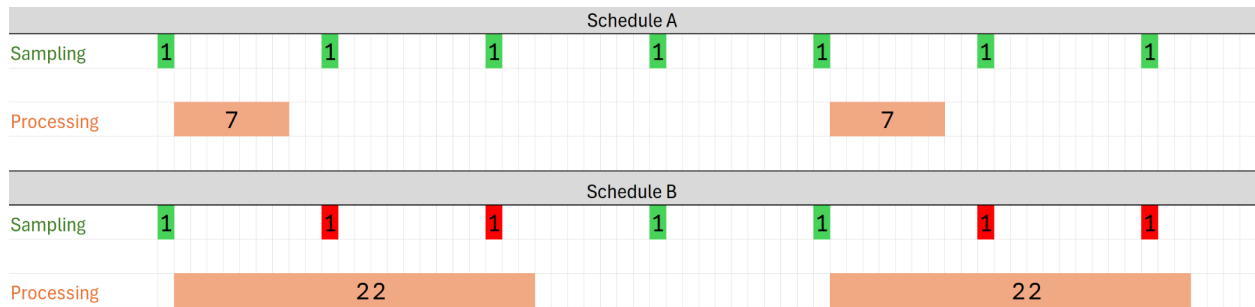


Figure 5: time constraints of data processing on the wearable. Schedule A shows a schedule that meets the time constraints, where processing ends before the next sampling point is acquired. If processing, including FFT calculation, takes longer than the time between sampling actions (Schedule B), some samples will either be skipped or delayed, the former case compromising accuracy and the latter case causing a continuously increasing lag.

## Compliance with Medical Device Regulations: Adhering to Safety Standards

**Output Requirement:** Compliance with Medical Devices Regulations (SOR/98-282) for Class I devices.

The device will be developed to align with the Medical Devices Regulations (SOR/98-282) as much as possible, which would ensure that it is classified as a Class I medical device [52]. This classification would confirm the device meets the necessary safety standards for non-invasive health monitoring technology and supports its potential for clinical-grade applications. However, given the time constraints and limited resources for the project, the device aims to achieve the best possible results within the project timeline while maintaining a focus on safety, functionality, and reliability. While all components, from sensors to communication systems, will strive to comply with international standards for medical devices, the project's scope may not fully encompass the comprehensive testing and certification required for market-ready clinical devices.

### 2.2.3 Final Design Concept Analysis: Evaluating Algorithmic Performance and Inference Efficiency

#### Algorithmic Accuracy: Evaluating Sensitivity, Specificity, and Generalizability

The performance of the TinyML model will be evaluated using the Clifford et al. Computing in Cardiology Challenge 2015 dataset [78] and the Charlton et al. MIMIC PERform AF dataset [79], specifically focusing on its sensitivity and specificity in detecting arrhythmias. Cross-validation will be employed to assess the model's generalizability and ensure it performs consistently across different subsets of the dataset. This process will help evaluate how well the model can classify unseen data, ensuring it does not overfit to the training set, as well as to eliminate the effect of randomness. Test set size was 20% while the remaining 80% was for training..

The confusion matrix will be utilized to assess the model's classification performance. The matrix provides a summary of the predictions made by the model and compares them to the actual outcomes, allowing us to quantify the number of true positives, false positives, true negatives, and false negatives. The following metrics will be derived from the confusion matrix:

$$\text{Sensitivity (True Positive Rate)} = \frac{\text{True Positives}}{\text{True Positives} + \text{False Negatives}}$$

$$\text{Specificity (True Negative Rate)} = \frac{\text{True Negatives}}{\text{True Negatives} + \text{False Positives}}$$

Minimizing both false positives and false negatives is critical for the clinical effectiveness of the model. These metrics are essential for ensuring that the model accurately identifies arrhythmias while minimizing the risks associated with misclassifications. The equations provided above were referenced from the Diagnostic Testing Accuracy study conducted at the University of Louisville [53].

To measure the inference performance of the TinyML model, a timer will be implemented in the code to calculate the time taken for each inference. This data will help evaluate whether the device meets the

response time requirement of 5 seconds or less. Additionally, the accuracy metric was used to assess model's predictive performance::

$$\text{Accuracy} = \frac{1}{n_{samples}} \sum_{i=0}^{n_{samples}-1} 1(\hat{y}_i = y_i)$$

Where  $1(x)$  is the indicator function (1 if  $x$  is true, 0 otherwise), and  $n_{samples}$  is the number of samples being predicted.

These evaluations will help ensure the device meets the project's goals for real-time performance and reliable arrhythmia detection. Alternative techniques such as the machine learning-based technique suggested by Brun and Ernst in their research to identify properties in program code that may lead to errors will also be considered [54].

#### Signal Sampling and Filtering: Optimizing ECG Signal Accuracy

To ensure accurate ECG signal analysis in wearable devices, the project incorporates best practices for filtering as outlined in GE HealthCare's guide, including the use of low-pass filters for frequency-based noise reduction and power-line filters to address electrical interference from the environment [55]. The device will capture ECG signals at  $\geq 300$  Hz, which satisfies the Nyquist sampling theorem criterion [3, 4, 22]. The FFT will be applied to identify relevant frequency components, such as heart rate frequency, to detect arrhythmia. The low-pass and high-pass filters will be implemented to remove noise outside the relevant frequency band (0.5–50 Hz). This ensures that the processed signal retains the key characteristics needed for accurate arrhythmia detection.

#### Criteria:

- Maximum ECG frequency ( $f_{max}$ ):  $\sim 150$  Hz [11].
- Sampling frequency ( $f_s$ ):  $f_s > 2 \times f_{max}$  (Nyquist criterion).
- Sampling frequency set at 512 Hz to ensure fidelity.
- **Filtering:** Low-pass and high-pass filters will be applied to remove noise outside the relevant frequency band (0.5–50 Hz). In addition to optional smoothing filters that preserve features like peaks and valleys such as the Savitzky-Golay filter as suggested in the following article [57].

#### Wearable Design: Size, Comfort, and Material Selection for Continuous Monitoring

The MAXREFDES104 Health Sensor Platform 3.0 [58] was selected as it features a collection of small, integrated components that are essential for monitoring health metrics in a compact form. This platform is designed with size efficiency in mind. The components in the MAXREFDES104 are designed to be small and lightweight, making it easier to integrate into a wearable device that can be worn continuously without discomfort.

Since the MAXREFDES104 Health Sensor Platform 3.0 is being utilized, and already includes components with a compact form factor and integrated features, tests will not be conducted for size or water resistance in the scope of the project.

#### Battery Life Considerations: Ensuring 24-Hour Continuous Monitoring

The ideal desired battery life would be a minimum of 24-hours to enable continuous monitoring. However, since the project utilizes a pre-existing device with a Li-Po 105mAh battery rather than designing a new wearable from scratch, considerations such as battery life are beyond the scope of this project. Thus, additional design and testing related to these aspects will not be undertaken in this project.

#### Power Consumption Optimization: Enhancing Energy Efficiency for Extended Device Operation

Power consumption will be optimized through the use of energy-efficient algorithms. The software will incorporate techniques such as low-power state management, computational optimizations, and model quantization to minimize processing requirements. One common approach, as discussed in research such as the work of Mohd et al. highlights the effectiveness of reducing model size and computational complexity to lower power consumption. The algorithms will be designed to perform necessary tasks with minimal computational overhead, thus reducing the overall energy consumption of the system [59]. Furthermore, the TinyML models will be specifically optimized for low-power microcontrollers, ensuring that the device can operate efficiently over extended periods without significant battery drain.

#### Real-Time Feedback Mechanism and Data Privacy: Ensuring User Interaction and Security

The wearable device will feature a separate LCD screen component for displaying real-time data. Since direct access to the device via wires is not feasible, bluetooth will be implemented as a practical necessity, but it is not part of the project's long-term concept. Data storage will remain exclusively on the device, eliminating the need for cloud integration, encryption, or external data transfer, ensuring simplicity and user privacy within the project's scope.

While our current implementation is focused on these localized features, we envision potential future iterations with advanced functionalities. These could include integrating and embedding the LCD screen onto the wearable (similar to smart watches), embedding the wearable into other healthcare systems, secure Bluetooth communication or WiFi connection with caregivers or doctors, and the use of robust encryption protocols to protect sensitive health data during transmission. Other feedback mechanisms such as a small vibrating motor or buzzer also show potential for real-time feedback which can be customizable for the individual patient's needs. However, such features are beyond the current project's scope and will not be addressed in this development cycle.

## 2.2.4 Assumptions, Limitations, and Constraints of Design Implementation

### Assumptions: Defining Usage and Operational Guidelines

- The wearable device will be used primarily by individuals in non-clinical settings for screening rather than diagnostic purposes. This implies that while the device will provide critical arrhythmia detection, it will not replace a healthcare professional's diagnosis.
- Users will need to follow instructions carefully for proper sensor placement and device operation to ensure the most accurate readings.
- Users will need to follow provided instructions regarding disposal of electronic waste or send back the device for proper handling and recycling of the components.

### Limitations: Identifying Constraints on Detection and Data

- Single-Lead ECG: The RhythmGuard device uses a single-lead ECG, which has limitations compared to multi-lead systems in detecting certain arrhythmias. For example, atrial fibrillation and other complex arrhythmias might be better detected with more leads. This is a trade-off between design simplicity, cost, and diagnostic accuracy.
- Training Data Limitations: The performance of the TinyML model relies heavily on the quality and variety of the training data (e.g., MIMIC dataset). Any inherent biases or data gaps in the training dataset could affect the model's accuracy and the generalizability to new patients or arrhythmia types.

### Constraints: Addressing Hardware and Battery Limitations

- Real-Time Processing: The wearable's real-time processing capabilities are constrained by the microcontroller's memory and computational power. This necessitates the optimization of algorithms (e.g., FFT, feature extraction) to ensure that they fit within the device's hardware limits while providing accurate and timely arrhythmia detection.
- Battery Capacity: The need to balance power consumption with continuous and accurate monitoring requires careful selection of components and algorithms.

## 2.3 Final Decision: Risk and Compliance Management Plan

### 2.3.1 Scope of Risk Management Activities in the Project Lifecycle

A comprehensive risk management strategy will be applied across the project's lifecycle, guided by the Failure Modes and Effect Analysis (FMEA). Table 2 outlines identified risks, their potential impacts, and mitigation strategies. Health and safety considerations include; accuracy and reliability, electrical Safety, quality Assurance, and user safety alerts.

*Limitations, Constraints, and Assumptions*

The risk management strategy assumes that the device will adhere to medical standards and will be used under typical conditions as outlined in the scope. The project assumes the availability of diverse data for testing, though real-world testing across diverse user populations may be limited during the prototyping phase.

### 2.3.2 Responsibility, Authorities, and Stakeholder Roles in Risk Management

Risk Management responsibilities are distributed as follows

- Engineering Team: Responsible for conducting FMEA, implementing mitigations, and ensuring compliance with technical safety standards
- Quality Assurance Team: Oversees testing, defect prevention, and manufacturing quality controls
- Compliance officer: Ensures adherence to ISO 13485, ISO/IEC 23894, ISO14001, IEC 60601-1-11[26, 27, 28, 29]

### 2.3.3 Criteria for Accepting and Managing Risks in Medical Device Development

The criteria for acceptable risk are based on the manufacturer's policy for determining acceptable residual risk, including [64]:

When determining the acceptability of risks associated with medical devices, the FDA conducts a benefit-risk assessment, where events such as recalls, new safety information, or device nonconformities may prompt regulatory actions [64]. These assessments evaluate both benefits and risks to inform decisions on product availability, compliance, and enforcement [64].

Relevant benefit factors will be reviewed such as clinical studies, patient input, device performance data, and comparative advantages over existing treatments [64]. The severity and likelihood of potential adverse effects will be considered, using data from sources such as medical device reports, inspection findings, and clinical feedback. Risk mitigation measures proposed by the manufacturer are also reviewed.

Additional factors, such as patient tolerance for risk, device alternatives, public health impact, and the urgency of addressing a health need, are integrated into the assessment. The outcome of the benefit-risk assessment informs decision making, which may include granting variances, allowing continued use of a nonconforming device during shortages, or taking compliance actions. High-benefit, low-risk scenarios may justify maintaining device availability, while low-benefit, high-risk scenarios are likely to prompt stricter actions [64].

### 2.3.4 Risk Identification, Analysis, and Evaluation Process

Table 3: FMEA Table [31, 32]

<b>Function</b>	<b>Failure</b>	<b>Effects of</b>	<b>(S)</b>	<b>Causes of Failure</b>	<b>(O)</b>	<b>(D)</b>	<b>RPN</b>	<b>Mitigation</b>
-----------------	----------------	-------------------	------------	--------------------------	------------	------------	------------	-------------------

	<b>Mode</b>	<b>Failure</b>						
ECG/PPG Sensors	Inaccurate arrhythmia detection	Missed diagnoses or false alarms	10	Sensor inaccuracies, movements, poor placement, poor electrode contact, interference	6	5	300	Validate with diverse real-world testing, and optimize the tinyML algorithm to account for inaccuracies in the model
TinyML Algorithm	Delayed arrhythmia detection, Inaccurate arrhythmia detection	Late/no medical intervention or false alarms	10	Low computational speed, poor optimization, or sampling, false positives/negatives, machine learning model limitations, bad choice of predictors	5	4	200	Optimize algorithm for efficiency, increase training data, avoid overfitting, and evaluate and tune models using cross-validation, and perform feature selection and elimination
Battery	Device stops functioning/electrical shock	Device stops functioning, harm to user	9	High current draw, faulty battery, circuit malfunction, poor insulation	4	3	108	Use low-voltage ICs and design, optimize power consumption, warning for battery levels
Device Firmware	Crashes	Device failure during critical time	9	Software bug	4	4	144	Conduct rigorous software testing and provide a factory reset option and alert the user of failure
Manufacturing	Defective product	Unpredictable malfunctions ranging from false data to complete failure	9	Poor quality control	5	4	180	Implement strict quality assurance
Enclosure	Breakage or water leak	Damage to internal components/	9	Improper material, design or assembly	5	4	180	Use robust material, redesign to be waterproof

		electrical shock, harm to user						
Electronic waste	Environmental hazards	Public health risk from improper disposal	7	Use of non-recyclable materials, electronic components	4	6	168	Educate users on proper disposal of electronic waste, and provide the option of sending back old devices for disassembly and reuse of parts
User error	Improper user operation, overreliance	Ineffective monitoring, delayed medical intervention	9	Poor user training, unclear instructions, user overestimated device capabilities	5	6	270	Provide clear instructional manuals and include warnings and disclaimers emphasizing the use of the device as a supplemental tool

### 2.3.5 Mitigation Strategies and Control Measures for Identified Risks

To address health and safety risks associated with this project, a comprehensive strategy will be implemented across all the developmental phases. During the implementation phase, the TinyML algorithm will use diverse datasets and real-world testing to ensure accuracy and reliability, while complying with medical standards like ISO/IEC 23894 [61]. In the prototyping phase, electrical safety will be prioritized by using low-voltage designs, insulated wiring, and insulated enclosures. Basic biocompatibility will be considered by selecting appropriate electrode materials, though extensive long-term wearability testing is beyond the current scope. For validation, the device will undergo testing to ensure functionality, however extensive testing with a diverse population to confirm performance consistency will be addressed in future phases. Manufacturing processes involving rigorous quality assurance and environmental responsibility measures, such as partnering with certified manufacturers, are critical for final production, they exceed the scope of this prototyping phase. During deployment, user-friendly training materials will be used to integrate safety alerts for issues like low battery, or improper sensor placement, and ensure that the device is used to supplement professional medical care rather than replace it.

2.3.6 Verification and Testing of Risk Control Measures  
Reviewing training materials to ensure users are well-informed about device operation and limitations [67].

- Testing and validation with diverse user populations to ensure performance consistency is beyond the scope of this project, and testing for the prototyping phase will mainly use open source datasets.
- Monitoring compliance with safety and environmental standards during prototyping and manufacturing will be critical for future phases and is not included within the current scope.
- 

### 2.3.7 Comprehensive Evaluation of Residual Risks and Their Impact

The overall residual risk of the device will be assessed using the following components:

1. Cumulative Risk Priority Numbers (RPNs): Residual risks identified during the FMEA will be quantified using RPNs. This assessment helps prioritize risks based on their severity, occurrence, and detectability, ensuring a systematic evaluation.
2. Cross-Functional Review: A multidisciplinary team will review the residual risks to ensure they are acceptable when weighed against the anticipated benefits of the device.
3. Iterative Testing and Stakeholder Feedback: Continuous testing during development and post-market surveillance will be conducted to monitor long-term safety and reliability. Input from stakeholders, including clinicians and patients, will provide insights into emerging risks.

The residual risk will only be deemed acceptable when the device's benefits substantially outweigh the identified risks, and appropriate mitigations are implemented to minimize any potential harm.

### 2.3.8 Ethical, Safety, and Environmental Considerations in Risk Management

#### *Informed Consent and Transparency in Device Use*

The ethical foundation of the wearable device is built on ensuring that users are fully informed about its capabilities, limitations, and potential risks. Prior to using the device, all users will be required to provide explicit, informed consent, which will be facilitated through a comprehensive consent process. This process will clearly explain that the device is not a substitute for professional medical evaluation, nor should it be relied upon for diagnostic purposes without professional consultation. Additionally, users will be made aware of the types of data being collected, such as ECG and PPG signals, and how this data will be used in the context of arrhythmia detection. Transparency about the potential risks of data bias and the limitations of the system is essential, as there may be instances where the device's algorithm may fail to detect arrhythmias or provide inaccurate feedback.

To further emphasize transparency, the device will include easy-to-understand user guides and consent forms that explain:

- The device's intended use and scope of application.
- Potential system limitations, including false positives or false negatives in arrhythmia detection.
- The possibility of bias in the machine learning models, particularly if certain demographics or health conditions are underrepresented in the training data.
- The storage, processing, and sharing of personal health data, ensuring that users are aware of their privacy rights and data protection measures.

This thorough informed consent process allows users to make a conscious, educated decision about whether to use the device, and ensures that they understand the balance between the benefits of early arrhythmia detection and the risks inherent in using a machine-learning-based tool for health monitoring [68].

#### *Ensuring Safety and Compliance with Medical Standards*

Ensuring the safety of users is paramount in the development of any wearable medical device. The device must meet the highest standards of safety and reliability, particularly when it comes to the risk of malfunctions that could compromise health outcomes. Risks include issues such as inaccurate arrhythmia detection, delayed or failed alerts, or faulty device performance that could lead to incorrect diagnoses or missed medical events. Additionally, there are electrical safety concerns related to faulty wiring, malfunctioning batteries, or substandard insulation, all of which can lead to electric shock, burns, or other hazards.

To mitigate these risks, the device will undergo rigorous testing under a variety of conditions to ensure its functionality, reliability, and safety across different environments (e.g., temperature, humidity, and mechanical stress). In addition to functionality testing, it will also be subjected to tests designed to validate electrical safety, ensuring that the device complies with international standards such as ISO 13485 (Quality Management Systems for medical devices) and IEC 60601-1 (standard for electrical safety in medical devices). These standards outline the requirements for medical devices to be safe, effective, and reliable. Specific focus will be placed on ensuring that the device's power circuitry operates within low-voltage, non-hazardous ranges to protect the user from electrical risks.

Adhering to these standards will ensure that the device:

- Is safe for prolonged wear.
- Delivers accurate, timely arrhythmia detection without undue risk of malfunctions.
- Meets electrical safety regulations, reducing the possibility of electrical hazards [63, 26, 29].

These safety measures are vital for ensuring the device not only provides value to users but also adheres to the necessary legal and regulatory frameworks to protect user well-being.

#### *Managing Algorithmic Fairness and Minimizing Bias*

The integration of machine learning algorithms in the device introduces the potential risk of algorithmic bias, which can affect the accuracy and fairness of health-related predictions. Machine

learning models can inadvertently perpetuate biases if they are trained on datasets that lack diversity, or if the data collection process itself is skewed by demographic or socio-economic factors. For example, if the training dataset does not adequately represent certain ethnic groups or individuals with specific health conditions, the algorithm may have reduced efficacy for those populations, leading to unequal health outcomes.

To prevent such biases, the AI models will be trained on a diverse dataset that reflects a wide range of ages, genders, ethnicities, and health conditions. Special attention will be given to ensuring that underrepresented groups are adequately represented, using techniques such as oversampling underrepresented categories, generating synthetic data, and ensuring diversity in clinical trial participants.

Furthermore, the algorithm's performance will be regularly evaluated and monitored to ensure that no group is unfairly disadvantaged. The development process will adhere to ISO/IEC 23894:2023, which provides guidelines for managing risks associated with AI systems in medical devices. This standard emphasizes the importance of ongoing risk assessments, accountability, and transparency in algorithm development, requiring developers to:

- Conduct fairness audits and risk assessments.
- Integrate procedures for mitigating biases throughout the AI development lifecycle.
- Use feedback loops to monitor real-world performance and correct any emerging biases.

Incorporating these measures into the design and development process ensures that the AI system is fair, equitable, and capable of delivering reliable health insights to all users, regardless of their demographic background [68, 61].

#### *Environmental Responsibility and Sustainability in Production*

As electronic waste (e-waste) becomes a growing global concern, the development of wearable devices must consider environmental sustainability from the outset. The production of wearables often involves the use of non-recyclable materials, hazardous substances like lead and mercury, and batteries that contribute significantly to environmental pollution if not disposed of responsibly. Addressing these issues is not only an ethical obligation but also an opportunity to create a product that aligns with broader environmental sustainability goals.

To minimize the environmental impact of the wearable device, the design will prioritize the use of eco-friendly materials, such as biodegradable plastics or recycled components, whenever possible. The manufacturing process will be guided by international standards like ISO 14001 (Environmental Management Systems) and RoHS (Restriction of Hazardous Substances), ensuring compliance with regulations that restrict the use of harmful chemicals and promote sustainable practices.

Additionally, the device will be designed with a focus on modularity, allowing components such as batteries and sensors to be easily replaced or upgraded. This design choice extends the device's lifecycle and reduces the amount of e-waste generated by encouraging repairs rather than disposals.

Additionally, users will be provided with clear guidance on how to dispose of the device responsibly, including information about authorized e-waste recycling programs. This will ensure that the device is not only eco-friendly during production but also during the end-of-life stage.

Collaborations with manufacturers committed to ethical, sustainable production practices will ensure that all materials used in the device meet high environmental standards. Regular environmental audits will be conducted to assess the environmental footprint of the device's production, transportation, and disposal stages. This will help track progress and ensure continuous improvement in environmental practices.

Furthermore, a portion of the device's profits may be allocated to funding environmental initiatives, such as supporting sustainable production practices, promoting e-waste recycling, or contributing to reforestation efforts, thus demonstrating a commitment to broader environmental responsibility [28, 36, 69, 71, 72].

## 2.4 Final Decision: Proof-of-Concept and Verification

This project has two critical components that must be proven for the final prototype to work. The first component examines the transferability of results from algorithms that are built for detecting arrhythmia trained on open source data to the use of data acquired by equipment with limited resources and capabilities such as the chosen wearable device. The second component examines the technical feasibility of conducting all the data acquisition and processing tasks on the wearable device while maintaining acceptable performance and meeting memory and time constraints.

### 2.4.1 Transferability of Wearable Device Data

#### Objective

The objective of the transferability component is to assess whether the signal acquired by the wearable device is comparable to MIMIC signals in terms of main characteristics including the QRS complex, P wave, T wave, and PPG features. MIMIC data is collected in controlled ICU environments under ideal conditions, which reduces noise and allows for high-quality multi-lead signals. In contrast, the wearable device operates in real-world settings, where it is more susceptible to noise and relies on a single lead, which poses challenges for signal fidelity. If the wearable signals demonstrate sufficient similarity to MIMIC signals, it would validate the use of MIMIC data to train machine learning models intended for the wearable device.

#### Verification Methodology

There was more concern with ECG signal transferability compared to PPG, since the latter is generally simpler in shape. For this reason, the verification method for transferability primarily focused on the ECG portion of predictors. Since the transferability component is highly dependent on the sensor's capabilities, the main prototype was the wearable itself. Wearable ECG signals (Figure 6) were compared to two other

signals: MIMIC III database waveform signals, and 3-lead lab circuit signals (Figure 7). Wearable signals and lab circuit signals were both acquired from the same individual. Following data acquisition, digital filtering and smoothing was applied to wearable signals and lab circuit signals to reduce noise. Two aspects were evaluated: the presence of the main ECG characteristics including the QRS complex, P waves, and T waves, for their important role in detecting and distinguishing arrhythmias, and the presence of the “healthy peaks” in the FFT, as described in section 2. The latter aspect is included due to its relatively noise-resistant nature compared to the former aspect, but the prototype could still pass the FFT test without having all important wave types, hence why checking the raw ECG is important.

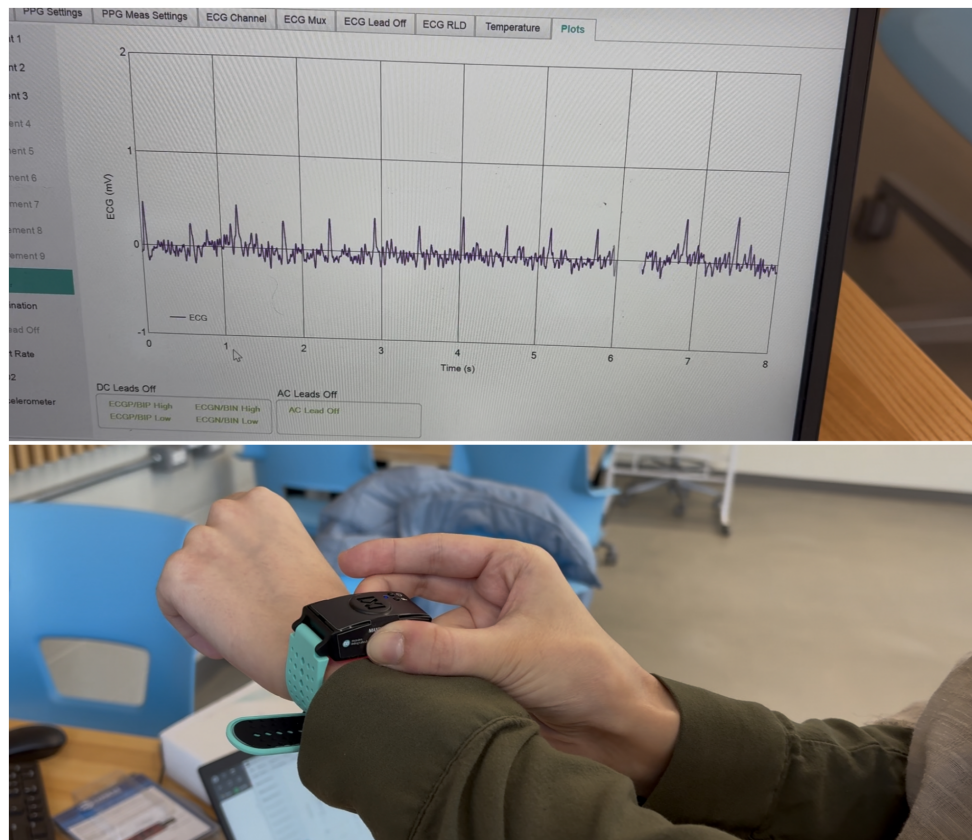
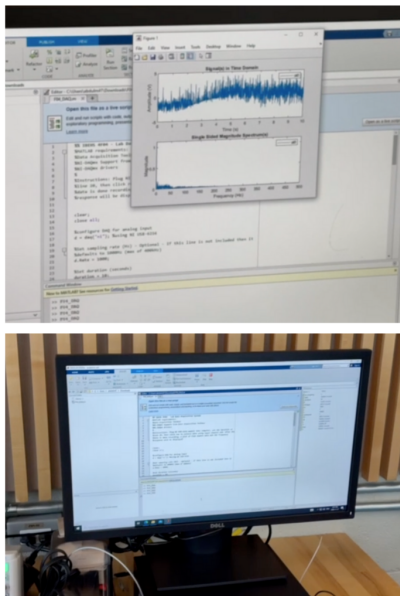


Figure 6: data acquisition using the wearable through bluetooth.



## Lab Setup

A circuit board with three ECG leads connected for signal processing in MATLAB.



Figure 7: circuit used for the 3-lead signal acquisition, consisting of amplifiers and a combination of high-pass and low-pass filters.

### Modeling and Analysis

As expected, the wearable device produced a lower-quality signal compared to the MIMIC waveform samples (Figure 8). Surprisingly, the wearable signal was similar to the 3-lead circuit signal, suggesting that the 1-lead configuration did not negatively impact quality as much as initially anticipated. Despite quality differences, the QRS complex, P wave, and T wave can all be seen in the filtered wearable sample. The FFT was subsequently calculated for all three samples, revealing that the wearable's FFT exhibited healthy peak traits similar to those of the lab signal and the MIMIC signal (Figure 9). Based on these findings, the prototype successfully passed the transferability tests.

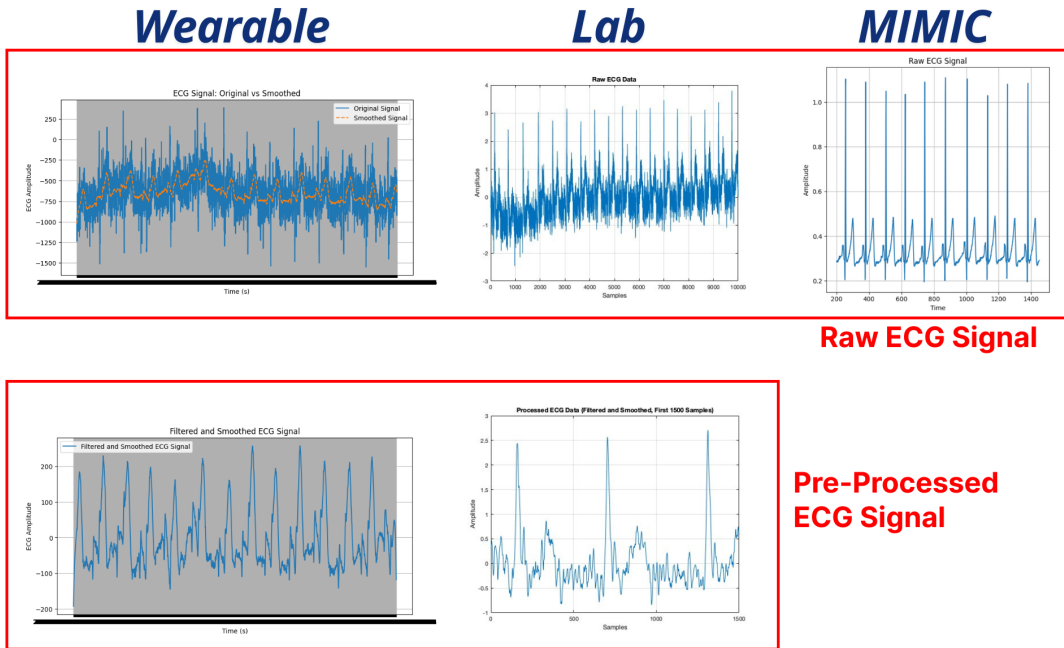


Figure 8: raw ECG signals (top) and processed ECG signals (bottom) from the wearable (left), 3-lead lab circuit (middle), and MIMIC (right). Since MIMIC waveforms had minimal noise, no filtering or smoothing was required.

# Wearable Lab MIMIC

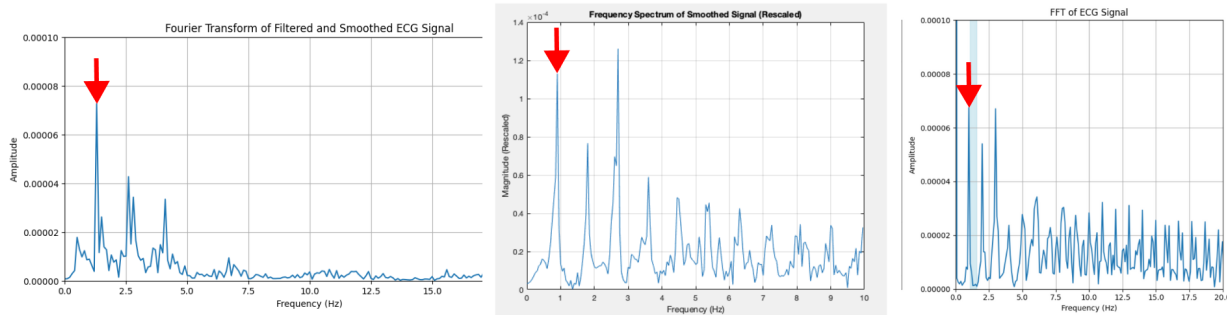


Figure 9: the FFT of the wearable, 3-lead lab circuit, and MIMIC samples, respectively. All three samples displayed the healthy peaks at the heart rate frequency and its multiples. The red arrows show the main peak which represents the heart rate frequency.

## 2.4.2 Technical Feasibility of Data Acquisition and Processing

### Objective

The objective for the second component, technical feasibility, was to ensure that the chosen input-processing methods could meet timing and memory constraints on a device with limited capabilities, such as the wearable.

### Verification Methodology

For simplicity and due to a delay the team faced in obtaining the NDA to program the wearable, the ESP32 microcontroller was used as a substitute for the wearable to represent the prototype for the technical feasibility component test. Although the ESP32 is not as functionally limited as the wearable, it is of similar specifications. Since the focus was data processing and not sensing, ECG signals were not detected through sensors, but rather sent through serial communication from a laptop. In other words, the laptop emulated a patient, while the ESP32 represented the wearable. The ESP32 was programmed to calculate the FFT of the signals it received every 1024 sample points of MIMIC data, which corresponded to just over 8 seconds (sampling frequency is 500 Hz). To confirm that the ESP32 was continuously and correctly calculating the FFT of the signal, the FFT results were periodically sent back to the laptop for real-time graphing. Additionally, to test timing, the number of elapsed milliseconds during FFT calculation was outputted. The prototype's passing criteria were defined as follows: the FFT results graph needed to match the FFT results calculated directly on the laptop (Figure 1), and the FFT calculation time had to be less than the sampling period, which is 1/500Hz or 2 ms. If the processing time exceeded this threshold, it would result in a conflict between sampling and processing, potentially causing skipped samples or interrupted FFT calculations.

## Modeling and Analysis

The FFT of the healthy and atrial fibrillation data sent to the ESP32 can be seen in figures 10 and 11 respectively. It is evident that the FFT graphs are similar to the ones discussed in section 2 and are equally distinguishable. This demonstrates that devices with limited computational power and capacity can successfully perform routine operations such as FFT without exceeding memory limits.

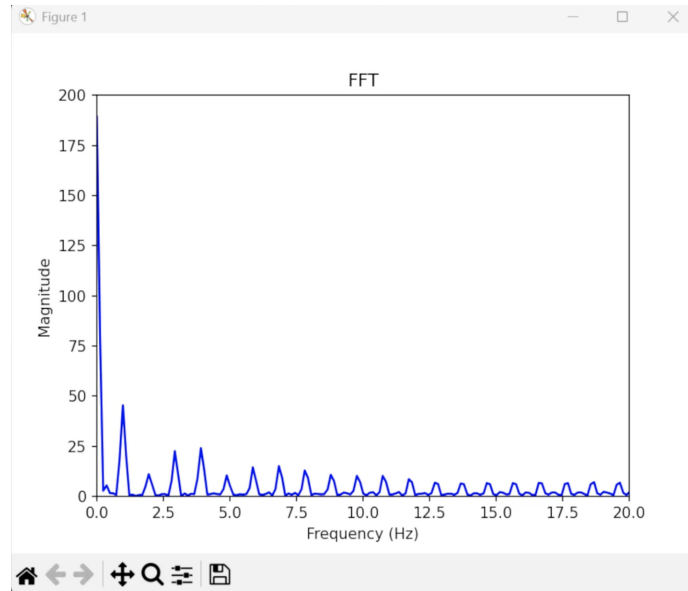


Figure 10: FFT of healthy ECG signal as calculated on the ESP32, graphed in real-time on the laptop.

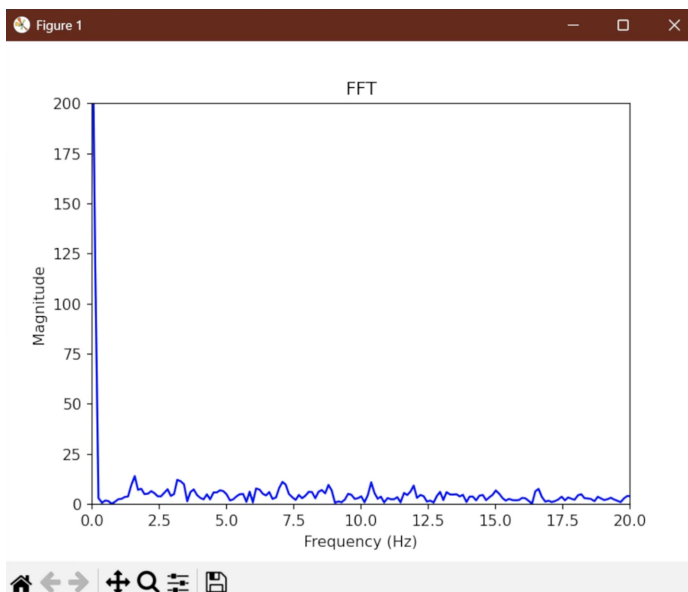


Figure 11: FFT of atrial fibrillation ECG signal as calculated on the ESP32, graphed in real-time on the laptop.

Unfortunately, the calculated time for FFT processing was found to be  $7 \pm 1$  ms, which exceeds the sampling period. Since the wearable has a single processor core and does not automatically sample points, this processing time must be reduced. A potential solution could involve manually coding the FFT function, which would allow for breaking up the calculation, creating a real-time scheduling approach, or even skipping the computation of less significant frequencies.

### 3.1 Design Prototype Plan

#### 3.1.1 Overview of Hardware Architecture and Integration

The wearable, MAXREFDES104, integrates a two-in-one PPG and ECG analog-front-end (AFE) sensor, a human body temperature sensor, a microcontroller, a power-management IC, and a 3-axis accelerometer. The complete platform, as illustrated in Figure 1, includes a 3D-printed enclosure and a biometric algorithm hub with embedded heart rate, oxygen saturation, and ECG algorithms. The MAXREFDES will interface with its corresponding computer GUI via Bluetooth, in which data will be printed to a CSV [58].

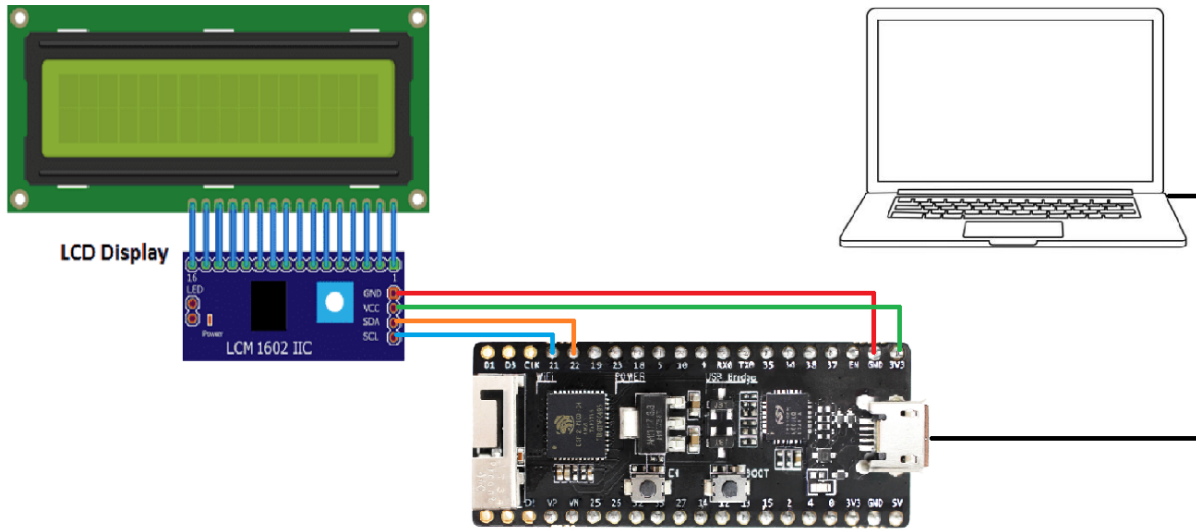


Figure 12: The hardware system consists of two separate components, the wearable and the ESP32 portion.

The ESP32 will be used to demonstrate the functionality of the software algorithms due to the lack of access provided to upload firmware onto the wearable. The TinyML algorithm and data processing algorithms will be implemented on the ESP32. The data obtained from the wearable sensors will be transferred via a computer to the ESP32 which will take the Fast Fourier Transform (FFT) and identify key features such as peaks, and valleys. The ESP32 will perform the machine learning algorithm to

identify heart arrhythmias in patients. The algorithm output and raw data can be streamed through Bluetooth to a computer GUI for demonstration, evaluation, and customized development. The Bluetooth feature interfaces with the computer, and allows for real-time data collection that can be sent to the ESP32 for processing. Once the TinyML algorithm has finished processing the data and reached a conclusion, the ESP32 will output real-time results to a 16x2 LCD Display. The display will alert the user if heart arrhythmia is detected.

This change of plans from using the wearable to using an ESP32 necessitates completing a comparison of the microprocessors as seen in Table 4. The ESP32-PICO-D4 has a faster dual-core processor while the MAX32666 has dual-cortex-M4 cores with FPU and DSP acceleration, making it more efficient for machine learning tasks like signal processing [2, 3]. The MAX32666 consumes significantly less power making it ideal for battery-powered tinyML applications, such as in the wearable. The main hurdle in using the MAX32666 versus the ESP32-PICO-D4 is that the latter offers 4MB of flash making it better for larger ML models, while the MAX32666's SRAM makes it more efficient for in-memory computations [4, 5].

Table 4: A comparison between the ESP32-PICO-D4 and the MAX32666 wearable device [2, 3]

Feature	<b>ESP32-PICO-D4</b>	<b>MAX32666</b>
<b>Processor</b>	Dual-core 32-bit LX6	Dual-core Arm Cortex-M4
<b>Clock Speed</b>	240 MHz	96 MHz (per core)
<b>Floating Point Unit (FPU)</b>	software-based	Hardware FPU (single precision)
<b>Power Consumption</b>	~200mW active	~30mW active
<b>Flash</b>	4 MB flash	1 MB Flash
<b>SRAM</b>	520 KB	560 KB
<b>External Memory Support</b>	Yes (SPI Flash)	No

### 3.1.2 Overview of Software Architecture and Integration

This section outlines the software design and implementation plan for the final prototype, focusing on ECG and PPG signal processing, feature extraction, and real-time data handling on the ESP32 microcontroller. As the project progresses from the proof-of-concept stage described in Chapter 2, this section details how the software will be structured to accommodate the updated prototype design while addressing limitations and mitigation strategies (see Figure 13).

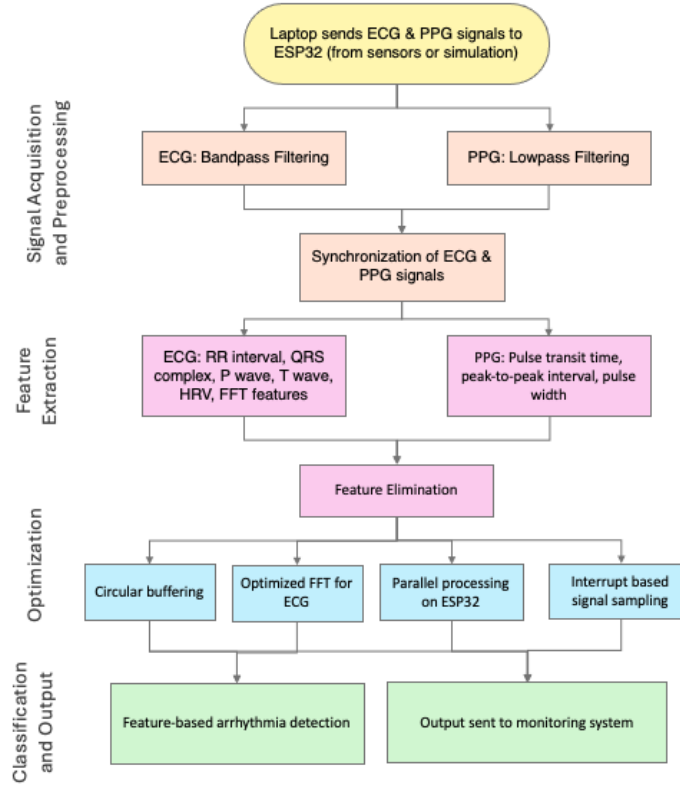


Figure 13: A flow chart outlining the process from signal acquisition and processing to feature extraction, optimization, classification, and output.

#### Data Preparation and Processing

The arrhythmia types considered were atrial fibrillation, ventricular fibrillation and flutter (unseparated), ventricular tachycardia, tachycardia, and bradycardia. Originally, the plan was to use MIMIC III data directly, since it has timestamps of the occurrence of different types of arrhythmias [77]. A limitation of using that data set, however, was that even assuming all the alarms were true alarms and timestamps were correct to the second, the presence of the timestamp did not guarantee the ECG and PPG of the patient were being recorded at that time. A straightforward yet time-consuming solution was to check the waveform header files and cross-reference them with arrhythmia timestamps to filter the waveform files. However, two smaller datasets were found that did not require as much processing: the Clifford et al. Computing in Cardiology Challenge 2015 dataset, and the Charlton et al. MIMIC PERform AF dataset [78, 79]. The latter had atrial fibrillation samples and controls, while the former had all the other types of interest, including healthy samples. Due to a difference in sampling frequency between the two data sources, the Charlton et al. signals were interpolated to increase the number of samples per second from 125 to 250 Hz, which matches the Clifford et al. dataset (see Figure 14).

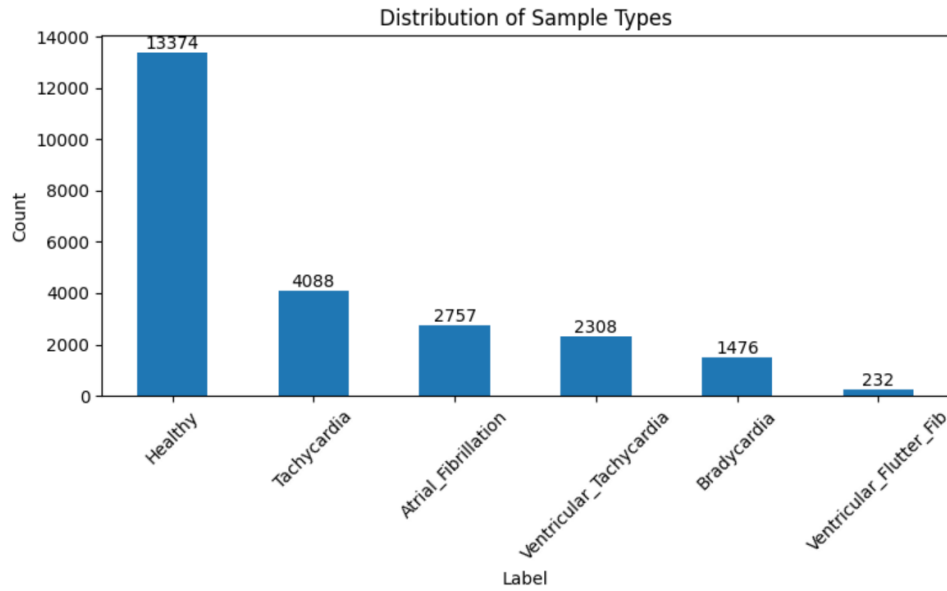


Figure 14: the counts of 8-second samples collected from the Clifford et al. and Charlton et al. datasets combined.

#### Feature Extraction and Clustering

Unsupervised clustering algorithms, such as UMAPs, will be used to assess whether the variability of a set of features is enough to distinguish the different arrhythmia types - from each other and from healthy heart rhythms. The features considered for the models will include those extracted from both ECG and PPG signals, combining time- and frequency-domain characteristics.

Examples of features found to be useful so far include the FFT number of peaks, number of valleys, peak-to-peak distance median, and peak-to-peak distance standard deviation (see Figure 15). It is important to note that the number of peaks in FFT does not correlate to the number of peaks in the time-domain (TD) signal, but is useful for determining the FFT pattern associated with a healthy rhythm and disturbed in arrhythmias. For tachycardia and bradycardia, time-domain features might be more useful, but that remains to be confirmed with UMAPs and test runs of machine learning models. Both the R peak and the S valley will be used in time-domain, even though the intervals between them should theoretically be the same. This is a form of redundancy in case the S characteristic is more dominant than the R characteristic (and therefore more accurate) due to electrode placement.

Table 5: Summary of key frequency-domain and time-domain features extracted from preprocessed ECG signals

Feature Name	Description

Difference of Medians (FFT)	The difference between the median of the FFT peaks and the median of the FFT valleys.
Median of Distances (FFT)	The median (in Hz) of the distances between FFT peaks.
Standard Deviation of Distances (FFT)	The standard deviation (in Hz) of the distances between FFT peaks.
Number of Peaks (FFT)	The total number of FFT peaks in the frequency range of interest.
Number of Valleys (FFT)	The total number of FFT valleys in the frequency range of interest.
RR Interval Median (TD)	The median (in seconds) of the RR intervals, where R is the ECG peak characteristic.
RR Interval Standard Deviation (TD)	The standard deviation (in seconds) of the RR intervals, where R is the ECG peak characteristic.
SS Interval Median (TD)	The median (in seconds) of the SS intervals, where S is the ECG valley characteristic.
SS Interval Standard Deviation (TD)	The standard deviation (in seconds) of the SS intervals, where S is the ECG valley characteristic.

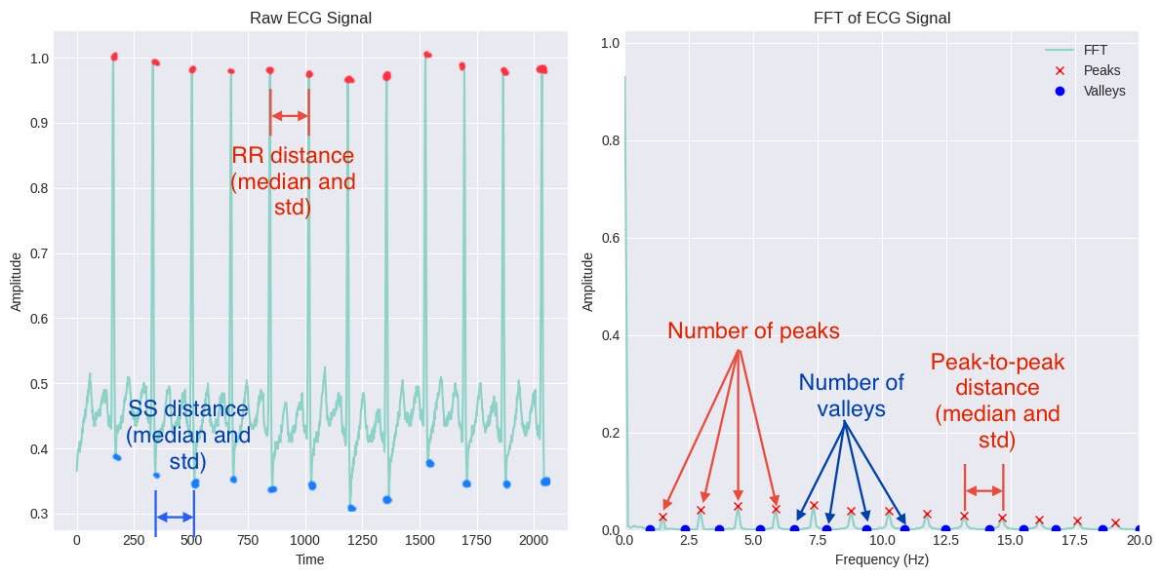


Figure 15: time-domain signal (left) and frequency domain signal (right) of a sample signal. Annotations on the right graph represent some features found to be useful in distinguishing some arrhythmias from healthy rhythms and from each other.

PPG models, on the other hand, will include both morphological and time-domain features. Key features found to be valuable include systolic and diastolic amplitude, pulse interval, peak-to-peak interval, and full width half maximum (FWHM). The systolic and diastolic amplitudes reflect changes in blood flow dynamics associated with arrhythmias, while the pulse interval and peak-to-peak interval are indicative of variations in heart rate and vascular response [80]. The features in Table 6 will be extracted from the preprocessed PPG signals, which undergo bandpass filtering, smoothing, and baseline removal to ensure accurate detection of peaks and valleys. An image showing the specific features being extracted from the PPG waveform is provided in Figure 15, which visually represents the morphological characteristics used in this study [80]. Note that these features will be evaluated for their sensitivity to the model and various classifications in order to identify which ones are essential. Time-domain features, such as pulse interval and peak-to-peak interval, will provide important information for distinguishing between different arrhythmia types, including tachycardia and bradycardia. Similarly, the effectiveness of these features in differentiating arrhythmias will be evaluated through unsupervised clustering methods like UMAP and tested in machine learning models. The detection of peaks and valleys within the PPG waveform is shown in Figure 16, emphasizing the role of these points in segmenting the signal for feature extraction.

Table 6: Summary of key morphological and time-domain features extracted from preprocessed PPG signals

Feature Name	Description
Systolic Amplitude (sa)	The peak amplitude of the systolic portion of the PPG waveform, reflecting the maximum blood flow during heart contraction.
Diastolic Amplitude (da)	The peak amplitude of the diastolic portion of the PPG waveform, representing the residual blood flow during heart relaxation.
Systolic Area (SA)	The area under the systolic portion of the PPG waveform, indicative of the total blood volume pumped during systole.
Diastolic Area (DA)	The area under the diastolic portion of the PPG waveform, representing the total blood volume remaining during diastole.
Systolic Time (St)	The time duration of the systolic phase in the PPG signal, reflecting how long the heart takes to pump blood during each beat.
Diastolic Time (Dt)	The time duration of the diastolic phase in the PPG signal, representing the heart's relaxation period between beats.
Pulse Interval (PI)	The time between two consecutive pulses in the PPG waveform, used to assess heart rate variability.
Peak-to-Peak Interval (PPI)	The time interval between the peaks of consecutive pulses, used to evaluate the overall rhythm of the heart.

Full-Width Half Maximum (FWHM)	The width of the systolic peak at half of its maximum amplitude, used to characterize the sharpness of the pulse waveform.
--------------------------------	--

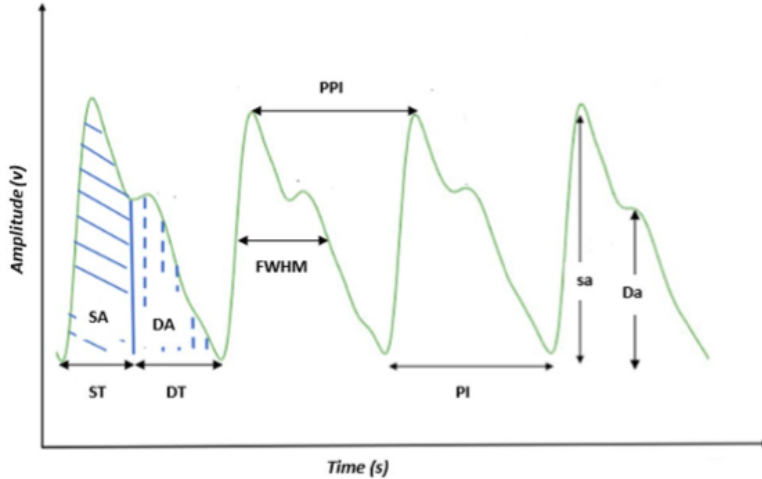


Figure 16: Visual representation of the specific features extracted from the PPG waveform, highlighting the morphological characteristics critical for analysis. Adapted from [80].

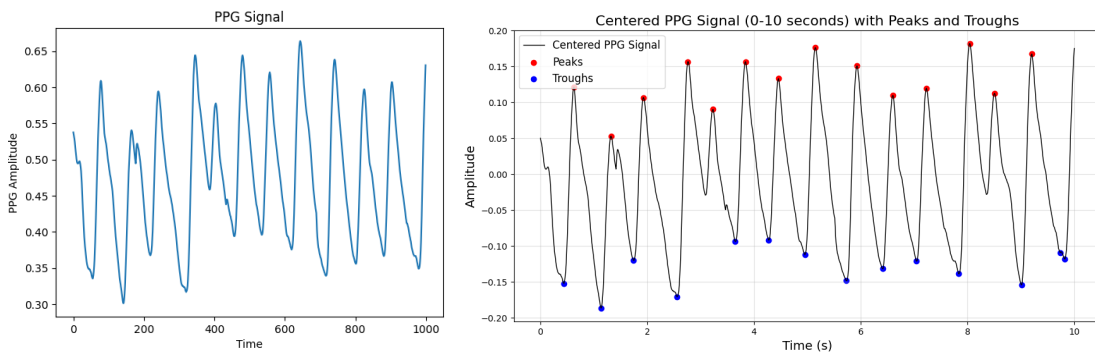


Figure 17: Detection of peaks and valleys within the PPG waveform, illustrating their significance in segmenting the signal for feature extraction.

### Real-Time Identification and Classification of Arrhythmia Types

To optimize arrhythmia detection and classification, the ECG and PPG signals will be integrated within the system to combine the complementary information provided by both signals. The ECG signal offers detailed electrical activity of the heart, while the PPG signal provides insights into the mechanical effects of heart function and vascular health. By leveraging both types of data, the system can improve classification accuracy and robustness. The integration will involve the simultaneous processing of both ECG and PPG signals. While each signal will undergo individual preprocessing steps, the key features

extracted from both will be combined for further analysis. The system will evaluate the interaction between these features using unsupervised clustering methods, such as UMAP, to examine the impact of both signals on the ability to distinguish arrhythmias. Additionally, machine learning models will be trained using features from both signals, aiming to improve performance by capturing a more complete picture of the patient's heart health. The final model will incorporate both ECG- and PPG-derived features to classify arrhythmias, with the expectation that the combination of both modalities will provide a more robust and accurate system.

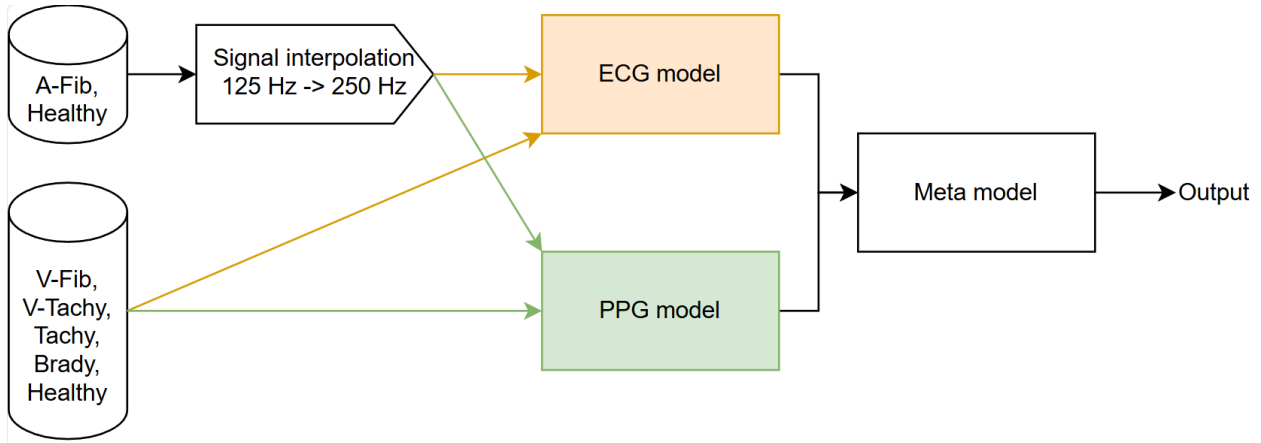


Figure 18: stacked ML model to form a decision based on both ECG and PPG data. ECG and PPG data are extracted from both datasets and separated so that each is fed to its corresponding model. The final result is determined by a meta model that forms the decision based on the outputs of the two models.

The goal is to implement a machine learning model capable of detecting arrhythmias (such as atrial fibrillation, ventricular fibrillation, tachycardia, and bradycardia) in real-time on the ESP32 microcontroller using TinyML techniques. This will enable the system to process ECG and PPG signals directly on the embedded device, providing low-latency detection of arrhythmias without needing constant connectivity to a more powerful server. The model selection for real-time arrhythmia detection on the ESP32 microcontroller will focus on lightweight machine learning models, such as decision trees, logistic regression, or naive Bayes. The chosen models will be evaluated based on their accuracy, computational efficiency, and ability to function within the ESP32's hardware limitations. This approach follows the principles demonstrated in Hassan et al.'s work on deploying TinyML-based healthcare applications in resource-constrained environments, such as real-time physiological monitoring and classification on edge devices [81].

To optimize the trained model for efficient operation on embedded devices, several techniques will be applied. Quantization will reduce memory and computation requirements by lowering the precision of the model's weights, improving inference speed and minimizing memory usage while maintaining acceptable accuracy. Additionally, pruning will eliminate less important components, such as neurons or weights, thereby reducing model size and enhancing computational efficiency. The optimized model will be converted into a format compatible with TinyML frameworks, ensuring efficient loading and execution on the device without exceeding its resource limitations. These optimization techniques align with the findings of Hassan et al., who demonstrated the effectiveness of quantization and pruning in reducing

computational overhead while maintaining model performance in embedded healthcare applications [81].

### Real-Time Scheduling for Signal Processing

The TinyML algorithm will be flashed onto the ESP32 to handle real-time data processing from the ECG/PPG sensors. Real-time inference will be performed on incoming signal data, using interrupt-based signal sampling to capture relevant data at specific intervals, avoiding overloading the device's CPU (Figure 19). The ESP32 will process signals, extract features, run the machine learning model, and provide real-time arrhythmia detection feedback. This method ensures minimal power consumption while maintaining system performance. This approach aligns with the implementation described in the study "Atrial Fibrillation and Sinus Rhythm Detection Using TinyML (Embedded Machine Learning)," which discusses deploying machine learning models on the ESP32 for real-time ECG data processing and arrhythmia detection [82].

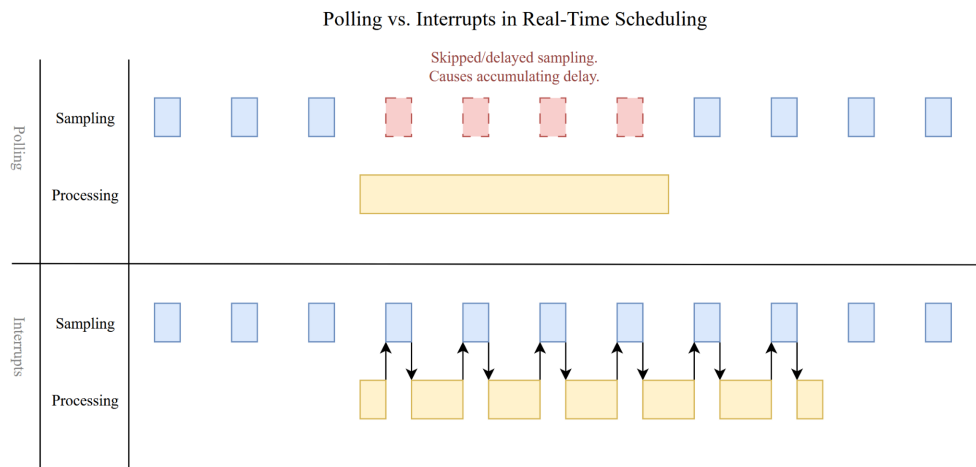


Figure 19: the management of sampling and processing real-time tasks. Although the usage of interrupts increases the duration of processing, it leads to all tasks meeting their deadlines since processing (every second) is less frequent than sampling (250 times per second).

When implementing interrupts on the Arduino using the built in interrupt library, there were difficulties adjusting the interrupt handler to capture the data every 8 ms. The issue caused delays in sampling which accumulated over time leading to missed data points. An alternative approach was taken by applying threading and taking advantage of ESP32's dual core. One thread was used to collect the data and store the samples in a circular buffer. Another thread was used to perform all data processing activities including taking the fast fourier transform of the ECG data and identifying features for the ML algorithm in the frequency and time domains. The data buffers have a common mutex lock which must be acquired by a thread to access the buffer. Once one thread possesses the mutex lock, other threads can not acquire the lock until the lock is released. The use of threads allows the data processing to run almost continuously while switching to the data sampling thread every 8 ms to collect a data point, thus reducing delays and creating an illusion of parallel execution.

#### 3.1.3 Overview of Casing for Hardware Hiding Design

Although the final goal of the software and hardware implementation will be on the wearable, the ESP32 and LCD will be used as proof of concept due to time and budget constraints. A 3D-printed housing will

be designed to hold the hardware components. This design consists of a base with an opening that can be used to connect the ESP32 to power or the computer. The second component of the design is a lid that covers the ESP32 protecting it from dust while revealing the LCD display such that users can read its messages.

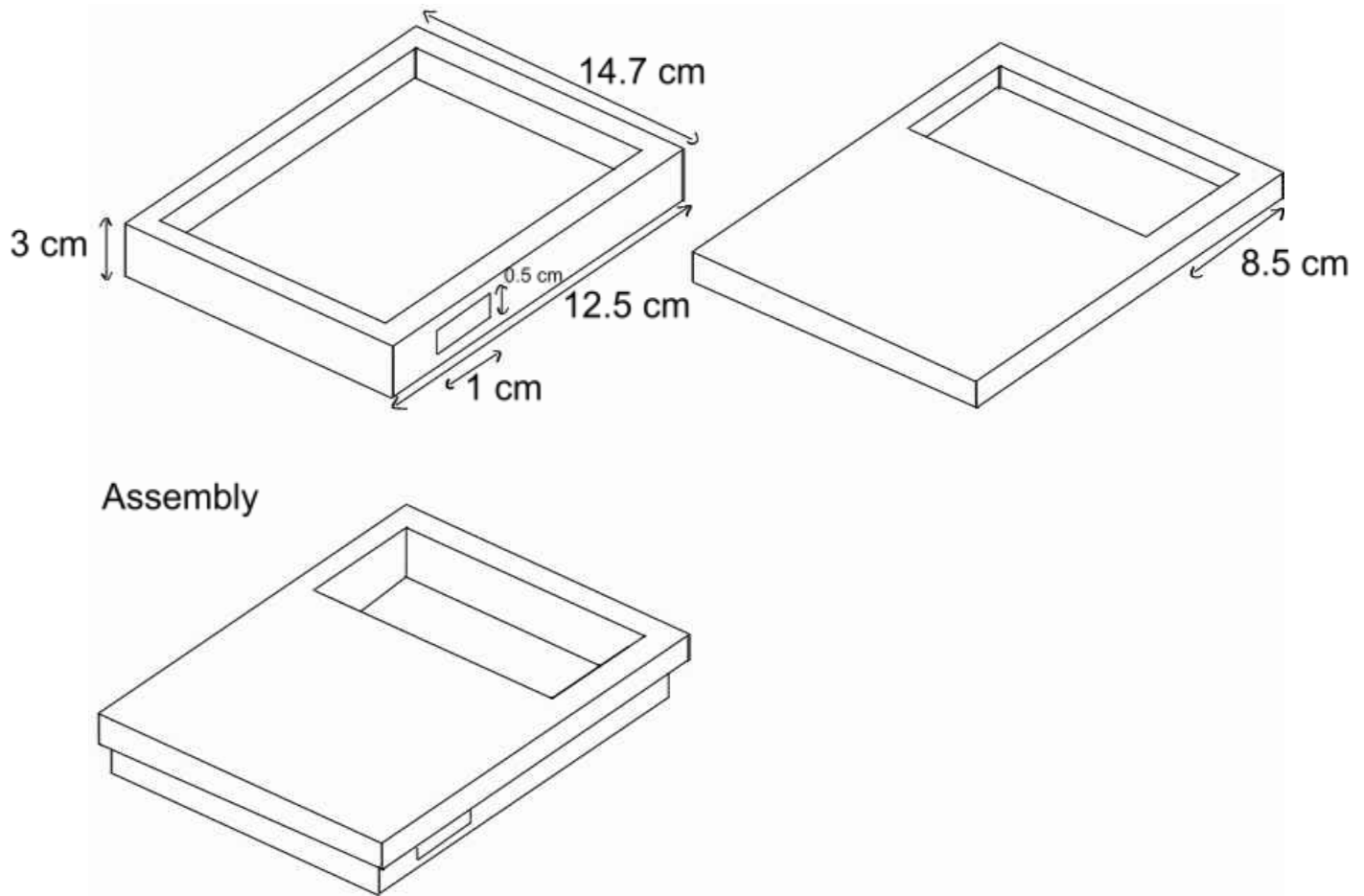


Figure 20: Initial iteration sketch for the hardware casing

The casing was modelled using AutoDesk Inventor and it consists of two parts: a base and a lid. The design initially had the LCD's screen mesh parallel to the lid which would require the user to look down from the top to read its text. The next iteration of the design has the LCD screen angled up such that one can read its contents from the front of the device. This setup makes the design more compact and allows the user to view results on the LCD screen even from a short distance. The casing was printed in PLA and assembled together ensuring to follow hardware hiding to protect the user from electrical components.

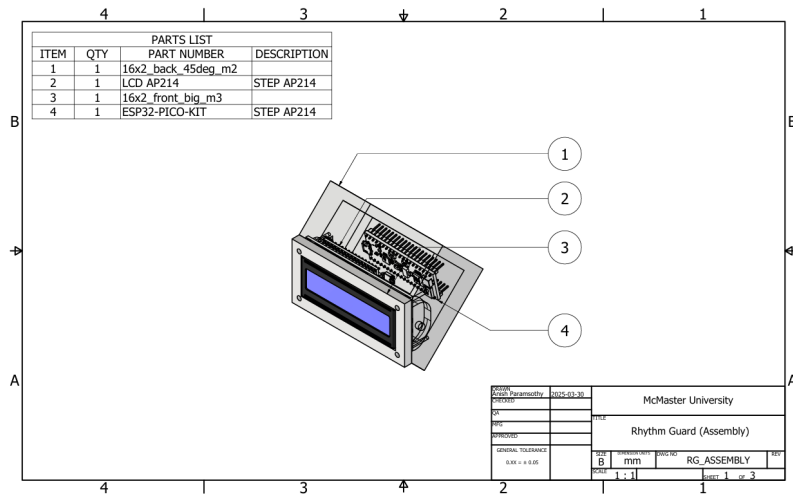
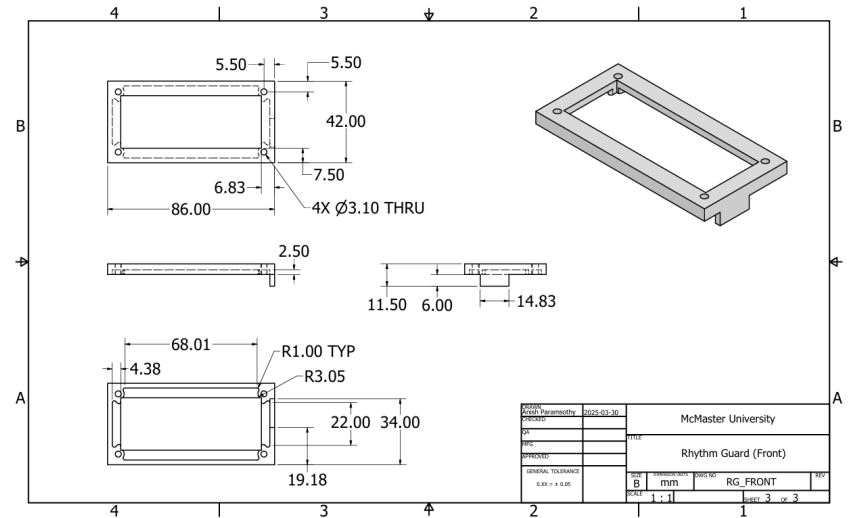
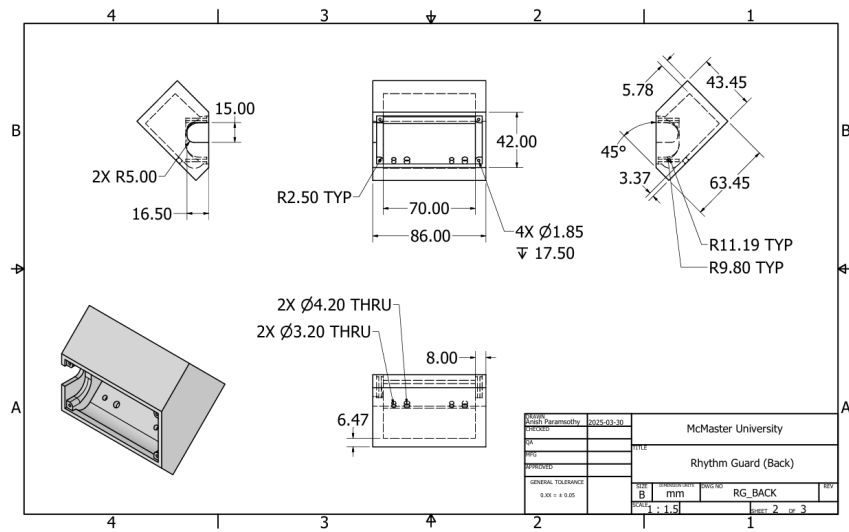


Figure 21: Engineering Drawings of the Final Mechanical Component

### 3.1.4 Assumptions, Limitations, and Constraints

#### Assumptions:

- The wearable device has sufficient computational power and memory to accommodate the signal processing and classification algorithms currently implemented on the ESP32 microcontroller.
- The Charlton et al. dataset and the Clifford et al. datasets use similar sensor equipment, meaning that the primary differences between atrial fibrillation (AFib) and other arrhythmia signals are due to pathology-related factors rather than differences in signal acquisition methods, hardware, or population [7, 8].
- The MAX32666 microcontroller's specs are better suited for this machine-learning model and would be able to operate to the same degree of effectiveness as the ESP32 (see Table 1).

#### Limitations:

1. The performance of the PPG model may be influenced by the skin tone of the user, as variations in skin pigmentation can affect the absorption and reflection of light, which in turn impacts the quality and accuracy of the PPG signal.
2. PPG signals can be sensitive to motion artifacts, which may degrade the quality of the signal, especially in a wearable device that is subject to everyday movements.
3. Imbalance in the Clifford et al. dataset can cause inaccuracies in some types of arrhythmia, due to the lack of Ventricular Fibrillation and Flutter samples compared to the other types of arrhythmias (see Figure 3).
4. Variability in the ECG electrode contact quality and differences in skin conditions and electrode placement can impact ECG signal quality, potentially leading to signal dropouts or increased noise
5. While the wearable device can assist doctors in monitoring and detecting arrhythmias by providing valuable real-time data, it is not intended to replace medical professionals' expertise. The device can serve as a helpful tool in the diagnostic process, but final decisions regarding treatment or diagnosis must always be made by qualified healthcare providers.

#### Constraints:

1. The wearable device (e.g. ESP32) has limitations in processing power and memory, which may constrain the complexity of the algorithms and the speed of real-time signal processing.
2. The sampling rate of the sensors may limit the resolution of the data, which could affect the accuracy of certain features, particularly at higher heart rates or in the presence of rapid arrhythmias.
3. The quality of data may vary depending on the sensor's placement, ambient light conditions, and other environmental factors, potentially limiting the overall performance of the model.
4. The need for low power consumption produces constraints on continuous data transmission intervals as Bluetooth and wi-fi data transmission may increase power consumption and reduce battery life.

### 3.1.5 Implementation of Mitigation Strategies

The ECG/PPG sensors may lead to inaccurate arrhythmia detection, resulting in missed diagnoses or false

alarms. To address this, validation should be performed using diverse real-world testing, and the tinyML algorithm should be optimized to account for inaccuracies in the model. Algorithms that merge data from both ECG and PPG should be used to provide a more reliable signal interpretation. For example, if one signal is corrupted or noisy, the other signal may still provide useful information. Additionally, appropriate signal processing techniques should be used to mitigate artifacts like motion or interference that might impact signal quality. Displaying a confidence score for each arrhythmia detection, categorized as low, medium, and high can help users interpret the algorithm's certainty. On the final prototype a sticker was added to the rear of the display outlining the % true positive, % false positive, % false negative, % true negative, % precision, and % sensitivity for each arrhythmia classification to ensure the user is aware of the accuracy of each result.

The TinyML algorithm may cause delayed or inaccurate arrhythmia detection, leading to false alarms, late medical intervention, or no medical intervention at all. To enhance the performance, the training data sets shall be increased while avoiding overfitting through cross-validation, and performing feature selection and elimination. Algorithm efficiency can be implemented by implementing an optimized FFT for ECG signal processing to ensure fast frequency-domain analysis, reducing computational overhead, using a circular buffer for efficient real-time signal storage and processing, minimizing memory usage and optimizing the handling of continuous data streams. Parallel processing shall also be employed on the ESP32 to offload computational tasks, allowing simultaneous signal analysis and feature extraction to speed up processing and enhance model performance. Data augmentation techniques should be applied to improve model robustness across varied patient profiles. Regular cross-validation, and feature elimination, and hyperparameter tuning should be conducted to improve prediction accuracy while minimizing overfitting. Removing and identifying redundant features, as well as standardizing datasets using healthy reference data can further enhance the model's accuracy and generalizability.

Battery-related issues could cause device failure or electrical shock. To prevent this low-voltage ICs should be used while optimizing power consumption and implementing battery level warnings. The wearable power management is handled by the MAX20360, a highly integrated and programmable power management solution designed for ultra-low-power wearable applications, and the MAX17260 cell fuel gauge which utilizes an advanced algorithm that combines the short-term accuracy and linearity of a coulomb counter with the long-term stability of a voltage-based fuel gauge, along with temperature compensation to provide industry-leading fuel gauge accuracy. This IC automatically compensates for cell aging, temperature, and discharge rate. Additionally, a haptic driver integration is included to enhance user feedback while operating within the power limits.

Firmware crashes may compromise device functionality. To ensure reliability, rigorous software testing shall be conducted and a factory reset option should be provided to alert users of failure. Automated tests should detect firmware failures, such as when it fails to respond, hangs, or enters an infinite loop, with watchdog timers integrated to reset the device when necessary [83]. Various stress conditions shall be tested such as high processor load, low battery, fluctuating temperatures and extreme input data to identify vulnerabilities related to resource management, real-time performance and error handling [84]. Memory leak testing should be performed by monitoring heap usage over time, tracking allocation/free calls, and detecting heap fragmentation to prevent long-term performance degradation and crashes. A recovery mode should also be included for the user to restore functionality in the event of a crash.

The device enclosure shall be constructed from robust material, to ensure waterproofing, preventing break or water leakage. To address concerns regarding electronic waste and environmental hazards, users should be educated on proper disposal of electronic waste, and provide the option of sending back old devices for

disassembly and reuse of parts. Lastly, user errors, including improper operation, or overreliance on the device should be mitigated by providing clear instructional manuals and including warnings and disclaimers emphasizing the use of the device as a supplemental tool. The ESD sensitive warning label was included in the final prototype to ensure users keep it away from electrical components.

## 3.2 Design Verification Plans

### 3.2.1 Verification Setup

The verification process for Rhythm Guard will focus on the system's functionality, performance, and reliability in detecting arrhythmias, as well as verifying the data transmission, processing and alert mechanism. For live healthy data the team will test the MAXREFDES104 wearable device on themselves to gather ECG/PPG data. However, to ensure consistency and thorough testing, the simulated healthy signal outputs will be compared with the simulated arrhythmia outputs.

#### Test environment and components

The testing will take place in a controlled environment with minimal electromagnetic interference to maintain data integrity. The required components include ECG and PPG sensors embedded into the wearable device for live data collection and simulation, as well as an ECG and PPG labeled dataset for thorough testing. An ESP32 microcontroller will be used for data transmission, processing, and classification to simulate the wearable's process. A laptop will send simulations using dataset data similar to those used for training, while an LCD screen will display real-time data and classification results. The setup follows the system architecture illustrated in Figure 1, ensuring that data transmission, processing, and classification occur as designed. The test environment and components are structured to maintain consistency and accuracy in results.

#### Verification strategy

The data transmission and processing tests will include three key evaluations: the Healthy Data Transmission Test, the Simulated Arrhythmia Transmission Test, and the Alert System Verification. In the Healthy Data Transmission Test, ECG and PPG data will be collected from a healthy team member using the wearable device. This data will be transmitted to the laptop and then forwarded to the ESP32 microcontroller to ensure the transmission path maintains data integrity and that the ESP32 processes the ECG and PPG signals correctly. The Simulated Arrhythmia Transmission Test will involve streaming pre-recorded ECG and PPG data, containing both healthy and arrhythmic events, from the laptop to the ESP32 microcontroller. This data, similar to what was used in the system's training phase, will be used to verify that the ESP32 correctly classifies and processes arrhythmias, responding appropriately with alerts or feedback mechanisms. Finally, in the Alert System Verification test, the system will trigger a predefined alert on the LCD screen based on the classification results from the ESP32. This step ensures that the ESP32's output triggers activate accurately in response to both healthy and arrhythmic data.

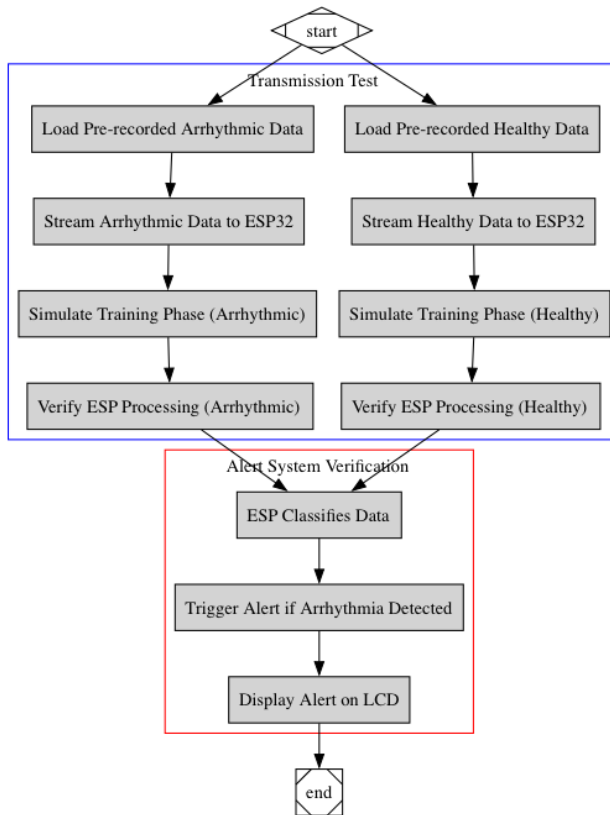


Figure 22: Data transmission and processing verification test flow chart.

The hardware verification setup includes several key tests to ensure the reliability and stability of the system. Power and connectivity testing will involve measuring the voltage and current supplied to the ESP32 microcontroller using a multimeter to confirm stable power delivery and uninterrupted communication between the wearable device, laptop, and ESP32. Extended runtime testing will be conducted to assess power stability and data transmission over time. Signal integrity and processing verification will compare raw ECG data received by the ESP32 with the original signal from the wearable device using a data logging tool such as MATLAB or Python. Additionally, a simulated interface test will introduce noise or electrical interference to evaluate the ESP32's ability to maintain signal integrity. The alert system and output testing will involve triggering the system with both healthy and simulated arrhythmic data and monitoring the LCD screen for correct visual alerts, with response time and accuracy checked using an oscilloscope or logic analyzer. Lastly, optional durability and environmental testing will subject the system to extended runtime stress, mild temperature and humidity variations, and mechanical stress, such as vibrations, to ensure the device remains functional in real-world conditions.

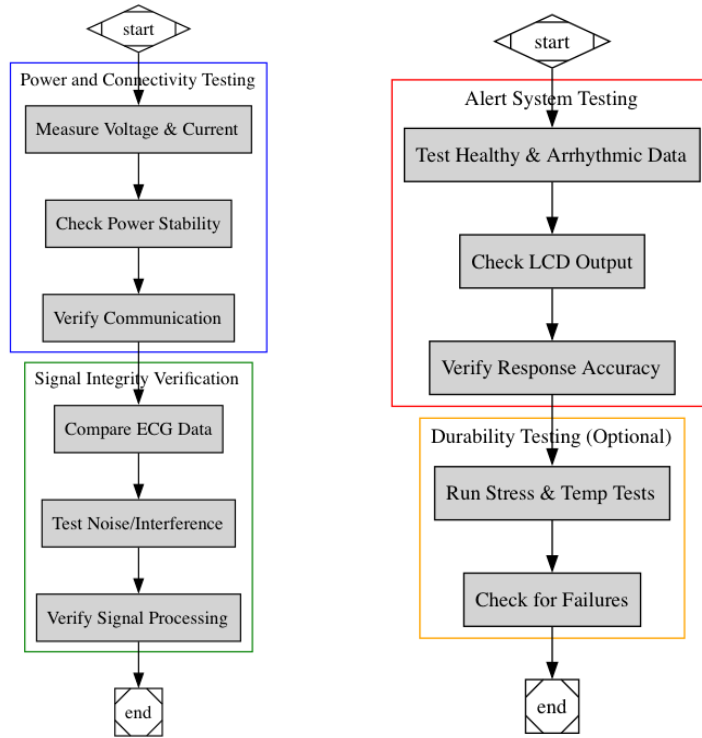


Figure 23: Power and signal verification test flow chart (Left) and alert and system durability verification test flow chart (right)

The software verification setup focuses on validating the Rhythm Guard algorithm and ensuring accurate data processing. Simulation models will be developed and executed to evaluate how the algorithm handles different heart rhythms, including arrhythmias. The simulated test data will be processed similarly to the training data, allowing for consistent comparison and validation of the algorithm's ability to correctly identify various arrhythmias in real time. Additionally, logging mechanisms will be implemented to track data processing, classification results, and anomaly detection. This ensures that no data is lost during classification and processing, with every event logged accurately, including timestamps and details for future analysis and debugging.

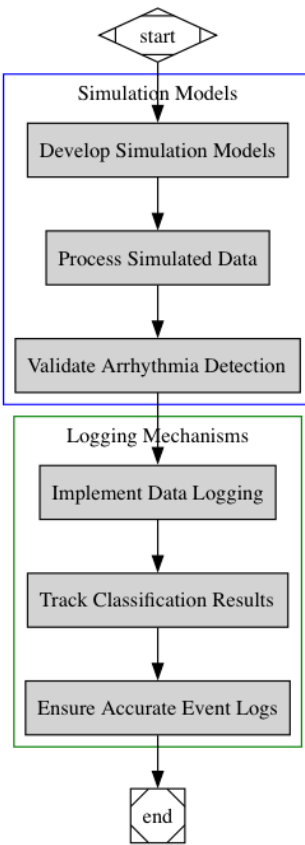


Figure 24: Software verification tests flowchart

Future work may involve user testing with real or simulated ECG/PPG data to evaluate the system's performance under varied physiological conditions. However, this is beyond the current scope and would require ethical approval and regulatory compliance.

### 3.2.2 Test Cases

The following test cases can be conducted to ensure the device is behaving as expected.

<b>Test Case 1: real-time scheduling</b>	Measure the time it takes to sample and process 30 seconds worth of data points.
<b>Expected Outcome</b>	Measured time should be exactly 30.000 seconds, since anything more indicates a delay in sampling caused by processing and calculations.

<b>Test Case 2: model</b>	Use a set of paired ECG and PPG intervals the ML model hasn't seen before, corresponding to patients it hasn't seen before, to test the model
---------------------------	---

<b>accuracy</b>	(zero-shot learning).
<b>Expected Outcome</b>	Sensitivity and specificity should both exceed or equal 90%.

<b>Test Case 3: device response rate</b>	Join an arrhythmia recording to a healthy recording and mark the time of transition as well as the time of output change on the LCD screen.
<b>Expected Outcome</b>	The delay between the two times should not exceed 5 seconds.

<b>Test Case 4*: durability</b>	Repeatedly do test cases 1-3, apply forces in the range 2-50 N, and redo the test cases.
<b>Expected Outcome</b>	Test case results should match up before and after applying force.

Test Case 4 is Out of Scope\*

<b>Test Case 5*: water resistance</b>	Repeatedly do test cases 1-3, submerge the device in water 1 m deep for 30 minutes, and redo the test cases.
<b>Expected Outcome</b>	Test case results should match up before and after submerging in water.

Test Case 5 is Out of Scope\*

<b>Test Case 6: heart rate classification</b>	Use ECG and PPG paired data only consisting of healthy, tachycardia, and bradycardia samples to test the ML model's heart rate classification.
<b>Expected Outcome</b>	Sensitivity and specificity should both exceed or equal 90%.

<b>Test Case 7: arrhythmia source prediction</b>	Use ECG and PPG paired data consisting of atrial fibrillation as atrial events, and ventricular flutter, ventricular fibrillation, and ventricular tachycardia as ventricular events, to test the ML model's ability to distinguish these two categories of arrhythmias.
<b>Expected Outcome</b>	Sensitivity and specificity should both exceed or equal 90%.

### 3.2.3 Verification Plans for Design Outputs

Table 7: The verification tests that can be conducted to check each design output corresponding to each design input.

<b>Design Inputs</b>	<b>ID</b>	<b>Design Outputs</b>	<b>Verification Test</b>
The device must have a long lasting battery life of at least 24 hours.	1	The device must comply with IEC 61960 standards for Secondary Lithium Cells and Batteries for Portable Applications to prove the battery's ability to continuously provide power under various circumstances [85].	Due to the costs of acquiring the testing equipment and the time required to complete these tests, the battery life verification is not within the scope of this project.
The device must achieve a minimum sensitivity and specificity of 90% for detection of heart arrhythmia.	2	Sensitivity and specificity can be calculated using the labeled datasets which mark the presence/absence of arrhythmia for each individual.	The algorithm will be tested using data from a labeled data set to cross reference the positives and negatives. Then the sensitivity and specificity will be calculated.
The sensors must have a sampling frequency greater than or equal to 300 Hz.	3	The Nyquist frequency must be at least 300 Hz because the highest frequency in an ECG signal is 150 Hz [87].	The number of samples collected in a second will be counted to calculate the sampling frequency.
The wearable must be small, noninvasive and compact.	4	The device must comply with the Medical Devices Regulations (SOR/98-282) definition of a Class I Medical Device from sections 10 to 20 to validate that the device is noninvasive [88].	The device must adhere to rules 4 to 7 of the Guidance on the Risk-Based Classification System [89].
	5	The wearable must accommodate for circumferences from 10 cm to 25 cm which is the range of wrist sizes in adults [90].	The circumference of the wearable can be measured manually using a measuring tape.
The wearable enclosure must be made of a durable and hypoallergenic material.	6	Verify Human Repeated Insult Patch Test (HRIPT) results on all materials used in the casing which will assess if the materials can pose allergies [91].	The result of HRIPT is the percentage of induced sensitization reactions observed in the total number of participants which should be less than 2.9% for all materials [92].

The device should be able to withstand scratches. The device must survive falls and should remain functional.	7	Successful scratch test results based on the ASTM D7027/ISO 19252 standards on materials used in the wearable casing [93].	The wearable should not exhibit failure from 2 to 50 N [94].
	8	Successful test results from Drop and Shock testing according to MIL-STD-810G [95].	The device should be dropped 10 times from a height of 168.27 cm after which the device must still be functional. This test will not be done to avoid permanent damage to the wearable.
The device must have a water resistance rating of at least IPX7.	9	Successful results from a 1-metre water submersion test of the final device for 30 minutes [96].	The wearable should have the same functionality after being submerged in a container of water that is 1-metre deep for 30 minutes.
The device response rate must not exceed 5 seconds.	10	Successful results from performance testing of the device under different scenarios (e.g. presence/absence of arrhythmia) where the device responds in less than 5 seconds and the software doesn't freeze in an infinite wait state [97].	The time for the diagnosis to be displayed on the LCD will be measured using an oscilloscope.

#### Test 1: Battery Life Validation and Compliance with IEC 61960 Standards

The machine learning algorithm requires a large amount of data to analyse and arrive at a diagnosis which requires the user to wear the device for a long time period. Therefore the device must have a long battery life. To verify the 24-hour battery life requirement and compliance with IEC 61960 standards, battery emulation and power analysis tools such as battery run-down tests, state of charge testing, power consumption profiling, temperature impact testing, aging and degradation testing, and event-based power testing will need to be performed as highlighted by Keysight [98]. The costs and time required to test the battery life are above the budget and timeframe of this project, hence this test will not be performed.

#### Test 2: Sensitivity and Specificity Assessment of Heart Arrhythmia Detection

The device must achieve a minimum sensitivity and specificity of 90% for detection of heart arrhythmia to meet the performance of the golden standard. Sensitivity and specificity can be calculated using equations (1) and (2) [86].

$$\text{Sensitivity} = \frac{\text{True Positives}}{\text{True Positives} + \text{False Negatives}} \quad (1)$$

$$\text{Specificity} = \frac{\text{True Negatives}}{\text{True Negatives} + \text{False Positives}} \quad (2)$$

A cohort study would be designed to evaluate sensitivity and specificity in realistic conditions. Since the prevalence of heart arrhythmia is expected to be 1.5-5%, a sample size of 3980 is required to achieve a p-value less than 0.05 and a power of 80% [99]. Due to the large sample size needed and the lack of

access to the wearable firmware, testing the project through the sensors and using a real cohort is outside this project's scope.

Instead, the Charlton et al. [79] and the Clifford et al. [78] datasets will be used to test the machine learning algorithm's sensitivity and specificity. The reported positives and negatives from the algorithm will be cross-referenced with the positives and negatives in the datasets to count the number of true/false positives and true/false negatives. Then the sensitivity and specificity will be calculated using the given formulas.

#### Test 3: Sampling Frequency Verification Based on ECG Signal Requirements

Applying the Shannon-Nyquist Theorem, the sampling frequency must be greater than or equal to twice the highest frequency that the device can measure to ensure enough data is collected and to avoid oversampling [100]. The highest frequency in an ECG signal is 150 Hz [87]. Therefore, the sensors must have a sampling frequency greater than or equal to 300 Hz. This means that sampling should happen at least 300 times per second. Therefore, the largest period between samples should be calculated to be 1/300, which is 3 ms.

The internal clock in the wearable can be used to measure the time between the collection of two data points also known as the sampling interval. This measurement will be taken for 100 data points to calculate the average sampling interval ( $\Delta t$ ). The sampling frequency (Fs) can be calculated from the sampling interval using formula (3) [101].

$$Fs = \frac{1}{\Delta t} \quad (1)$$

#### Test 4: Verification of Non-Invasiveness and Class I Medical Device Compliance

The device is intended to be used independently by the user without any supervision so it must be noninvasive and easy to use as specified in the definition of Class I Medical Devices. The device must comply with the Medical Devices Regulations (SOR/98-282) definition of a Class I Medical Device from sections 10 to 20 to validate that the device is noninvasive [102].

This can be verified by checking if the device adheres to rules 4 to 7 of the Guidance on the Risk-Based Classification System. The device must pass the following criteria mentioned in the rules. The device usage must not be intended for injured skin. The device must not channel or store gases, liquids, tissues or body fluids. The device must not modify the biological or chemical composition of body fluids or liquids. The device must not be connected to a Class II, III, or IV device. The device must not act as a calibrator, tester or quality control support [103] We will prepare a checklist with rules 4 to 7 and verify that the device satisfies all the rules.

#### Test 5: Wearable Adjustability Assessment for Diverse Wrist Sizes

The wearable will be used by a variety of individuals of different sizes so it must be adjustable for all users' wrist sizes. The wearable must accommodate for circumferences from 10 cm to 25 cm which is the range of wrist sizes in adults [90]. The circumference of the wearable can be measured manually using a measuring tape to assess if it satisfies the size requirements.

#### Test 6: Allergenicity Assessment via Human Repeated Insult Patch Test (HRIPT)

The wearable will be used for long time periods regularly by the user so it shouldn't trigger any allergic reactions that would cause the user to discontinue its usage. Verify Human Repeated Insult Patch Test (HRIPT) results on all materials used in the casing which will assess if the materials can pose allergies.

At least 100 participants that are between the ages of 18 and 70 will be recruited. 0.3 mL or g of each material used in the casing of the wearable is placed on an individual test patch and the patches are applied to normal skin on the back from 15 to 40 minutes. A control patch with saline is also applied. The procedure is repeated until 9 induction applications of the test article are made. The patch sites are scored for the presence and severity of erythema, edema, papules, vesicles, and bullae.

Then 10 days after the last test, a single patch is applied to a naive site on the back. Those who exhibit skin reactivity undergo one final test where occlusive and semi-occlusive patches are applied along with the control to the back [104]. The result of HRIPT is the percentage of induced sensitization reactions observed in the total number of participants which should be less than 2.9% for all materials [92]. Due to the cost and time required to complete the HRIPT, this test will be omitted.

#### Test 7: Scratch Resistance Testing of Wearable Casing Materials

Since the user will be wearing the device for long time periods regularly, the device may be handled roughly by accident. The device should be able to withstand the slight rough handling and still be functional. Scratch tests based on the ASTM D7027/ISO 19252 standards on materials used in the wearable casing can be used to assess the durability of the device [79].

Test Mode A will be performed where a scratch is applied onto the surface of the wearable under an increasing normal load from 2 to 50 N over a distance of 0.1 m at a constant scratch rate of 0.1 m/s. The material should not exhibit failure from 2 to 50 N [105]. Since the wearable must be returned to its rightful owner at the end of this project, the wearable can not be subjected to any tests that may cause damage. Therefore, this test will be omitted.

#### Test 8: Drop Resistance Testing Based on Average Adult Height

The average height of adults in Canada from ages 60 to 79 is 165.32 cm so the device must survive height falls from this height [106]. The Drop and Shock test will be performed according to MIL-STD-810G to assess the ability of the wearable to survive falls. The device should be dropped 10 times from a height of 170 cm after which the device must still be functional [95]. This test will not be done to avoid permanent damage to the wearable.

#### Test 9: Water Resistance Evaluation Using 1-Metre Submersion Test

While the device is not intended to be used when engaging with water, it's possible that light splashes can occur while washing hands for example or rain can come in contact with the device. The device must be able to survive these mild contact scenarios with water and still remain functional. The water resistance ability of the wearable will be assessed using the 1-metre water submersion test [96].

The wearable will be submerged in a container of water that is 1-metre deep for 30 minutes. After the device is removed from water it will be dried and tested for functionality. The device's ECG and PPG sensors will be assessed for accuracy in comparison to the golden standard procedures on the same group of participants. Then, the machine learning algorithm and data processing algorithms will be tested using the datasets to verify that the device can still correctly diagnose people using the ECG and PPG parameters. This entire test will be repeated on the wearable in 3 trials. This test will not be done to avoid permanent damage to the wearable.

#### Test 10: Hardware Response Time Measurement for Real-Time User Feedback

Users tend to lose attention or become disinterested once software takes more than 5 seconds to respond. Thus to make the device easy to use and satisfactory for users its response rate must be reasonable. It's also important to have a quick response rate to have the effect of real-time data collection and feedback response effect on the user.

The hardware response time rate refers to the time it takes for the LED to display the results of the machine learning algorithm on the LCD. This can be measured by connecting an oscilloscope to pins 7-14 on the LCD which receive the data that will be displayed. The oscilloscope will display a voltage vs time graph from which the duration when the pins are high can be observed using the oscilloscope's measure functions. The pulse width will correspond to the response time. The hardware response time will be assessed for both scenarios of arrhythmia and no arrhythmia and the average will be taken across multiple trials [107]. Due to the limit of time and resources for this project, the number of trials will be limited to 10 for the arrhythmia and no arrhythmia scenarios.

### 3.2.4 Verification Plans for Mitigation Strategies

Risk: inaccurate arrhythmia detection

Two mitigation strategies will be used to resolve inaccurate arrhythmia detection, using appropriate signal processing techniques, and displaying a confidence score for each arrhythmia detection.

Signal processing techniques to minimize inaccurate arrhythmia detection involve using adaptive filtering techniques to remove motion artifacts and baseline wander. Motion artifacts refer to unwanted noise introduced in the system due to movement, and typically manifest as high-frequency noise in the signal. By designing a band-pass filter, it is able to suppress unwanted noise components that lie outside the physiological range of 0.05-100 Hz [108]. Baseline wander refers to the slow, low-frequency variations in the signal, typically caused by breathing, electrode drift, or poor skin contact. These manifest as low-frequency fluctuations and can distort the true signal [109]. The applied adaptive filter method will be based on the NRFIR filter described in the J.A. Van Alste et al. paper, which outlines a filter with a reduced number of coefficients [109]. The second mitigation strategy for inaccurate arrhythmia detection is to display a confidence score for each arrhythmia detection, indicating how certain the algorithm is about its results (e.g., low, medium, or high confidence). This provides users with additional context on the reliability of the results, helping them make informed decisions. In cases of low confidence, the system can prompt users to retake measurements or seek medical advice. Additionally, tracking confidence scores over time can help refine the model and improve detection accuracy through continuous learning and updates.

Verification plan

In order to verify the effectiveness of the proposed signal processing methods and the confidence scores, the following verification plans will be performed. To verify the effectiveness of the signal processing methods a combination of open-source datasets, and real-time validation using data collected from the biomedical instrumentation lab will be used. Performance metrics will be evaluated by using (1) signal-to-noise ratio (SNR), (2) Root Mean Square Error (RMSE), and (3) power spectral density (PSD) analysis. The verification approach would require introducing synthetic baseline drift and motion artifacts by adding noise from recorded accelerometer data to a clean reference ECG signal from the datasets. (1) The SNR measures the level of the desired ECG signal relative to the background noise, with higher SNR values indicating a clearer signal with the desired value being 10.064, the highest value of white Gaussian noise that was detected [110]. (2) The RMSE will be used to measure deviation from the clean signal with lower RMSE values signifying better performance with the desired value being 0.1576, the highest value of white Gaussian noise detected [39, 40]. (3) PSD analysis provides information into the power distribution of the ECG signal across different frequency components. Typical ECG signals exhibit prominent peaks in the PSD at frequencies corresponding to the heart rate (1 Hz), T wave (~4Hz), p wave (~7Hz), and the QRS complex (10 Hz). The PSD will be computed using FFT on the ESP32

microcontroller. It will be estimated by squaring the FFT magnitude and normalizing it by the number of samples [112].

The confidence score for each arrhythmia is to be verified by using different verification objectives such as (1) confidence probability alignment, (2) Edge case evaluation, and (3) Performance under noise. For (1) datasets with known probability outputs will be used to validate the confidence scores, ensuring that they accurately reflect the expected probability distribution and meet the defined thresholds [113]. For (2), predictions with values that are close to the classification boundaries and assess the model's confidence score around these thresholds to ensure they are correct. (3) Based on the previous mitigation strategy, various noise types should be introduced in the ECG signal, such as Gaussian noise, baseline wander, and motion artifacts.

#### Risk: delayed or inaccurate arrhythmia detection

The two mitigation strategies that will be used to minimize delayed or inaccurate arrhythmia detection will be the implementation of optimized FFT for ECG signal processing, employing parallel processing, and feature elimination.

Implement optimized FFT for ECG signal processing to ensure fast frequency-domain analysis, reducing computational overhead. Optimizing the FFT mainly relies on focusing only on relevant frequency components while ignoring unnecessary calculations; the Relevant ECG frequencies lie between 0.05 and 100Hz, and ignoring any negative frequencies as they are redundant in real-valued signals. The second method would be to employ parallel processing on the ESP32 to offload computational tasks, allowing simultaneous signal analysis and feature extraction to speed up processing and enhance model performance. The final mitigation strategy is to regularly use cross-validation and to implement feature elimination techniques to remove irrelevant features that do not contribute to the prediction accuracy. Recursive feature elimination (RFE) is a feature selection algorithm that fits a model and removes the weakest feature until the specified number of features is reached [114].

#### Verification plan

To verify the effectiveness of FFT optimization and parallel processing, the following verification plans will be followed. The verification process for the FFT optimization would require the comparison of the optimized FFT to the non-optimized FFT by conducting (1) computational benchmarking, (2) Accuracy, and (3) memory profiling tests. Profiling tools such as python's "timeit" function allows for comparison of execution times [115]. This will involve running both FFTs on the ESP32, and observing the time differential between the two sets of FFT. This will also need to be evaluated alongside the (2) accuracy of the model, as in theory the optimization completed should not affect the accuracy of the data. Finally for (3) the memory\_profiler function can be called to track memory consumption, and will be evaluated for both the optimized and non-optimized FFT [116]. To verify the impact of parallel processing, processing time can be assessed by measuring and comparing the time it takes for parallel and sequential processing to run. The internal clock on the MAX17260 can be used to measure the execution time of the machine learning algorithm. The execution time on sequential and parallel processing can be used to calculate the speed-up ratio which is a metric of algorithm performance and speed. A speed-up value greater than 1 indicates that the algorithm has been optimized compared to its previous version [117].

$$S_p = T_i/T_p$$

$T_i$  = execution time of the original algorithm.

$T_p$  = execution time of the optimized algorithm.

$S_p$  = speed-up ratio

To verify the final mitigation strategy, the model will be trained on a labeled dataset with and without feature elimination algorithms to compare the difference in accuracy.

$$\text{Accuracy} = \frac{\text{Correct Predictions}}{\text{Total Predictions}}$$

The number of correct predictions will be the number of diagnoses by the model that correctly aligns with the number of diagnoses found in the labeled dataset. Improvement in the performance of the model can be observed when the accuracy after feature elimination is closer to one in comparison to the accuracy of the model without feature elimination [118].

Risk: device firmware crashes

The last mitigation strategy that will need to be implemented is to develop automated tests to detect when the firmware fails to respond, hangs, or enters an infinite loop, and integrate watchdog timers to reset the device in case the firmware enters an unresponsive state.

Verification plan

In order to verify firmware fails, many test cases will need to be implemented such as (1) Hardware or memory failure simulation, (2) communication failures, (3) long-term stress test, (4) power cycle test, and (5) device recovery. It would be necessary to simulate hardware failure scenarios that involve faulty sensory data, and memory corruption to observe how the firmware handles these failures, and whether the device can self-recover by resetting without external intervention. Communication failures should be simulated and the watchdog timer should be triggered if the firmware fails to handle these issues and doesn't continue to wait indefinitely. Long-term stress tests should be conducted in which the device firmware is run for extended periods of time, and the watchdog timer should successfully reset the device upon any failure. The device shall also be power-cycled multiple items to observe if the firmware initialized correctly after being reset by the watchdog timer. The device shall also fully recover after a watchdog reset without any manual intervention; all hardware and software components should return to operational state [48, 49].

## 4.1 Implementation

Embedded Software Architecture and Pipeline Overview

The software prototype consists of two main components: the feature extraction code and the embedded machine learning model, both implemented in C++ to operate efficiently on the ESP32-PICO-D4 microcontroller. The implementation was developed with a focus on real-time performance, modularity, and low power consumption, tailored to the constraints of the embedded system.

*Core Software Implementation Pipeline Components*

### 1. Feature Engineering, Extraction, and Dimensionality Reduction

A comprehensive set of ECG and PPG features was collected, analysed, and resampled where necessary to support robust arrhythmia classification. These features were derived through a combination of

evidence-based selection from literature and team-driven brainstorming (see Tables 2 and 3). They encompassed a range of physiological markers, including:

- Time-domain ECG features such as RR intervals, QRS width, heart rate variability (HRV), and morphology-based indicators like P wave and T wave presence.
- Time-domain PPG features include pulse width, rise and fall times, peak-to-peak intervals, and pulse transit time (PTT) derived by aligning ECG R-peaks with PPG peaks.
- Frequency-domain features extracted using Fast Fourier Transform (FFT) to capture periodicities and spectral differences between rhythms, especially useful in identifying atrial fibrillation.

Due to the absence of C++ libraries for biomedical signal processing on embedded systems, all feature calculations were implemented manually in C++ to ensure full compatibility with the ESP32. The only exception was FFT, which leveraged an external library based on the Cooley-Tukey algorithm, offering a time complexity of  $O(n \log n)$ . This approach provided an efficient balance between accuracy and performance for computing frequency-domain features in real time.

After implementing the full feature set, an iterative feature selection and reduction process was performed. The trained Random Forest model, embedded with the ESP32, automatically calculated the relative importance of each feature. Features were ranked and progressively eliminated from least to most important to reduce model complexity and computation time.

However, rather than using only the overall accuracy metric, the confusion matrix was monitored at every step to ensure that no specific arrhythmia class—particularly minority types such as ventricular flutter or bradycardia—was disproportionately affected. This helped preserve class-wise sensitivity while minimizing overfitting.

The iterative pruning process continued until the model's classification performance began to decline. At this point, the remaining subset was finalized as the optimal feature set, balancing predictive power and resource efficiency. This approach ensured that the system could maintain high accuracy and responsiveness on a constrained embedded platform, without compromising its ability to differentiate between arrhythmia types.

## 2. Machine Learning Model Selection and Embedded Integration

Following feature extraction, several machine learning algorithms were evaluated using cross-validation to determine the optimal approach for arrhythmia classification. The Random Forest classifier consistently outperformed other models in both accuracy and generalizability, particularly when using the combined ECG + PPG feature set. This setup yielded better performance than ECG-only, PPG-only, or even stacked model configurations (see Figure 6), highlighting the complementary value of multimodal signal input.

Once trained, the final Random Forest model was converted into embedded-compatible C++ code using a custom Python script. The translated model consists of 50 decision trees, each implemented as a series of

nested `if` statements, with predictions aggregated through majority voting to determine the final classification result. This raw logic was integrated as a function within the ESP32 firmware.

By converting the model into pure C++ rather than relying on external inference libraries, the system achieved full compatibility with the ESP32's architecture while preserving inference speed and accuracy in a resource-constrained environment.

### 3. Sampling and Multithreading in a Resource-Constrained Environment:

In a resource-constrained environment like the ESP32, efficient task management is essential to ensure real-time performance. To handle this, the system employs multithreading using a built-in library, which allows for concurrent data sampling and processing. The ESP32, with its dual-core architecture, allows tasks to be bound to each core, ensuring that they do not compete for resources.

The ECG and PPG data are stored in separate circular FIFO buffers (first-in, first-out), which act as shared buffers accessible by both threads. Each thread has its own local buffer to handle its respective task, ensuring that the threads do not directly interfere with each other's data processing. This architecture allows the sampling thread to collect ECG and PPG data every 8 ms, while the processing thread performs FFT calculation, feature extraction, and arrhythmia prediction without delaying the sampling.

Figure 25 below illustrates the multithreading architecture, showing how the ECG and PPG data are handled in separate circular FIFO buffers and shared between threads for efficient sampling and processing. The diagram highlights the roles of each thread—sampling and processing—and how their respective local buffers prevent interference while ensuring continuous data flow and real-time performance.

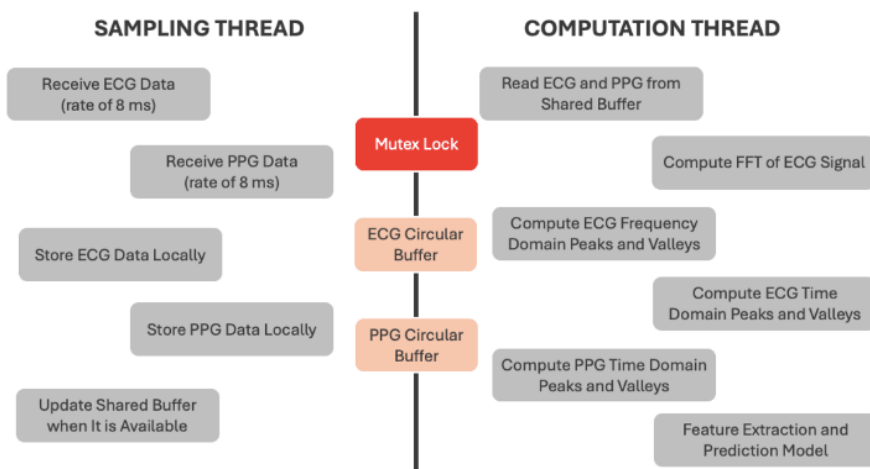


Figure 25: Diagram showing the multithreading architecture with separate circular FIFO buffers for ECG and PPG data. One thread handles sampling every 8 ms, while the other performs FFT, feature extraction, and arrhythmia prediction without data interference.

By using the circular FIFO buffers, the system can ensure that data is continuously updated and accessible to both threads without risking data corruption. This design prevents any task from blocking or delaying the other, ensuring that sampling occurs at the required frequency while still allowing for accurate and timely processing of the signals.

This approach optimizes the performance of the system in a resource-limited environment, balancing real-time data collection and computationally expensive tasks such as FFT and feature extraction, without compromising the sampling rate.

#### **4. Testing and Model Evaluation:**

To avoid overfitting and gain a comprehensive understanding of the model's accuracy, both cross-validation and zero-shot learning were employed. Zero-shot learning involves testing the model on data from patients it hasn't encountered during training, ensuring the model's generalizability to new, unseen cases. The Random Forest model, which automatically calculates feature importances, was used for feature elimination. The least important features were removed incrementally, and the model's performance was monitored for significant accuracy degradation. To ensure that no arrhythmia type was negatively impacted, the full confusion matrix, rather than just the overall accuracy score, was used as the evaluation metric. This approach prevented the removal of features critical to specific arrhythmia types, ensuring a balanced performance across all classes.

#### **5. Model Verification and Validation:**

To ensure the features had sufficient predictive power, Uniform Manifold Approximation and Projection (UMAP) was used to visualize how well different arrhythmia classes could be distinguished based on the available data. To validate the feature extraction process, the feature values of identical samples were compared between C++ (for ESP32) and Python implementations. This comparison ensured that the features were consistent across languages, allowing the model trained in Python to be effectively transferred to the ESP32.

For threading verification, the time elapsed between consecutive samples was measured to confirm that the sampling period remained consistent, regardless of the time-consuming feature calculation process. The device's performance was also video recorded while making predictions, and the refresh time between predictions was estimated from the video to ensure the system's real-time capabilities met the project requirements.

In addition, model performance was evaluated by calculating precision, sensitivity, true positives (TP), true negatives (TN), false positives (FP), and false negatives (FN). These metrics provided a

comprehensive assessment of the model's accuracy in detecting different arrhythmia types, helping to fine-tune its performance.

#### Hardware Prototype Design and Implementation for Real-Time ECG and PPG Data Processing

The hardware prototype consists of an ESP32 microcontroller for real-time data processing, a 16x2 LCD display for user feedback, and a computer to simulate patient data such as ECG and PPG waveforms. The computer sends data to the ESP32 through USB serial communication at a sampling rate of 125 Hz. To manage timing precision and CPU efficiency a multi-threaded approach was implemented to take advantage of the ESP32's dual-core architecture. One of the threads was used for data collection, in which the incoming PPG and ECG signals were stored in separate circular buffers. The second thread handled all data processing operations, such as applying the fast fourier transform, and extracting the features used by the TinyML model. A mutex-lock ensures synchronization of the access to the buffers, allowing the threads to run concurrently while avoiding data corruption. The ESP32 is able to process and classify the data in real-time and display the classification on the I2C-connected LCD.

#### Design Implementation:

**Building:** The system was built using an ESP32 microcontroller, a 16x2 I2C LCD display, and a computer acting as the data source. The components were assembled and integrated into a 3D-printed housing. The LCD was connected to the ESP32 via GPIO pins 21, 22, GND, and 5V. The ESP32 firmware was developed using Arduino, which incorporated prebuilt libraries for serial communication, I2C LCD control, and FFT computation.

**Testing:** Testing began by confirming that the ESP32 correctly received and stored data from the computer. Simulated ECG and PPG waveforms were streamed to validate signal consistency and timing. The FFT and feature extractions were then tested using known input signals to ensure correct outputs.

The system was evaluated for:

- Buffer integrity during continuous streaming
- Consistency of FFT results
- Correct TinyML predictions using labeled datasets
- Accuracy of LCD messages corresponding to classification outcomes

**Verification:** To verify system performance, the following steps were taken:

- Pre-labeled biosignal data was streamed into the ESP32, and the classifications were compared against ground truths
- The system was stress-tested with extended full datasets to ensure it could maintain a stable sampling rate and inference speed without data loss or crashes.
- The real-time LCD output was monitored for consistent and responsive feedback based on the model's results.

#### Mechanical

The final mechanical prototype consists of a custom 3D printed housing designed to hold the ESP32 and LCD modules, as seen in figure 10, with the final output being in figure 26. The enclosure was designed in

Autodesk Inventor, and is composed of two parts: the base and a lid which is held by 4 screws. The base features an opening on the side allowing for the micro usb connection to the ESP32 for communication. The lid fits securely over the base, providing protection for internal components while exposing the LCD for user interaction. The housing was printed using PLA filament.

### **Design Implementation:**

**Building:** The housing design was exported from Autodesk Inventor and sliced using a PRUSA slicer. The base and lid were printed separately and assembled using 4 screws at the mounting holes.

**Testing:** Fit tests were conducted with the ESP32 and the LCD modules to ensure proper alignment and secure testing within the casing. .STEP models of the ESP23 and LCD were imported in the assembly to complete the initial fit test

**Verification:** The mechanical design was verified by assembling the complete prototype and confirming usability, specifically the visibility of the LCD, and accessibility of power connections.



Figure 26: Final 3D printed mechanical design

## 4.2 Results and Discussion

### Software

#### Signal Sampling and Threading Performance on the ESP32

The system was designed to operate with a fixed sampling frequency of 125 Hz, corresponding to a sampling period of 8 ms. This was implemented using a multi-threaded architecture to ensure concurrent data acquisition, processing, and LCD feedback. Our threading model successfully maintained a consistent average of 8 ms intervals over extended runs without significant drift or lag, verifying its

reliability in real-time operation (Figure 27). This timing consistency is critical in embedded systems where sampling jitter can lead to signal distortion or misalignment with expected heart event intervals (e.g., RR peaks).

```
FFT result line: 8 ms. Skipping this line.  
FFT result line: 9 ms. Skipping this line.  
FFT result line: 9 ms. Skipping this line.  
FFT result line: 7 ms. Skipping this line.  
FFT result line: 9 ms. Skipping this line.  
FFT result line: 9 ms. Skipping this line.  
FFT result line: 9 ms. Skipping this line.  
FFT result line: 7 ms. Skipping this line.  
FFT result line: 8 ms. Skipping this line.  
FFT result line: 9 ms. Skipping this line.  
FFT result line: 9 ms. Skipping this line.  
FFT result line: 8 ms. Skipping this line.  
FFT result line: 9 ms. Skipping this line.  
FFT result line: 8 ms. Skipping this line.  
FFT result line: 8 ms. Skipping this line.
```

Figure 27: resultant sampling period after threading

While 125 Hz meets the minimum threshold for coarse ECG analysis, it introduces aliasing risks for high-frequency components. Many clinically important ECG components (e.g., QRS detail or P-wave morphology) reside closer to 100–150 Hz. With 125 Hz, the Nyquist limit of 62.5 Hz may truncate these, reducing model granularity. However, key time-domain features such as rr\_median and rr\_std are still effectively captured at this rate, making the setup suitable for broad arrhythmia detection tasks like AFIB, bradycardia, and tachycardia classification.

#### Feature Extraction and Class Variability

Feature engineering was central to the software pipeline. A random forest model was trained on all samples to obtain the feature importances. Starting from the least important features, feature elimination was performed, retraining the model with each feature removed in turn. Removing the 14 least important features had no impact on model performance, but removing the 15th (diastolic\_time) greatly degraded model accuracy. Therefore, the model can be reduced to the top 5 most important features:

- num\_peaks, num\_valleys (ECG frequency-domain)
- rr\_median, rr\_std (ECG time-domain)
- diastolic\_time (PPG time-domain)

Figure 28 shows the accuracy of the model with 19 features compared to the top 5 features only, proving the remaining features had no significant contribution or were redundant. A scatter plot of num\_peaks vs. num\_valleys (Figure 29) revealed visually separable clusters for some arrhythmia classes, suggesting the discriminative potential of these statistics.



Figure 28: Confusion matrices before and after feature elimination. The left matrix shows the model's performance with all features, while the right reflects improved classification accuracy after removing less informative features.

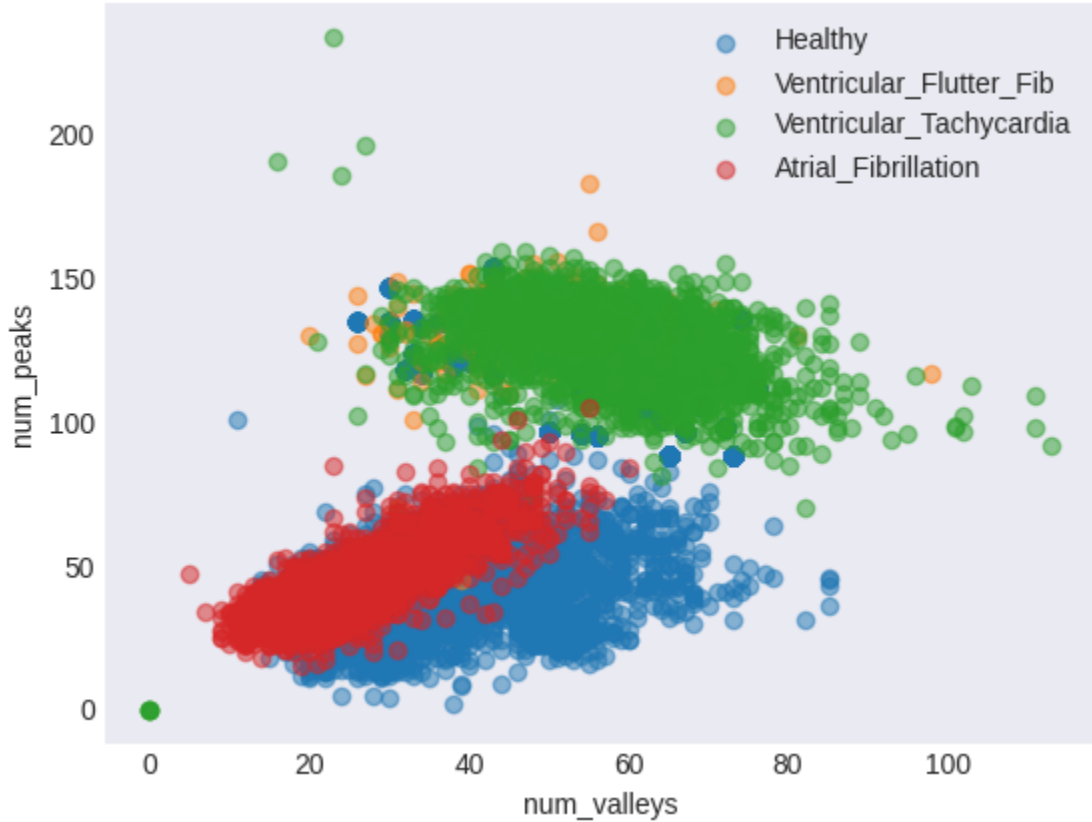


Figure 29: Scatter plot showing the variance in num\_peaks and num\_valleys across selected arrhythmia types, highlighting their potential for distinguishing between classes.

To further evaluate class separability, UMAP (Uniform Manifold Approximation and Projection) was used to reduce the high-dimensional feature space into 2D for visualization purposes. As shown in Figures (30, 31, 32) different arrhythmia classes showed distinct clustering, validating that the selected features encode meaningful rhythm characteristics.

## UMAP projection

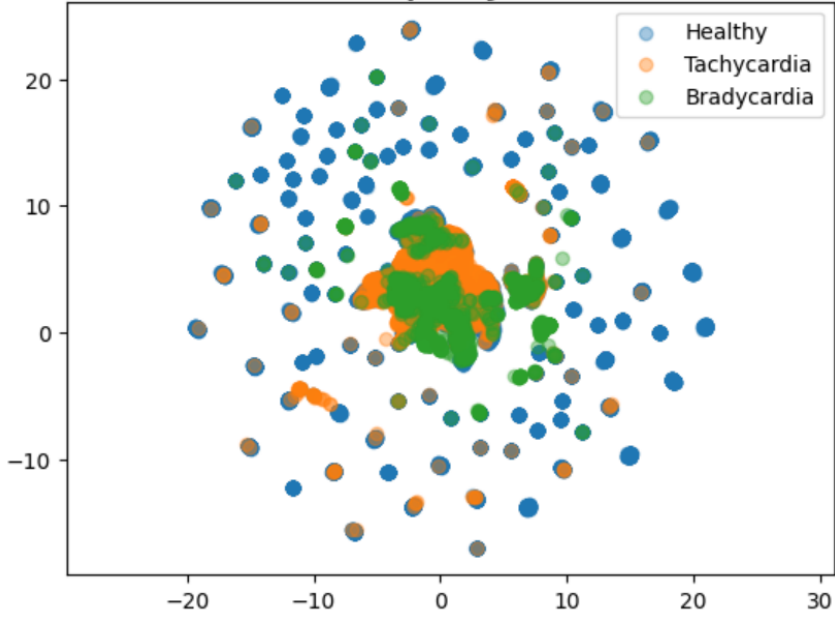


Figure 30: UMAP projection illustrating the variance between healthy, tachycardia, and bradycardia samples.

## UMAP projection

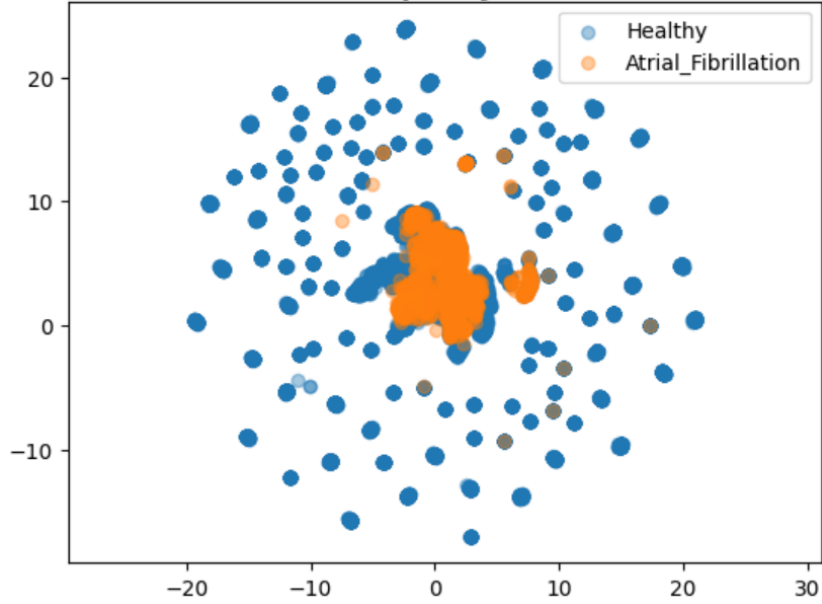


Figure 31: UMAP visualization highlighting the variance between healthy and atrial fibrillation samples.

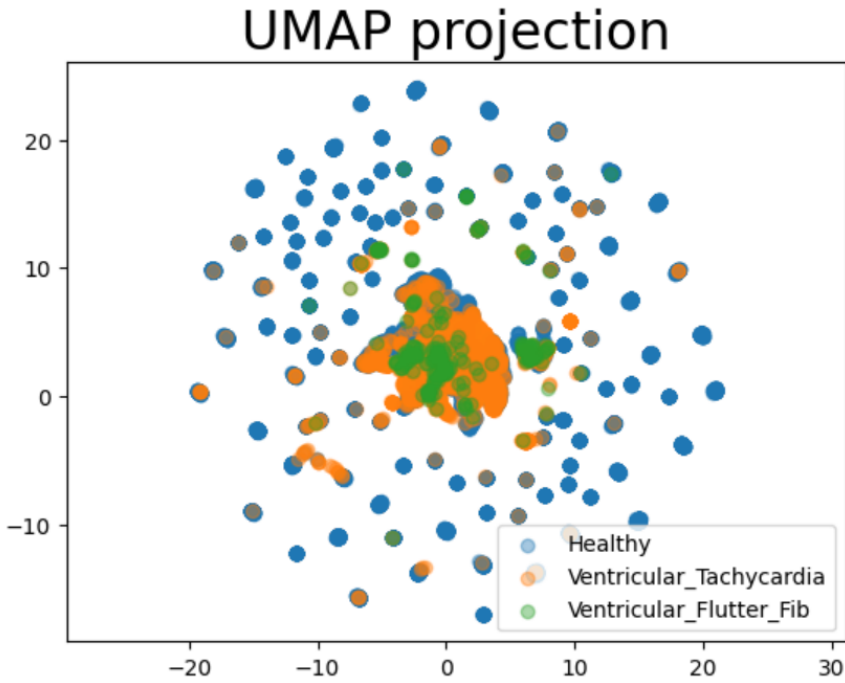


Figure 32: UMAP showing variance between ventricular tachycardia and ventricular flutter/fibrillation

#### Machine Learning Model Accuracy and Verification Results

Four experimental setups were used to evaluate model structure and hardware/software constraints: ECG-only model, PPG-only model, stacked model (Figure 18) and combined model. As shown in Figure 33, confusion matrices were generated for each configuration, highlighting trade-offs between complexity, accuracy, and resource use. The best performance was observed in the configuration using a single random forest classifier with all five selected features (combined model), achieving sub-5s inference time and moderate sensitivity.

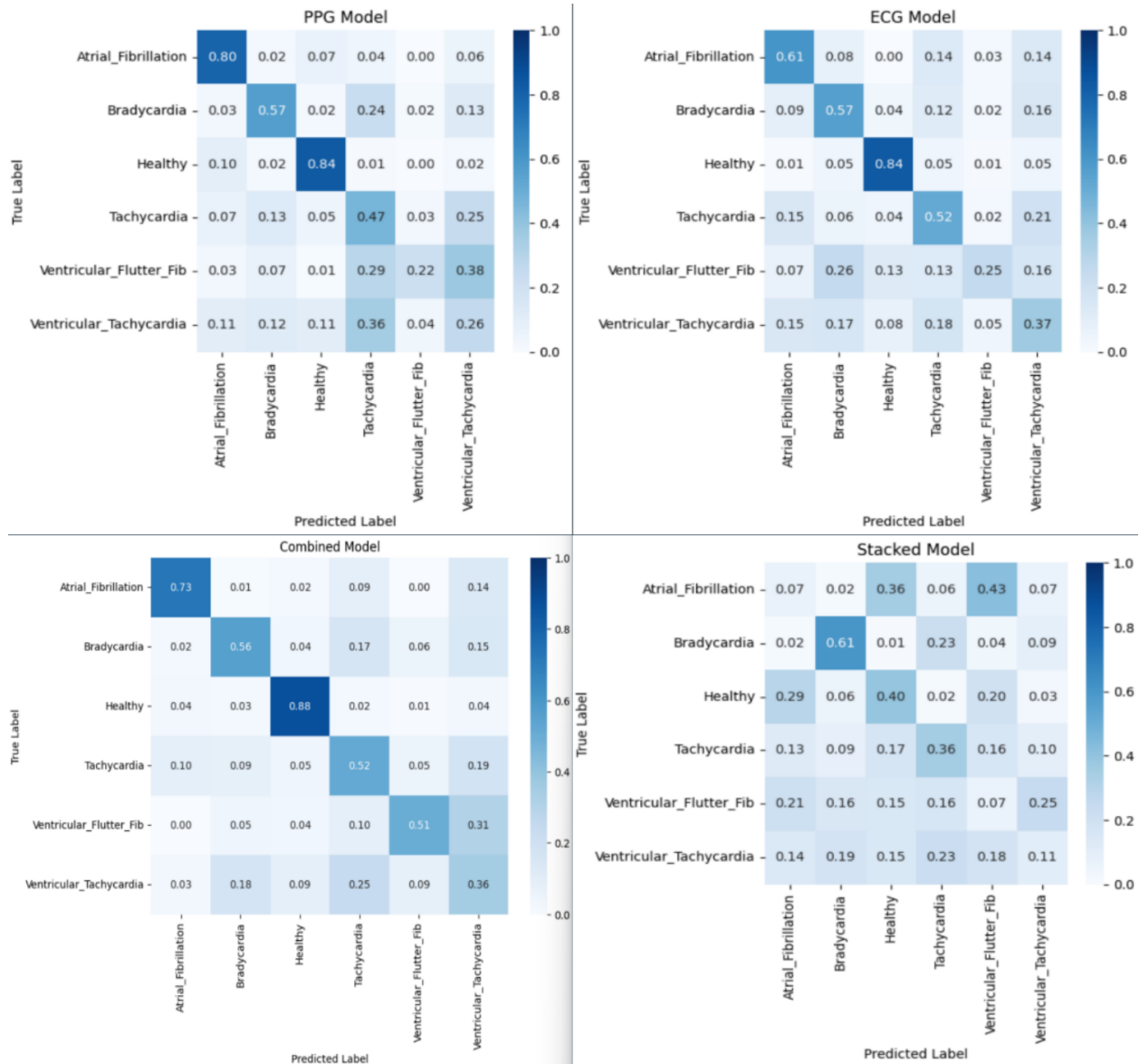


Figure 33: Confusion matrices comparing classification accuracy across four setups. Top left: PPG model; top right: ECG model; bottom left: combined PPG and ECG model; bottom right: final optimized model.

As shown in Table 8, the model's performance varies across different arrhythmia types. Precision was generally low, with the highest for healthy samples (15.6%), followed by bradycardia (12.1%) and tachycardia (10.5%). Atrial fibrillation (AFib) had the lowest precision at 7.17%, suggesting a higher rate of false positives for this class. Sensitivity values, however, were comparatively better, especially for healthy (79.2%) and bradycardia (64.6%) classifications. Tachycardia and ventricular flutter/fibrillation achieved moderate sensitivity (50% and 51%, respectively), while AFib and ventricular tachycardia showed the lowest sensitivities at 35% and 40%, respectively. These results highlight the model's stronger ability to detect healthy and bradycardia cases, while detection of other arrhythmias remains more

challenging. All in all, while precision was low due to class imbalance and overlapping feature spaces, sensitivity values were more promising, particularly for bradycardia and healthy cases.

Table 8: Summary of overall classification results, including true positives (TP), true negatives (TN), false positives (FP), false negatives (FN), precision, and sensitivity for each arrhythmia type.

<b>Arrhythmia Classification</b>	<b>True Positive (%)</b>	<b>False Positive (%)</b>	<b>False Negative (%)</b>	<b>True Negative (%)</b>	<b>Precision (%)</b>	<b>Sensitivity (%)</b>
<b>Atrial Fibrillation</b>	<b>5.83</b>	<b>7.83</b>	<b>10.83</b>	<b>75.5</b>	<b>7.17</b>	<b>35.0</b>
<b>Bradycardia</b>	<b>10.67</b>	<b>5.83</b>	<b>5.83</b>	<b>77.67</b>	<b>12.1</b>	<b>64.7</b>
<b>Healthy</b>	<b>13.33</b>	<b>5.17</b>	<b>3.5</b>	<b>78.00</b>	<b>15.6</b>	<b>79.2</b>
<b>Tachycardia</b>	<b>8.33</b>	<b>12.67</b>	<b>8.33</b>	<b>70.67</b>	<b>10.5</b>	<b>50.0</b>
<b>Ventricular Flutter Fibrillation</b>	<b>8.5</b>	<b>4.67</b>	<b>8.17</b>	<b>78.67</b>	<b>9.75</b>	<b>51.0</b>
<b>Ventricular Tachycardia</b>	<b>6.67</b>	<b>10.50</b>	<b>10.00</b>	<b>72.83</b>	<b>8.39</b>	<b>40.0</b>

#### Dataset Limitations and Software Implications

The use of pre-recorded datasets introduced key constraints on software validation. These datasets lacked:

- Real-time variability (e.g., motion artifacts, poor electrode contact)
- Demographic diversity (skin tone, body composition affecting PPG)
- Real-world noise typically observed in wearable sensors

This limited the model's ability to generalize, resulting in high false positive rates and reducing real-world robustness. Additionally, the datasets were imbalanced, leading to skewed performance metrics (e.g., lower precision for rare arrhythmias like ventricular flutter).

#### Hardware

##### Memory Overflow

The system was designed to operate with a fixed sampling frequency of 125 Hz, corresponding to a sampling period of 8 ms. This rate was chosen as a trade-off between signal fidelity and memory management as multithreading ensured concurrent data acquisition, processing, and LCD feedback. However, testing was not thoroughly tested for extremely large datasets, or for over extended durations.

This poses a potential risk of buffer overflow, especially with continuous operation. In earlier iterations, when using a sampling frequency of 250Hz, both the ECG and PPG buffers overflowed overtime, leading to data corruption and instability in the processing pipeline. Reducing the sampling rate to 125 Hz was intended to mitigate that issue, but there has not been sufficient long-duration testing conducted to confirm the problem has been fully resolved. As such, memory limitations remain as a constraint.

### LCD Screen

The LCD screen showed negligible latency. However, shaking the device caused a persistent glitch in the LCD, which started showing illegible characters. This glitch was only fixed by restarting the device, which proves it was not the wiring, but the device and LCD screen losing I2C synchronization.

## 4.3 Future Work

### Software

#### **Expanding Datasets**

The first step in future work will be to find additional datasets, particularly those containing more patient data on ventricular flutter fibrillation. The current iteration of the ML algorithm was trained on data from only six patients for each category, as only six patients with ventricular flutter fibrillation were present in the datasets. Therefore, the performance of the ML algorithm will improve once it is trained on more data.

#### **Addressing Wearable vs. Open-Source ECG Data Differences**

Next, addressing the differences between ECG data found in wearables and ECG data in open-source datasets is a key challenge. A potential solution could be to establish a "standard form" to which ECG signals could be converted. Alternatively, a more complex solution would involve collecting arrhythmia data directly from patients using the wearable device.

#### **Optimizing Peak Detection**

Peak detection should also be further tuned to achieve the best differentiation between arrhythmia types, rather than simply optimizing for perfect peak identification, as was done in this experiment. This will help improve the model's ability to distinguish between arrhythmia types more accurately.

#### **Handling Signal Shifts**

To address vertical shifts in signals, a high-pass filter should be implemented before standardization. Currently, standardization only accounts for variability between patient files but not within the same file, leading to potential inaccuracies.

#### **Reducing Calculation Time for Faster Predictions**

From a timing perspective, reducing calculation time will be crucial for increasing the prediction rate. Future work will focus on improving the system's real-time performance by sampling data at a faster rate (e.g., 4 ms instead of 8 ms). This will allow the system to provide more frequent predictions and enhance its real-time capabilities.

### **Wearable Integration and C++ to C Transition**

Once the firmware for the wearable is available, the machine learning model code and feature extraction routines should be translated from C++ to C, and the program should be fully integrated with the wearable sensors to create a fully operational device. This will ensure that the wearable device is able to collect and process data seamlessly.

### **Generalizing the Model for Multiple Wearables**

Efforts will also focus on improving the accuracy of the model and generalizing it for compatibility with any wearable device. To achieve this, the system should be designed to be flexible, with a modular approach to sensor input, signal preprocessing, and feature extraction. The model should be trained on data from multiple wearable devices to account for differences in sensor hardware, placement, and signal quality.

### **Device-Specific Calibration and Feature Extraction**

Additionally, incorporating device-specific calibration routines and adapting the feature extraction methods based on the device's capabilities will ensure that the system can work across different wearables with varying sensor specifications and processing power.

### **Using Annotated Data to Improve Model Accuracy**

Finally, increasing the use of more annotated and labeled data, particularly data that tracks transitions from healthy to arrhythmia states (e.g., from healthy to atrial fibrillation), will improve model accuracy. This will enable the system to detect early signs of arrhythmias and classify different stages of heart conditions more accurately.

### **Refining Chunk Labeling and Segmentation**

An important challenge to address is that while we know a patient file may contain arrhythmias like atrial fibrillation (AFIB), we cannot always be certain that each chunk or window of data accurately represents that arrhythmia. To mitigate this, further refinement of chunk labeling or the use of advanced segmentation techniques will be needed to ensure that the model can make reliable predictions from small, variable segments of data.

## **Hardware**

The current design of the device uses ECG and PPG data from published datasets to train and test the ML algorithm. Upon refining the ML algorithm, ECG and PPG sensors should be interfaced with the microcontroller to control live data from a real human subject. Appropriate sensor modules must be selected such that they are small and compact to fit in a wearable device while also providing accurate data. It may be necessary to conduct research on different sensors to identify ones that perform well on various people. Additionally, an accelerometer should be incorporated to understand the patient's physical activity which can assist with analyzing the shape of the ECG data. The patient's acceleration can contribute to monitoring heart rate and identifying abnormalities.

Furthermore, the use of analog sensors will definitely be accompanied by noise which must be removed using analog filtering. A bandstop filter with a cutoff frequency of 60 Hz is recommended to

remove the transmission line noise. A low pass filter will be required for the ECG signal to remove frequencies above 50 Hz and another low pass filter will be applied to the PPG signal to eliminate frequencies above 5 Hz to remove irrelevant data [122].

Since the I2C communication method between the ESP32 and the LCD screen is prone to glitches upon vibrations, a time-independent method of communication would be more reliable. The problem is that without I2C, more output pins are needed from the ESP32 to connect to the LCD's input pins. Given the limited number of strings intended to be displayed on the LCD (6 conditions, plus error feedback strings), only 3 pins are needed to indicate the current state, and logic gates can be used to determine the value of all LCD pins.

While the ESP32 is a relatively small microcontroller, it's still too large to be implemented into a wearable device that users can don comfortably for a long time period. Next steps include using a smaller microcontroller which will require further optimizations of the ML algorithm and data processing as the microcontroller may have less memory. The use of an external EEPROM may be considered to have additional memory to allow the increase of sampling frequency and the processing of larger data samples.

### Mechanical

Once the final hardware components of the device have been selected for the wearable, a new casing must be designed to house all the components and follow hardware hiding. The casing must also have an attachment mechanism such that it can be fastened to the body at an appropriate location from which the sensors can collect relevant data. Materials that are durable and comfortable against the skin will be selected for the casing.

## 4.4 Reflections and Recommendations

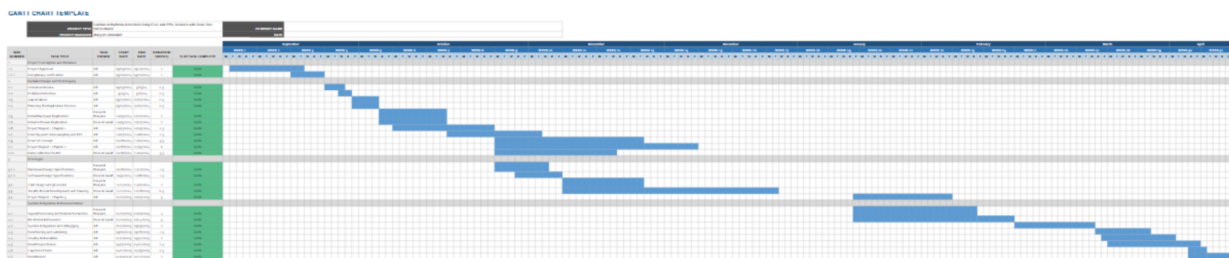


Figure 34: Updated Gantt chart to reflect changes

The initial Gantt Chart allotted more time for identifying the project objectives than what was actually needed. The initial mentorship from our supervisor Dr. Hassan helped reduce the time needed to complete the literature review, problem definition, gap analysis and planning of the process to replicate Dr. Hassan's work. Furthermore, the initial Gantt Chart missed some crucial tasks that our team worked on which took a fair bit of time. These tasks include taking the FFT of the ECG signal, consistent sampling of data points, finding labelled datasets to test the ML algorithm, designing the housing for the hardware components, signal processing and feature extraction, capstone poster and final demo. Additionally, we removed the task for hardware sourcing because our team already had the ESP32 and LCD which are the

only hardware components that were used. The new Gantt chart above reflects all of these changes.

The initial project proposal design aimed to develop a system that could perform real-time arrhythmia detection using ECG and PPG data, processed by an ESP32. Data collection was to be completed by the MAXREFDES104, and sent to the ESP32 to process the data and complete the TinyML. The initial proposal served as a solid foundation, clearly defining the scope; a focus on real-time processing and low power machine learning. The goal to use the ESP32 as a processing unit was feasible based on prior research completed by Dr. Hassan [48, 51, 81]. The major challenge that arose involved firmware restrictions for the MAXREFDES104 platform. This roadblock required a shift to simulated patient data, and a simplification of the machine learning, as there was previous intention to include features related to accelerometer data, but the idea was disregarded after the plan became to use open source datasets for training and validation rather than wearable data, since the datasets did not include accelerometer data or motion information. While this change allowed for algorithm testing and the development of the machine learning algorithm, it deviated from the original vision of having a real wearable for data collection.

The proof of concept aimed to validate the data collected using the wearable was suitable for processing using the machine learning algorithm. The initial goal was to verify that the recorded ECG and PPG data from the wearable were similar to the simulated ECG and PPG data used for training. The primary task was to extract the ECG frequency-domain features via Fast Fourier Transform (FFT), followed by identifying the peaks and valleys in the signal to compare the results to the dataset. The approach was successful in confirming that the ECG FFT and peaks and valleys features from the recorded data were comparable to those from the simulated dataset. While the system was able to perform well with the recorded data, the proof-of-concept was limited by the absence of real, noisy data. The recorded data did not fully represent the complexities and variability of real-world ECG and PPG signals, which could have impacted the comparison results.

The final design implementation aimed to ensure that the system could operate as intended with data processing and real-time feedback. While the system successfully met these goals, the shift from using real wearable sensors to simulated data introduced significant limitations in terms of external validation. The final prototype was functional and stable, and it fulfilled the core project goals: handling continuous data input, processing it in real time, and delivering alerts via the LCD interface. Multi-threading allowed for efficient management of concurrent tasks, while feature extraction using FFT and time-domain techniques enabled the identification of meaningful patterns in the ECG and PPG signals. The TinyML model performed reasonably well given the constraints of the embedded system and the training dataset. However, a major limitation was the dataset itself—publicly available data lacked diversity in patient profiles, signal noise, and real-world variability. The absence of real-time wearable data further restricted the model's ability to generalize and adapt to unpredictable user conditions, such as movement artifacts or varying skin tones affecting PPG quality. As a result, while the system performed well in simulated conditions, its real-world diagnostic accuracy remains unvalidated, highlighting the need for future testing with live, on-device sensor data.

Kavya

“I wish I had known how hectic capstone will get towards the end of March so we could have managed our time and tasks better.”

Noor

“I wish I had known obtaining the firmware wasn’t guaranteed and should have been requested early to change our plans early.”

Sarah

“I wish we had integrated software and embedded systems from the beginning, rather than viewing them as separate components. Early collaboration would have streamlined our project.”

Maryem

“I wish we had been able to get the promised resources from our supervisor, as we faced roadblocks with the manufacturer that limited our progress”

## Conclusion

Cardiac arrhythmias are irregular heart rhythms that, if left undetected, can lead to life-threatening events such as stroke or cardiac arrest. Current detection methods typically require clinical equipment and specialist interpretation, making them inaccessible for continuous, at-home monitoring. Wearable devices do exist but often fall short in terms of usability, real-time performance, or diagnostic accuracy. In response, our team developed *RhythmGuard*, a wearable, real-time arrhythmia detection system designed to be compact, user-friendly, and cost-effective. It combines single-lead ECG and PPG signals with a TinyML-powered classification algorithm that runs locally on-device. Initially, we considered using the ESP32 microcontroller due to its affordability and processing capabilities. While it proved comparable in performance to other health platforms, we ultimately implemented the prototype using the MAXREFDES104 due to its integrated sensor suite and streamlined development process. *RhythmGuard* provides visual alerts via an LCD screen and stores data locally, addressing both privacy and accessibility concerns. This project aimed to fill the gap in affordable, continuous arrhythmia monitoring by delivering a low-resource solution that empowers users to track their heart health outside clinical environments.

The final system was designed to capture ECG and PPG signals, extract relevant features using time- and frequency-domain techniques, and perform classification using a TinyML model trained on public datasets such as MIMIC and the Clifford et al. 2015 Challenge data. We validated model performance using standard classification metrics and cross-validation. While the model did not meet the original target of  $\geq 90\%$  sensitivity and specificity, it demonstrated promising accuracy and was able to distinguish between normal and arrhythmic signals under controlled conditions. Key challenges included limited training data diversity, signal noise, and computational constraints on the MAXREFDES104 platform. Nevertheless, the system successfully achieved real-time processing with a response rate under five seconds, met basic usability standards, and complied with Class I medical device design guidelines. Testing also confirmed local data handling, aligning with ethical and privacy standards. Though the

model's diagnostic performance requires improvement, RhythmGuard proves that a low-power, wearable device can feasibly support continuous arrhythmia detection.

Future work will focus on refining both software and hardware components to increase model performance and expand device functionality. On the software side, expanding and diversifying the dataset will help improve generalizability and reduce bias. Enhancing signal quality through more advanced filtering techniques, incorporating additional biosignal features, and implementing a multi-class classification model will strengthen diagnostic accuracy. Optimization of the TinyML pipeline—including model quantization and low-power scheduling—can further reduce latency and energy use. On the hardware side, transitioning to a custom PCB or reintroducing the ESP32 could enable better integration, and longer battery life can support extended wear. Additional user feedback mechanisms, such as vibration or auditory alerts, can improve accessibility for older or visually impaired users. Finally, integrating secure wireless communication (e.g., encrypted Bluetooth or WiFi) could allow optional clinician connectivity for remote monitoring and support broader healthcare integration. These improvements will position RhythmGuard as a more robust, inclusive, and clinically viable solution for real-time arrhythmia monitoring.

## References

- [1] D. Dube, D. S. Kumar, and S. K. Gupta, “An empirical study of the IOT Arrhythmia Detection Methods: Review and research gaps,” *2021 International Conference on Computer Communication and Informatics (ICCCI)*, vol. 11, pp. 1–8, Jan. 2021. doi:10.1109/iccci50826.2021.9402472
- [2] J. K. Sajeev, A. N. Koshy, and A. W. Teh, “Wearable devices for cardiac arrhythmia detection: A new contender?,” *Internal Medicine Journal*, vol. 49, no. 5, pp. 570–573, May 2019. doi:10.1111/imj.14274
- [3] A. Isin and S. Ozdalili, “Cardiac arrhythmia detection using Deep Learning,” *Procedia Computer Science*, vol. 120, pp. 268–275, 2017. doi:10.1016/j.procs.2017.11.238
- [4] S. Singhal and M. Kumar, “A systematic review on artificial intelligence-based techniques for diagnosis of cardiovascular arrhythmia diseases: Challenges and opportunities,” *Archives of Computational Methods in Engineering*, vol. 30, no. 2, pp. 865–888, Sep. 2022. doi:10.1007/s11831-022-09823-7
- [5] When smartwatches contribute to health anxiety in patients ...., [https://www.cvdigitalhealthjournal.com/article/S2666-6936\(20\)30008-6/fulltext](https://www.cvdigitalhealthjournal.com/article/S2666-6936(20)30008-6/fulltext) (accessed Oct. 25, 2024).
- [6] R. B. Schnabel et al., “Early diagnosis and better rhythm management to improve outcomes in patients with atrial fibrillation: The 8th AFNET/Ehra Consensus Conference,” *EP Europace*, vol. 25, no. 1, pp. 6–27, Jul. 2022. doi:10.1093/europace/euac062
- [7] P. Arun Kumar, “EcoDesign for medical devices: Barriers and opportunities to ecoeffective design of Medical Devices,” Royal College of Art, <https://researchonline.rca.ac.uk/id/eprint/4467> (accessed Oct. 25, 2024).
- [8] P. Travis and P. Khetrapal Singh, “Time to deliver: Accelerating more equitable access to better quality primary health-care services in the WHO south-east asia region,” *WHO South-East Asia Journal of Public Health*, vol. 8, no. 1, p. 1, 2019. doi:10.4103/2224-3151.255341

- [9] D. Abbott, “Linux and real-time,” in Linux for Embedded and Real-Time Applications, Elsevier, 2018, pp. 257–270.
- [10] J. Malmqvist, J. Engdahl, G. Sjölund, and P. Doliwa, “Sensitivity and specificity of handheld one lead ECG detecting atrial fibrillation in an outpatient clinic setting,” Journal of Electrocardiology, vol. 83, pp. 106–110, Mar. 2024.  
doi:10.1016/j.jelectrocard.2024.02.001
- [11] O. Kwon et al., “Electrocardiogram sampling frequency range acceptable for heart ratevariability analysis,” Healthcare Informatics Research, vol. 24, no. 3, p. 198, 2018.  
doi:10.4258/hir.2018.24.3.198
- [12] J. Hoxmeier and C. DiCesare, "System Response Time and User Satisfaction: An Experimental Study of Browser-based Applications" AMCIS 2000 Proceedings. 347, 2000..
- [13] S. Zheng, “Mucus mimic hydrogel coating for lubricous, antibiofouling and anti-inflammatory urinary catheters,” ACS Applied Materials & Interfaces, vol. 16, no. 35, Aug. 2024. doi:10.1021/acsami.4c13051.s001
- [14] “Method for testing IPX7 performance of waterproof device and waterproof device,” by 夏凯凯, 华函 Feb. 15, 2017 CN106404313A Available:  
<https://patents.google.com/patent/CN106404313A/en>
- [15] “Diagnosis,” NHLBI, NIH. [Online]. Available:  
<https://www.nhlbi.nih.gov/health/arrhythmias/diagnosis>. [Accessed: 25-Oct-2024].
- [16] E. A. Ashley and J. Niebauer, Arrhythmia. London, England: REMEDICA, 2004.
- [17] N. Paradkar and S. R. Chowdhury, “Cardiac arrhythmia detection using photoplethysmography,” Annu. Int. Conf. IEEE Eng. Med. Biol. Soc., vol. 2017, pp. 113–116, 2017.
- [18] Neha, H. K. Sardana, R. Kanwade, and S. Tewary, “Arrhythmia detection and classification using ECG and PPG techniques: a review,” Phys. Eng. Sci. Med., vol. 44, no. 4, pp. 1027–1048, 2021.

- [19] D. Castaneda, A. Esparza, M. Ghamari, C. Soltanpur, and H. Nazeran, “A review on wearable photoplethysmography sensors and their potential future applications in health care,” *Int. J. Biosens. Bioelectron.*, vol. 4, no. 4, pp. 195–202, 2018.
- [20] T. van der Ploeg, P. C. Austin, and E. W. Steyerberg, “Modern modelling techniques are data hungry: a simulation study for predicting dichotomous endpoints,” *BMC Med. Res. Methodol.*, vol. 14, no. 1, 2014.
- [21] . Mandala and T. C. Di, “ECG parameters for malignant ventricular arrhythmias: A comprehensive review,” *J. Med. Biol. Eng.*, vol. 37, no. 4, pp. 441–453, 2017.
- [22] P. Virtanen et al., “SciPy 1.0: fundamental algorithms for scientific computing in Python,” *Nat. Methods*, vol. 17, no. 3, pp. 261–272, 2020.
- [23] B. Liu et al., “Safety issues caused by internal short circuits in lithium-ion batteries,” *Journal of Materials Chemistry A*, vol. 6, no. 43, pp. 21475–21484, 2018.  
doi:10.1039/c8ta08997c
- [24] L. Wang, Y. Zhang, and P. G. Bruce, “Batteries for wearables,” National science review, <https://pmc.ncbi.nlm.nih.gov/articles/PMC9843125/#:~:text=and%20thermal%20abuse%20overheat%2C%20thermal,mechanical%20damage%20to%20the%20battery>. (accessed Oct. 25, 2024).
- [25] Z. Wang, W. Li, L. Chen, Z. Zhan, and H. Duan, “3D printable silicone rubber for long-lasting and weather-resistant wearable devices,” *ACS Applied Polymer Materials*, vol. 4, no. 4, pp. 2384–2392, Mar. 2022. doi:10.1021/acsapm.1c01674
- [26] S. Rath and N. Kaplish, “Allergic contact dermatitis to silicone causing PAP intolerance (p1-1.virtual),” *Neurology*, vol. 98, no. 18\_supplement, May 2022.  
doi:10.1212/wnl.98.18\_supplement.3672
- [27] Y. Muramatsu et al., “Silicone allergy associated with intraocular silicone ball prosthesis in a dog,” *The Canadian veterinary journal = La revue veterinaire canadienne*, <https://pmc.ncbi.nlm.nih.gov/articles/PMC8543662/#:~:text=In%20contrast%20silicone%20allergy%2C%20manifested,1%2C9%2C10> (accessed Oct. 25, 2024).
- [28] M. James E. Ip, “Wearable devices for cardiac rhythm diagnosis and management,” *JAMA*, [https://jamanetwork.com/journals/jama/article-abstract/2721089?casa\\_token=Dt](https://jamanetwork.com/journals/jama/article-abstract/2721089?casa_token=Dt)

CY0j8wzYAAAAA%3Aip2-TufDwYBXbMm9bq-fI8fAC4wpmm7pFm5mpMOhqD07t9F0zjIS\_Cf1cV6OKAEH4XWyX6nERY (accessed Oct. 25, 2024).

- [29] M. Strik et al., “Smartwatch-based detection of cardiac arrhythmias: Beyond the differentiation between sinus rhythm and atrial fibrillation,” *Heart Rhythm*, vol. 18, no. 9, pp. 1524–1532, Sep. 2021. doi:10.1016/j.hrthm.2021.06.1176
- [30] J. P. da Silva, “Privacy Data Ethics of Wearable Digital Health Technology,” Center for Digital Health | Engineering | Brown University,  
<https://cdh.brown.edu/news/2023-05-04/ethics-wearables#:~:text=As%20many%20wearable%20devices%20share,this%20data%20is%20being%20used.&text=This%20leads%20to%20privacy%20concerns,the%20individual's%20knowledge%20or%20consent>. (accessed Oct. 25, 2024).
- [31] P. J. Colvon, P. N. DeYoung, N.-O. A. Bosompra, and R. L. Owens, “Limiting racial disparities and bias for wearable devices in Health Science Research,” *Sleep*, vol. 43, no. 10, Sep. 2020. doi:10.1093/sleep/zsaa159
- [32] “Medical Devices—quality management systems—requirements for regulatory purposes,” ANSI/AAMI/ISO 13485:2016/(R)2019; Medical devices—Quality management systems—Requirements for regulatory purposes, Mar. 2016.  
doi:10.2345/9781570206047.ch1
- [33] “Medical Electrical Equipment — part 1-11: General requirements for basic safety and essential performance — collateral standard: Requirements for medical electrical equipment and medical electrical systems used in the Home Healthcare Environment,” ANSI/AAMI HA60601-1-11:2015; MEDICAL ELECTRICAL EQUIPMENT — Part 1-11: General requirements for basic safety and essential performance — Collateral Standard: Requirements for medical electrical equipment and medical electrical systems used in the home healthcare environment, Aug. 2015. doi:10.2345/9781570205934.ch1
- [34] ANSI/AAMI/ISO 14971:2019; medical devices—application of risk management to medical devices, May 2019. doi:10.2345/9781570207181
- [35] L. S. Branch, “Consolidated federal laws of canada, Personal Information Protection and Electronic Documents act,” Personal Information Protection and Electronic Documents Act, <https://laws-lois.justice.gc.ca/eng/acts/p-8.6/> (accessed Oct. 25, 2024).

- [36] Secondary cells and batteries containing alkaline or other non-acid electrolytes – Secondary lithium cells and batteries for portable applications, IEC 61960-4, 2020.
- [37] F. Babar *et al.*, “Sensitivity and specificity of wearables for atrial fibrillation in elderly populations: A systematic review,” *Current Cardiology Reports*, vol. 25, no. 7, pp. 761–779, May 2023. doi:10.1007/s11886-023-01898-3
- [38] Y. Zhu, R. Guo, P. Zhang, and A. Bhandari, “Frequency estimation via Sub-Nyquist Unlimited sampling,” *ICASSP 2024 - 2024 IEEE International Conference on Acoustics, Speech and Signal Processing (ICASSP)*, pp. 9636–9640, Apr. 2024. doi:10.1109/icassp48485.2024.10447003
- [39] L. S. Branch, “Consolidated federal laws of canada, Medical Devices Regulations,” Medical Devices Regulations, <https://laws-lois.justice.gc.ca/eng/regulations/sor-98-282/fulltext.html> (accessed Dec. 5, 2024).
- [40] L. M. Pereira *et al.*, “Wrist circumference cutoff points for determining excess weight levels and predicting cardiometabolic risk in adults,” *International Journal of Environmental Research and Public Health*, vol. 21, no. 5, p. 549, Apr. 2024. doi:10.3390/ijerph21050549
- [41] D. A. Basketter, “The human repeated insult Patch Test in the 21st Century: A commentary,” *Cutaneous and Ocular Toxicology*, vol. 28, no. 2, pp. 49–53, Jun. 2009. doi:10.1080/15569520902938032
- [42] Standard Test Method for Evaluation of Scratch Resistance of Polymeric Coatings and Plastics Using an Instrumented Scratch Machine, ASTM D7027/ISO 19252, 2020.
- [43] DEPARTMENT OF DEFENSE TEST METHOD STANDARD: ENVIRONMENTAL ENGINEERING CONSIDERATIONS AND LABORATORY TESTS, MIL-STD-810G, 2008.
- [44] S. Kummerl, D. Mantle, N. Patel, R. Munje, and P. Chen, “Dust and water resistance testing methodology for environmental sensors,” *International Symposium on Microelectronics*, vol. 2019, no. 1, pp. 000423–000427, Oct. 2019. doi:10.4071/2380-4505-2019.1.000423
- [45] D. Manishkumar Dave Amit, “Performance testing: Methodology for determining scalability of web systems,” *International Journal of Science and Research (IJSR)*, vol.

13, no. 1, pp. 1254–1261, Jan. 2024. doi:10.21275/sr24121010827

- [46] “Disease screening - statistics teaching tools - New York State Department of Health,” New York State Department of Health, <https://www.health.ny.gov/diseases/chronic/discreen.htm> (accessed Dec. 5, 2024).
- [47] A. Johnson, T. Pollard, and R. Mark, “Mimic-III clinical database,” MIMIC-III Clinical Database v1.4, <https://physionet.org/content/mimiciii/1.4/> (accessed Dec. 5, 2024).
- [48] B. Sun et al., “The case for tinyml in Healthcare: Cnns for real-time on-edge blood pressure estimation: Proceedings of the 38th ACM/SIGAPP Symposium on Applied Computing,” ACM Conferences, <https://dl.acm.org/doi/abs/10.1145/3555776.3577747> (accessed Nov. 25, 2024).
- [49] F. Babar *et al.*, “Sensitivity and specificity of wearables for atrial fibrillation in elderly populations: A systematic review,” *Current Cardiology Reports*, vol. 25, no. 7, pp. 761–779, May 2023. doi:10.1007/s11886-023-01898-3
- [50] (PDF) automatic feature extraction of ECG signal using Fast Fourier transform, [https://www.researchgate.net/publication/295813369\\_Automatic\\_Feature\\_Extraction\\_of\\_ECG\\_Signal\\_Using\\_Fast\\_Fourier\\_Transform](https://www.researchgate.net/publication/295813369_Automatic_Feature_Extraction_of_ECG_Signal_Using_Fast_Fourier_Transform) (accessed Dec. 5, 2024).
- [51] B. Sun and M. Hassan, “HW/SW collaborative techniques for accelerating tinyml inference time at no cost,” *2024 27th Euromicro Conference on Digital System Design (DSD)*, pp. 512–520, Aug. 2024. doi:10.1109/dsd64264.2024.00074
- [52] L. S. Branch, “Consolidated federal laws of canada, Medical Devices Regulations,” Medical Devices Regulations, <https://laws-lois.justice.gc.ca/eng/regulations/sor-98-282/> (accessed Dec. 5, 2024).
- [53] J. Shreffler, “Diagnostic testing accuracy: Sensitivity, specificity, predictive values and likelihood ratios,” StatPearls [Internet]., <https://www.ncbi.nlm.nih.gov/books/NBK557491/> (accessed Dec. 5, 2024).
- [54] Y. Brun and M. D. Ernst, “Finding latent code errors via machine learning over program executions,” *Proceedings. 26th International Conference on Software Engineering*, pp. 480–490, Jun. 2004. doi:10.1109/icse.2004.1317470

- [55] "A guide to ECG signal filtering | GE Healthcare (United States)," GE HealthCare, <https://www.gehealthcare.com/insights/article/a-guide-to-ecg-signal-filtering> (accessed Dec. 5, 2024).
- [56] L. Lévesque, "Nyquist sampling theorem: Understanding the illusion of a spinning wheel captured with a video camera," *Physics Education*, vol. 49, no. 6, pp. 697–705, Oct. 2014. doi:10.1088/0031-9120/49/6/697
- [57] H. Azami, K. Mohammadi, and B. Bozorgtabar, "An improved signal segmentation using moving average and Savitzky-Golay filter," *Journal of Signal and Information Processing*, vol. 03, no. 01, pp. 39–44, 2012. doi:10.4236/jsip.2012.31006
- [58] "MAXREFDES104," MAXREFDES104 | reference design | Analog Devices, <https://www.analog.com/en/resources/reference-designs/maxrefdes104.html> (accessed Dec. 5, 2024).
- [59] B. J. Mohd, K. M. Ahmad Yousef, A. AlMajali, and T. Hayajneh, "Quantization-based optimization algorithm for hardware implementation of Convolution Neural Networks," *Electronics*, vol. 13, no. 9, p. 1727, Apr. 2024. doi:10.3390/electronics13091727
- [60] "ISO 13485: Medical Devices – Quality Management Systems – Requirements for Regulatory Purposes," 2016. [Online]. Available: <https://www.iso.org/iso-13485-medical-devices.html>. [Accessed: Dec. 5, 2024].
- [61] "ISO/IEC 23894:2023 - Information Technology — Artificial Intelligence — Guidance on Risk Management," 2023. [Online]. Available: <https://www.iso.org/standard/77304.html>. [Accessed: Dec. 5, 2024].
- [62] "ISO 14001:2015 - Environmental Management Systems — Requirements with Guidance for Use," 2015. [Online]. Available: <https://www.iso.org/standard/60857.html>. [Accessed: Dec. 5, 2024].
- [63] "IEC 60601-1-11:2015 - Medical Electrical Equipment — Part 1-11: General Requirements for Basic Safety and Essential Performance — Requirements for Medical Electrical Equipment and Medical Electrical Systems Used in the Home Healthcare Environment," 2015. [Online]. Available: <https://www.iso.org/standard/65529.html>. [Accessed: Dec. 5, 2024].

- [64] Risk in medical device product availability, compliance, ...., <https://www.fda.gov/files/medical%20devices/published/Factors-to-Consider-Regarding-Benefit-Risk-in-Medical-Device-Product-Availability--Compliance--and-Enforcement-De-cisions---Guidance-for-Industry-and-Food-and-Drug-Administration-Staff.pdf> (accessed Dec. 5, 2024).
- [65] “What is FMEA? failure mode & effects analysis | ASQ,” Failure Mode and Effects Analysis (FMEA), <https://asq.org/quality-resources/fmea> (accessed Dec. 5, 2024).
- [66] D. Hemapriya, P. Viswanath, V. M. Mithra, S. Nagalakshmi, and G. Umarani, “Wearable Medical Devices — design challenges and issues,” *2017 International Conference on Innovations in Green Energy and Healthcare Technologies (IGEHT)*, pp. 1–6, Nov. 2017. doi:10.1109/igeht.2017.8094096
- [67] "ISO 14971:2019 - Medical Devices — Application of Risk Management to Medical Devices," 2019. [Online]. Available: <https://www.iso.org/standard/72704.html>. [Accessed: Dec. 5, 2024].
- [68] S. Gerke, T. Minssen, and G. Cohen, “Ethical and legal challenges of artificial intelligence-driven healthcare,” *Artificial Intelligence in Healthcare*, pp. 295–336, Jun. 2020. doi:10.1016/b978-0-12-818438-7.00012-5
- [68] E. Ferrara, *Fairness and bias in Artificial Intelligence: A brief survey of sources, impacts, and mitigation strategies (preprint)*, Apr. 2023. doi:10.2196/preprints.48399
- [69] “Global e-waste monitor 2024: Electronic waste rising five times faster than documented e-waste recycling | unitar,” unitar, <https://unitar.org/about/news-stories/press/global-e-waste-monitor-2024-electronic-waste-rising-five-times-faster-documented-e-waste-recycling> (accessed Dec. 5, 2024).
- [70] “RoHS directive,” Environment, [https://environment.ec.europa.eu/topics/waste-and-recycling/rohs-directive\\_en#:~:text=Restriction%20of%20Hazardous%20Substances%20in,the%20environment%20and%20public%20health](https://environment.ec.europa.eu/topics/waste-and-recycling/rohs-directive_en#:~:text=Restriction%20of%20Hazardous%20Substances%20in,the%20environment%20and%20public%20health) (accessed Dec. 5, 2024).
- [71] “Electronics Recycling in Ontario,” Recycle My Electronics, <https://recyclemyelectronics.ca/on> (accessed Dec. 5, 2024).

- [72] E. A. Bennett, “The efficacy of voluntary standards, Sustainability Certifications, and ethical labels,” *Research Handbook on Global Governance, Business and Human Rights*, Mar. 2022. doi:10.4337/9781788979832.00016
- [73] General Description, “MAX32665/MAX32666 Low-Power Arm Cortex-M4 with FPU-Based Microcontroller with Bluetooth 5 for Wearables,” *Analog.com*. [Online]. Available: <https://www.analog.com/media/en/technical-documentation/data-sheets/max32665-max32666.pdf> . [Accessed: 08-Feb-2025].
- [74] ESP32-Pico Series, [https://www.espressif.com/sites/default/files/documentation/esp32-pico\\_series\\_datasheet\\_en.pdf](https://www.espressif.com/sites/default/files/documentation/esp32-pico_series_datasheet_en.pdf) [Accessed Feb. 8, 2025].
- [75] K. Heyman, “SRAM in AI: The Future of Memory,” Semiconductor Engineering, <https://semiengineering.com/sram-in-ai-the-future-of-memory/> [Accessed Feb. 7, 2025].
- [76] B. Sudharsan, P. Patel, J. G. Breslin, and M. I. Ali, “Enabling machine learning on the edge using SRAM conserving efficient neural networks execution approach,” in *Lecture Notes in Computer Science*, Cham: Springer International Publishing, 2021, pp. 20–35.
- [77] A. Johnson, T. Pollard, and R. Mark, “Mimic-III clinical database,” MIMIC-III Clinical Database v1.4, <https://physionet.org/content/mimiciii/1.4/> [Accessed Feb. 7, 2025].
- [78] G. D. Clifford, I. Silva, B. Moody, and R. Mark, “Reducing false arrhythmia alarms in the ICU: The physionet/computing in cardiology challenge 2015,” Reducing False Arrhythmia Alarms in the ICU: The PhysioNet/Computing in Cardiology Challenge 2015 v1.0.0, <https://doi.org/10.13026/xxnk-d535> [Accessed Feb. 7, 2025].
- [79] P. H. Charlton, “Mimic perform datasets,” Zenodo, <https://zenodo.org/records/6973963> [Accessed Feb. 7, 2025].
- [80] Q. Qananwah, M. Ababneh, and A. Dagamseh, “Cardiac arrhythmias classification using Photoplethysmography Database,” *Scientific Reports*, vol. 14, no. 1, Feb. 2024. doi:10.1038/s41598-024-53142-9
- [81] K. Ahmed and M. Hassan, “TinyCare: A tinyML-based low-cost continuous blood pressure estimation on the extreme edge,” 2022 IEEE 10th International Conference on Healthcare Informatics (ICHI), pp. 264–275, Jun. 2022. doi:10.1109/ichi54592.2022.00047
- [82] G. V. Silva, M. D. Lima, J. A. Filho, and M. J. Rovai, “Atrial fibrillation and sinus rhythm detection using tinyml (embedded machine learning),” *IFMBE Proceedings*, pp. 633–644, Jan.

2024. doi:10.1007/978-3-031-49407-9\_63

- [83] “What is a watchdog timer and why is it important?,” SSZTAH7 Technical article | TI.com, <https://www.ti.com/document-viewer/lit/html/ssztah7> [Accessed Feb. 7, 2025].
- [84] “Embien technologies::Embedded System Testing Methods,” Embien, <https://www.embien.com/blog/embedded-system-testing-methods-black-box-and-white-box-testing> [Accessed Feb. 7, 2025].
- [85] Secondary cells and batteries containing alkaline or other non-acid electrolytes – Secondary lithium cells and batteries for portable applications, IEC 61960-4, 2020.
- [86] F. Babar et al., “Sensitivity and specificity of wearables for atrial fibrillation in elderly populations: A systematic review,” Current Cardiology Reports, vol. 25, no. 7, pp. 761–779, May 2023. doi:10.1007/s11886-023-01898-3
- [87] J. W. Mason, E. W. Hancock, and L. S. Gettes, “Recommendations for the standardization and interpretation of the electrocardiogram,” Circulation, vol. 115, no. 10, pp. 1325–1332, Mar. 2007. doi:10.1161/circulationaha.106.180201
- [88] L. S. Branch, “Consolidated federal laws of canada, Medical Devices Regulations,” Medical Devices Regulations, <https://laws-lois.justice.gc.ca/eng/regulations/sor-98-282/fulltext.html> [Accessed Dec. 5, 2024].
- [89] H. Canada, “Government of Canada,” Canada.ca, <https://www.canada.ca/en/health-canada/services/drugs-health-products/medical-devices/application-information/guidance-documents/guidance-document-guidance-risk-based-classification-system-non-vitro-diagnostic.html#a32> [Accessed Feb. 7, 2025].
- [90] L. M. Pereira et al., “Wrist circumference cutoff points for determining excess weight levels and predicting cardiometabolic risk in adults,” International Journal of Environmental Research and Public Health, vol. 21, no. 5, p. 549, Apr. 2024. doi:10.3390/ijerph21050549
- [91] D. A. Basketter, “The human repeated insult Patch Test in the 21st Century: A commentary,” Cutaneous and Ocular Toxicology, vol. 28, no. 2, pp. 49–53, Jun. 2009. doi:10.1080/15569520902938032
- [92] V. T. Politano and A. M. Api, “The Research Institute for Fragrance Materials’ Human Repeated Insult Patch Test Protocol,” Regulatory Toxicology and Pharmacology, vol. 52, no. 1, pp. 35–38, Oct. 2008. doi:10.1016/j.yrtph.2007.11.004

- [93] Standard Test Method for Evaluation of Scratch Resistance of Polymeric Coatings and Plastics Using an Instrumented Scratch Machine, ASTM D7027/ISO 19252, 2020.
- [94] Test method for evaluation of scratch resistance of polymeric coatings and plastics using an instrumented scratch machine. doi:10.1520/d7027-13
- [95] DEPARTMENT OF DEFENSE TEST METHOD STANDARD: ENVIRONMENTAL ENGINEERING CONSIDERATIONS AND LABORATORY TESTS, MIL-STD-810G, 2008.
- [96] S. Kummerl, D. Mantle, N. Patel, R. Munje, and P. Chen, “Dust and water resistance testing methodology for environmental sensors,” International Symposium on Microelectronics, vol. 2019, no. 1, pp. 000423–000427, Oct. 2019.  
doi:10.4071/2380-4505-2019.1.000423
- [97] D. Manishkumar Dave Amit, “Performance testing: Methodology for determining scalability of web systems,” International Journal of Science and Research (IJSR), vol. 13, no. 1, pp. 1254–1261, Jan. 2024. doi:10.21275/sr24121010827
- [98] Keysight, “How to validate low-power device battery life,” Keysight, <https://www.keysight.com/us/en/solutions/validate-low-power-device-battery-life.html> [Accessed Feb. 7, 2025].
- [99] D. S. Desai and S. Hajouli, “Arrhythmias,” StatPearls, StatPearls Publishing, 2023.
- [100] Y. Zhu, R. Guo, P. Zhang, and A. Bhandari, “Frequency estimation via Sub-Nyquist Unlimited sampling,” ICASSP 2024 - 2024 IEEE International Conference on Acoustics, Speech and Signal Processing (ICASSP), pp. 9636–9640, Apr. 2024.  
doi:10.1109/icassp48485.2024.10447003
- [101] Siemens Digital Industries Software Community, <https://community.sw.siemens.com/s/article/digital-signal-processing-sampling-rates-bandwidth-spectral-lines-and-more> (accessed Feb. 7, 2025).
- [102] L. S. Branch, “Consolidated federal laws of canada, Medical Devices Regulations,” Medical Devices Regulations, <https://laws-lois.justice.gc.ca/eng/regulations/sor-98-282/fulltext.html> [Accessed Dec. 5, 2024].
- [103] H. Canada, “Government of Canada,” Canada.ca, <https://www.canada.ca/en/health-canada/services/drugs-health-products/medical-devices/application-information/guidance-documents/guidance-document-guidance-risk-based-classification-syst>

m-non-vitro-diagnostic.html#a32 [Accessed Feb. 7, 2025].

- [104] V. T. Politano and A. M. Api, “The Research Institute for Fragrance Materials’ Human Repeated Insult Patch Test Protocol,” *Regulatory Toxicology and Pharmacology*, vol. 52, no. 1, pp. 35–38, Oct. 2008. doi:10.1016/j.yrtph.2007.11.004
- [105] Test method for evaluation of scratch resistance of polymeric coatings and plastics using an instrumented scratch machine. doi:10.1520/d7027-13
- [106] Government of Canada, Statistics Canada, Anthropometry measures of the household population, <https://www150.statcan.gc.ca/t1/tbl1/en/tv.action?pid=1310031901> [Accessed Feb. 7, 2025].
- [107] Y. Yang, W. Xia, L. Han, F. Ding, and J. Xie, “Research on high precision yime measurement and analysis method based on oscilloscope,” *Journal of Physics: Conference Series*, vol. 1865, no. 2, p. 022057, Apr. 2021. doi:10.1088/1742-6596/1865/2/022057
- [108] L. G. Tereshchenko and M. E. Josephson, “Frequency content and characteristics of ventricular conduction,” *Journal of electrocardiology*, <https://pmc.ncbi.nlm.nih.gov/articles/PMC4624499/> [Accessed Feb. 7, 2025].
- [109] J. A. Van Alste and T. S. Schilder, “Removal of base-line wander and power-line interference from the ECG by an efficient FIR filter with a reduced number of taps,” *IEEE Transactions on Biomedical Engineering*, vol. BME-32, no. 12, pp. 1052–1060, Dec. 1985. doi:10.1109/tbme.1985.325514
- [110] P. Bing et al., “A novel approach for denoising electrocardiogram signals to detect cardiovascular diseases using an efficient hybrid scheme,” *Frontiers in Cardiovascular Medicine*, vol. 11, Apr. 2024. doi:10.3389/fcvm.2024.1277123
- [111] P. Madan, V. Singh, D. P. Singh, M. Diwakar, and A. Kishor, “Denoising of ECG signals using weighted stationary wavelet total variation,” *Biomedical Signal Processing and Control*, vol. 73, p. 103478, Mar. 2022. doi:10.1016/j.bspc.2021.103478
- [112] I. Dotsinsky, “Review of ‘advanced methods and tools for ECG Data Analysis’, by Gari D. Clifford, Francisco Azuaje and Patrick E. McSharry (editors),” *BioMedical Engineering OnLine*, vol. 6, no. 1, p. 18, 2007. doi:10.1186/1475-925x-6-18
- [113] A. Kumar, R. D. Morabito, S. Umbet, J. Kabbara, and A. Emami, “Confidence under the hood: An investigation into the confidence-Probability Alignment in Large Language Models,” *Annu Meet Assoc Comput Linguistics*, vol. abs/2405.16282, 2024.
- [114] I. Guyon, J. Weston, S. Barnhill, and V. Vapnik, *Mach. Learn.*, vol. 46, no. 1/3, pp. 389–422,

2002.

- [115] “timeit — Measure execution time of small code snippets,” Python documentation. [Online]. Available: <https://docs.python.org/3/library/timeit.html>. [Accessed: 08-Feb-2025].
- [116] PyPI · the python package index, <https://pypi.org/project/memory-profiler/> [Accessed Feb. 7, 2025].
- [117] N. M. Adams, S. P. J. Kirby, P. Harris, and D. B. Clegg, “A review of parallel processing for statistical computation,” *Stat. Comput.*, vol. 6, no. 1, pp. 37–49, 1996.
- [118] O. Rainio, J. Teuho, and R. Klén, “Evaluation metrics and statistical tests for machine learning,” *Sci. Rep.*, vol. 14, no. 1, pp. 1–14, 2024.
- [119] Nrc.gov. [Online]. Available: <https://www.nrc.gov/docs/ML1215/ML12151A426.pdf>. [Accessed: 08-Feb-2025].
- [120] Fastercapital.com. [Online]. Available: <https://fastercapital.com/content/Firmware-Testing--How-to-Test-the-Software-Embedded-in-Your-Product-s-Hardware.html>. [Accessed: 08-Feb-2025].
- [121] M. Stuart, A. B. Turman, J. Shaw, N. Walsh, and V. Nguyen, “Effects of aging on vibration detection thresholds at various body regions,” *BMC Geriatr.*, vol. 3, no. 1, p. 1, 2003.
- [122] Á. Solé Morillo, J. Lambert Cause, V.-E. Baciu, B. da Silva, J. C. Garcia-Naranjo, and J. Stiens, “PPG EduKit: An adjustable photoplethysmography evaluation system for educational activities,” *Sensors (Basel)*, vol. 22, no. 4, p. 1389, 2022.